

# What is the role of fish intestine as environment-organism barrier? Mechanistic investigations using fish intestinal cells on a chip

THÈSE N° 8708 (2018)

PRÉSENTÉE LE 22 JUIN 2018

À LA FACULTÉ DES SCIENCES ET TECHNIQUES DE L'INGÉNIEUR  
LABORATOIRE DE MICROSYSTÈMES 4  
PROGRAMME DOCTORAL EN BIOTECHNOLOGIE ET GÉNIE BIOLOGIQUE

ÉCOLE POLYTECHNIQUE FÉDÉRALE DE LAUSANNE

POUR L'OBTENTION DU GRADE DE DOCTEUR ÈS SCIENCES

PAR

**Carolin DRIESCHNER**

acceptée sur proposition du jury:

Prof. P. De Los Rios, président du jury  
Prof. Ph. Renaud, Prof. K. Schirmer, directeurs de thèse  
Prof. A. van den Berg, rapporteur  
Prof. H. Segner, rapporteur  
Prof. S. Sturla, rapporteuse



ÉCOLE POLYTECHNIQUE  
FÉDÉRALE DE LAUSANNE

Suisse  
2018



*To all people  
who feel a deep connection to water,  
in all its beautiful shapes.*

*water is life*



# Acknowledgments

This work was carried out at the laboratory of microsystems 4 (LMIS4) at EPFL and the department of environmental toxicology (Utox) at eawag. This is the opportunity for me to thank the people I had the chance to meet and work with.

First and foremost, I would like to gratefully thank my doctoral supervisors Kristin Schirmer and Philippe Renaud. You are both brilliant scientists and it has been a honor and pleasure to work with you! Thank you for your unmeasurable support, guidance, encouragement and inspiration throughout the past 5 years. You made my Ph.D. time to a creative, productive and stimulating period of my life.

Besides my advisors, I would like to thank the rest of my thesis committee: Prof. Shana Sturla, Prof. Albert van den Berg and Prof. Helmut Segner for reviewing my thesis and giving valuable feedback. I have been lucky working in two groups with open-minded people, who were at any time unhesitant to share their knowledge with me. I have been enjoying the nice working atmospheres and was able to learn so much from my colleagues, of whom some became friends. My special thanks goes to Matteo, Robert and Songmei for their scientific support during the first time of my Ph.D and Sarah for completing experiments with the "Flying Spaghetti Monster". I thank my fellow labmates from Utox, in particular Hannah, Alena, Alex, Melanie, Stephan, Fred, Jenny, Nadine and Muris for helpful discussions, wonderful hiking trips and awesome pool parties. Thanks to the people from LMIS4, specifically to Guillaume, David, Ela, Jonathan, Amélie, Sophie, Fabien and Damien for constructive advices, funny Satellite evenings and fantastic ski touring trips.

This dissertation would not have been possible without funding from the Swiss National Science Foundation and is therefore acknowledged.

Last but not least, I would like to thank my family: my parents, sister and grandparents for supporting and encouraging me, in particular during the final stage of my Ph.D. Most importantly I wish to thank my love Michael and Benno our little sunshine. I'm lucky to have you both by my side, making my life entirely happy, colorful and adventurous on every single day.



## Abstract

The gut of fish belongs to the most essential barriers that mark the border between the organism and its surrounding environment. The pivotal barrier function, allowing absorption of nutrients from the diet while simultaneously protecting the organism from pathogens and contaminants, is accomplished by a single layer of epithelial cells lining the intestinal lumen. *In vitro*, this barrier has been mimicked by culturing fish epithelial intestinal cells on conventional permeable membranes within a two-chamber system, which creates an upper and a lower compartment representing the intestinal lumen and blood circulation, respectively. This simplified approach, however, has at least three important limitations: The first being restricted diffusion through the several micrometer thick commercial membranes, which moreover have quite limited porosity; the second being a lack of interaction with other intestinal cell types; and the third being absence of mechanical stimulation, such as shear forces from fluid flow to better simulate the physiology of the intestine. To overcome these limitations, this thesis focuses on the recreation of the piscine intestinal microenvironment by combining cells derived from the intestine of fish, precisely epithelial and fibroblast cell lines from rainbow trout (*Oncorhynchus mykiss*), with engineered microsystems. The applied stepwise approach encompasses (a) the development of an ultrathin permeable membrane as novel support for barrier forming cells, (b) followed by combining epithelial cells and fibroblasts for intestinal architecture reconstruction, and (c) exposure to fluid flow to mimic the mechanical forces occurring on the epithelial-lumen interface.

Artificial ultrathin membranes for intestinal cell culture were found to better mimic features of the delicate, highly permeable basement membrane that underlines the epithelial cells *in vivo* compared to conventional porous supports. Two types of membranes were fabricated in this study. The first was an anodized aluminum oxide membrane that features densely packed pores in the nanometer range and allows for fast diffusion of small molecules. This type of membrane is ideal for high quality microscopy and supports epithelial polarization. However, membranes release, albeit non-cytotoxic, concentrations of aluminum ions, which might be critical for toxicological investigations. Therefore, a second type of an ultrathin membrane, namely a silicon nitride membrane, was fabricated. It has pores in the micrometer range, is optically transparent and has been applied beyond static exposures for microfluidic studies.

To initiate co-culture of epithelial cells with fibroblasts, an intestinal fibroblast cell line from rainbow trout needed to be characterized first. The cells feature typical fibroblast morphology and behavior

and appear to be infinite. The combination of epithelial and fibroblast cells, when in direct contact, had no beneficial effect on barrier tightness. Cell culture on opposite sides of ultrathin alumina membranes, however, resulted in increased trans-epithelial electrical resistance, suggesting enhanced barrier tightness from cellular cross-talk.

A uniquely designed microfluidic bioreactor with integrated ultrathin silicon nitride membranes as substrate for cell growth was finally developed to allow for realistic flow conditions on epithelial cells. The arising fluid shear stress on epithelial monolayers and epithelial-fibroblast co-cultures positively affected barrier resistance when applied at a moderate rate. This physiological adaptation allows for better comparability to the fish intestine *in vivo* compared to cells cultured under static conditions. This finding highlights the importance of mechanical stimulation for realistic organ mimicry within *in vitro* systems.

To conclude, this thesis demonstrates the benefits of recreating a more physiologically realistic microenvironment for epithelial cell cultures from fish intestine. By introducing ultrathin permeable membranes as novel culture substrate, adding a fibroblast cell line and shear stress, the novel *in vitro* intestinal barrier model now better reflects intestinal properties of the *in vivo* counterpart and allows for improved exposure and transport phenomena during experimental uptake studies, e.g. for chemical pollutants. This thesis therefore paves the way for improved understanding of normal and impaired physiology of the fish intestine and better *in vitro* to *in vivo* extrapolation while contributing to a reduced need of animal experiments.

## **Keywords**

gut-on-chip, fish, intestine, rainbow trout (*Oncorhynchus mykiss*), ultrathin membrane, RTgutGC, RTgutF, impedance, microfluidic bioreactor, toxicity

# Zusammenfassung

Der Fischdarm gehört zu den wichtigsten Barrieren, welche den Organismus von seiner umgebenden Umwelt abgrenzen. Die zentrale Funktion dieser Barriere besteht darin, Nährstoffe aus der Nahrung aufzunehmen und gleichzeitig den Organismus vor Krankheitserregern und Schadstoffen zu schützen. Dies wird durch eine einzige Schicht von Epithelzellen erreicht, die das Innere des Darms auskleiden. Die Nachahmung dieser Barriere *in vitro* wurde bisher durch die Kultivierung von Darmepithelzellen vom Fisch auf konventionellen permeablen Membranen in einem Zweikammersystems erreicht. Dieses System besteht aus zwei Kompartimenten, wobei das obere das Darmlumen und das untere die Blutzirkulation darstellt. Dieser vereinfachte Ansatz weist jedoch mindestens drei beträchtliche Einschränkungen auf. Erstens ist die Diffusion durch die mehrere Mikrometer dicke, kommerzielle Membrane nur beschränkt möglich, zudem ist die Porosität der Membran gering. Zweitens fehlt im System die Interaktion mit anderen Darmzelltypen; und drittens fehlt es an mechanischen Reizen, wie Scherkräfte verursacht durch das Fließen von Flüssigkeiten, welche die Physiologie des Darms besser simulieren. Um diese Einschränkungen zu überwinden, liegt der Fokus dieser Dissertation auf der Wiederherstellung der natürlichen intestinalen Mikroumgebung, wie sie in Fischen vorhanden ist. Dies wird durch die Kombination einer Darmepithel- und Darmfibroblasten-Zelllinie der Regenbogenforelle (*Oncorhynchus mykiss*), und technisch konstruierten Mikrosystemen erreicht. Der Forschungsansatz umfasst (a) die Entwicklung einer ultradünnen, permeablen Membran als neuartigen Träger für die Barriere-bildenden Zellen; (b) die Kombination von Epithelzellen und Fibroblasten um die natürliche Darmstruktur nachzubilden und (c) die Exposition mit einem Flüssigkeitsstrom, welcher die an der Grenze zwischen Epithel und Darmlumen auftretenden mechanischen Kräfte nachahmt.

Im Organismus sind die Epithelzellen von der filigranen und hochpermeablen Basalmembran unterlegt. Es wurde gezeigt dass die artifiziellen ultradünnen Membranen, welche für die intestinale Zellkultur entwickelt wurden, diese Eigenschaften viel besser nachbilden können als herkömmliche, kommerziell erhältliche Membran Systeme. Für die vorliegende Dissertation wurden zwei Membrantypen hergestellt: Die Erste ist eine anodisierte Aluminiumoxid Membran, welche dicht gepackte Poren im Nanometerbereich aufweist und eine schnelle Diffusion von kleinen Molekülen ermöglicht. Dieser Membrantyp ist ideal für hochwertige Mikroskopie und unterstützt zudem die Polarisierung der Epithelzellen. Jedoch setzt diese Membran, wenn auch in nicht-zytotoxischen Konzentrationen, Aluminium Ionen frei, welche für toxikologische Untersuchungen kritisch sein könnten. Daher wurde eine zweite Art von ultradünne Membranen hergestellt, welche aus

Siliziumnitrid besteht. Diese besitzt Poren im Mikrometerbereich, ist optisch transparent und wurde speziell für mikrofluidische Untersuchungen angewendet.

Vor der Verwendung in der Co-Kultur musste zunächst eine neuartige intestinale Fibroblasten-Zelllinie der Regenbogenforelle charakterisiert werden. Diese Zellen weisen die typische Morphologie und das Verhalten von Fibroblasten auf, außerdem ist ihre Lebensdauer unendlich. Ein direkter Zellkontakt zwischen Epithel- und Fibroblasten-Zellen hatte keinen positiven Einfluss auf die Dichte der Barriere. Im Gegensatz hierzu zeigte die Kultivierung der Zellen auf gegenüberliegenden Seiten der ultradünnen Aluminiumoxid Membran einen erhöhten elektrischen Widerstand des Epithels auf. Dies lässt auf eine erhöhte Barrieredichte hindeuten, welche vermutlich durch die Kommunikation der beiden Zelltypen verursacht wird.

Um die Auswirkung eines Flüssigkeitenstromes auf die Zellen zu untersuchen, wurde ein spezieller Bioreaktor für mikrofluidische Anwendungen entwickelt. Dieser Reaktor beinhaltet die ultradünnen Siliziumnitrid Membranen als Wachstumsunterlage für die Zellen und ermöglicht es, realistische Strömungsbedingungen für die Epithelzellen nachzustellen. Die auftretenden Scherkräfte, welche durch einen angemessenen Flüssigkeitsstrom verursacht wurden, hatten eine positive Wirkung auf die Resistenz von einfachen Epithelzellschichten und Epithel-Fibroblasten-Co-Kulturen. Diese physiologische Anpassung ermöglicht eine bessere Vergleichbarkeit zum *in vivo* Fischdarm, als Zellen welche unter herkömmlichen, statischen Bedingungen kultiviert werden. Weiterhin unterstreicht dieses Ergebnis die Bedeutung von mechanischen Reizen für die realistische Nachbildung von Organen in *in vitro* Systemen.

Die vorliegende Dissertation verdeutlicht die Vorteile der Nachstellung einer physiologisch realistischen Mikroumgebung für epitheliale Zellkulturen vom Fischdarm. Die Einführung ultradünner permeabler Membranen als neues Kultursubstrat, das Hinzufügen einer Fibroblasten Zelllinie und Einführung zusätzlicher Scherkräfte ermöglichen ein neuartiges *in vitro* Barrieremodell, welches die intestinalen Eigenschaften im Organismus besser nachstellt. Zudem ermöglicht dieses Modell realistischere Expositions- und Transportphänomene für experimentelle Aufnahmestudien z.B. von chemischen Schadstoffen. Diese Studie bereitet somit den Weg für ein verbessertes Verständnis der normalen und geschädigten Physiologie des Fischdarms, ermöglicht eine realistischere *in vitro* zu *in vivo* Extrapolation und trägt dadurch zu einem reduzierten Bedarf an Versuchstieren bei.

## Schlüsselwörter

Darm-auf-dem-Chip, Fisch, Darm, Regenbogenforelle (*Oncorhynchus mykiss*), ultradünne Membran, RTgutGC, RTgutF, Impedanz, mikrofluidischer Bioreaktor, Toxizität



# Table of Contents

Acknowledgments .....	i
Abstract .....	iii
Zusammenfassung .....	v
Table of Contents .....	ix
List of Figures .....	xi
<b>Chapter 1. Introduction .....</b>	<b>1</b>
1.1 Scope .....	1
1.2 Background .....	2
1.2.1 <i>The potential of fish cells in ecotoxicology</i> .....	2
1.2.2 <i>Key aspects of the fish intestine</i> .....	3
1.2.3 <i>Piscine intestinal models</i> .....	5
1.2.4 <i>The pioneers: human gut-on-chip devices</i> .....	7
1.2.5 <i>Recreation of an artificial basement membrane</i> .....	9
1.2.6 <i>Impedance based monitoring of barrier function</i> .....	12
1.3 Research strategy .....	14
1.3.1 <i>Problem definition</i> .....	14
1.3.2 <i>Research objectives</i> .....	14
1.3.3 <i>Thesis structure</i> .....	15
<b>Chapter 2. Ultrathin alumina membranes as scaffold for epithelial cell culture from the intestine of rainbow trout (<i>Oncorhynchus mykiss</i>) .....</b>	<b>17</b>
2.1 Introduction .....	18
2.2 Material and methods .....	20
2.3 Results and discussion .....	26
2.4 Conclusion .....	36
2.5 Supplemental material .....	37
<b>Chapter 3. Characterization of a fibroblast-like cell line from the intestine of rainbow trout and its potential role in an advanced intestinal barrier model .....</b>	<b>41</b>
3.1 Introduction .....	42
3.2 Material and methods .....	44
3.3 Results and discussion .....	52
3.4 Conclusion .....	59
3.5 Supplemental material .....	60
<b>Chapter 4. 'Fish-gut-on-chip': Development of a microfluidic bioreactor to study the role of the fish intestine as environment-organism barrier in vitro .....</b>	<b>63</b>

4.1	Introduction.....	64
4.2	Material and methods.....	66
4.3	Results and discussion .....	72
4.4	Conclusion.....	80
<b>Chapter 5.</b>	<b>Conclusion and future perspective .....</b>	<b>81</b>
5.1	Ultrathin permeable membranes as novel culture interface .....	81
5.2	Role of cellular complexity of the intestinal barrier <i>in vitro</i> .....	83
5.3	Potential of the perfused fish-gut-on-chip .....	83
	<b>Bibliography.....</b>	<b>85</b>
	<b>Glossary.....</b>	<b>99</b>
	<b>Curriculum Vitae CAROLIN DRIESCHNER .....</b>	<b>101</b>

# List of Figures

Figure 1.1 The cell as basic unit in ecotoxicology.....	2
Figure 1.2 General arrangement of the fish intestine. ....	4
Figure 1.3 The two-compartment model as applied for piscine intestinal cells. ....	7
Figure 1.4 Examples of human <i>in vitro</i> gut models from literature (2009-2016). ....	9
Figure 1.5 Porous substrates for cell culture application.....	11
Figure 1.6 Simplified equivalent circuit for impedance measurements.....	13
Figure 2.1 Ultrathin nanoporous alumina supports. ....	27
Figure 2.2 Pore size histograms of alumina membrane.....	28
Figure 2.3 Comparison of membrane permeability between commercial PET and custom made alumina membranes in the absence of cells. ....	29
Figure 2.4 Alumina membranes as cell culture interface for rainbow trout intestinal epithelial cells.....	30
Figure 2.5 Cell growth, polarization and epithelial resistance of rainbow trout intestinal epithelial cells (RTgutGC) cultured on alumina membranes.....	32
Figure 2.6 Impedance-based toxicity testing on mature epithelia.....	33
Figure 2.7 Al release from membranes and prevention. ....	35
Figure 3.1. Impedance spectra and corresponding phase angle analysis.....	49
Figure 3.2 General characterization of RTgutF cultured on conventional support. ....	53
Figure 3.3 Frequency dependent impedimetric monitoring for cultures on electric cell-substrate for impedance sensing (ECIS). ....	55
Figure 3.4 Mono- and co-cultures on ultrathin alumina membranes.....	57
Figure 4.1 Silicon nitride porous supports. ....	73
Figure 4.2. The fish-gut-on-chip model.....	74
Figure 4.3. Impact of shear stress on epithelial barrier organization.....	77
Figure 4.4. Co-culture of piscine intestinal epithelial (RTgutGC) and fibroblast (RTgutF) cell lines. ....	79

## Supplemental figures

Figure S 2.1 Fabrication process of ultrathin anodic aluminum oxide membranes.....	37
Figure S 2.2 Impedimetric characterization of RTgutGC cells grown on alumina supports. ....	37
Figure S 2.3 Membrane permeability of alumina versus commercial PET membrane.....	38
Figure S 2.4 Microscopy through alumina membrane.....	38
Figure S 2.5 Epithelial resistance of RTgutGC. ....	39
Figure S 3.1. Morphology of RTgutF cells at passage 3.....	60
Figure S 3.2 Relative telomerase activity of three fish- and one mammalian cell line. ....	61
Figure S 3.3 Expression of tight junction protein ZO-1 in RTgutF and RTgutGC cells. ....	62



# Chapter 1. Introduction

Epithelial barriers serve as gate keepers between different biological compartments or between an organism and its surrounding environment. A number of *in vitro* epithelial cell barrier models have been developed as alternatives to animal experiments to answer a range of questions relevant to biomedicine and human toxicology. In contrast, only one model has been established for the fish intestine with the intention to provide insights into uptake and defense mechanisms of chemicals and nanomaterials, to name one type of application (Minghetti *et al.* 2017). The long-term vision of such developments is the evaluation of risks or benefits of newly developed chemicals or products *in vitro* and accurately extrapolate the results to fish and ecosystem health before market release. Other applications of a fish intestinal model include physiological studies e.g. to better understand nutrient absorption and pathogen defense.

## 1.1 Scope

This thesis focuses on the refinement of the current *in vitro* fish intestinal barrier model by engineering an artificial microenvironment for intestinal cell lines derived from rainbow trout (*Oncorhynchus mykiss*) to better mimic realistic, biologically relevant exposure and transport phenomena. Herein, knowledge on physiological aspects of the fish intestine set the framework for the development of suitable cell culture micro-devices. Such devices should facilitate control of the cellular microenvironment with high spatial and temporal resolution and provide access and instrumentation for simple and fast evaluation of cellular parameters such as morphology, differentiation state and vitality. This introductory chapter aims to provide an overview of the use of fish cells in ecotoxicology, intestinal tissue architecture and physiology, current intestinal barrier models of fish, the principle of organ-mimicry on microchip format, micro-technological innovations for permeable cell culture supports and methods for evaluation of epithelial barrier properties with emphasis on non-invasive, real-time impedance spectroscopy.

## 1.2 Background

### 1.2.1 The potential of fish cells in ecotoxicology

Fish in large number serve as experimental animals for toxicity testing of chemicals and water samples. Fish are the most diverse group of vertebrates inhabiting the aquatic environment and as such are indicators of ecosystem health (Castano *et al.* 2003). In accordance with several legislations, such as the European legislation on the Registration, Evaluation, Authorization and Restriction of Chemicals (REACH), an increasing number of fish tests need to be performed for regulatory purposes to estimate the risk of new and existing chemical products. These tests include the evaluation of acute toxicity, chronic effects, effects on distinct developmental stages, reproduction and bioconcentration (Rovida and Hartung 2009). In order to conduct REACH in an ethically and financially acceptable manner, the European Commission encourages the development and application of alternative test strategies (Lilienblum *et al.* 2008). Herein, the attractiveness of fish cell lines is increasing thanks to recent achievements in, for example, predicting fish acute toxicity and fish growth using a rainbow trout gill cell line (Stadnicka *et al.* 2012, Tanneberger *et al.* 2012). Further, the establishment of cell lines from various tissues and species enable mechanistic investigations of the specific mode of action of a chemical, to extrapolate effects from the basic unit of life, the cell, to the whole organism (Figure 1.1) and finally to fish populations (Bols *et al.* 2005, Schirmer 2006, Bols *et al.* 2017).

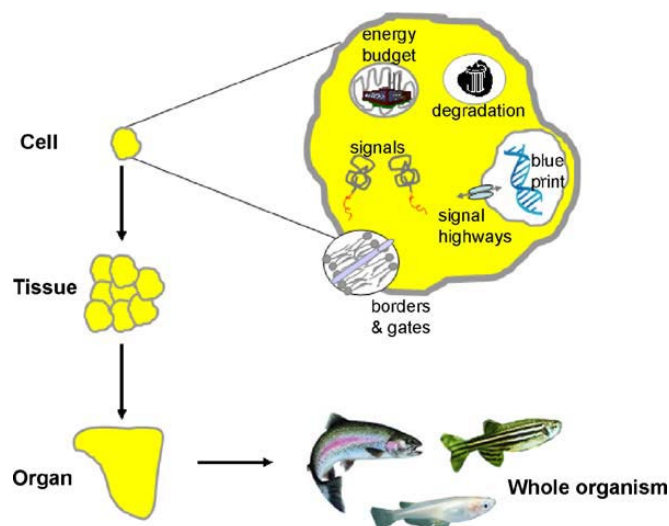


**Figure 1.1** The cell as basic unit in ecotoxicology.

Sensitive target sites within vertebrate cells allow for mechanistic investigations of chemical mode-of-action and extrapolation of impaired organ function and whole organism health. (Figure from Schirmer (2006))

One more recent development for broadening the use of fish, and specifically rainbow trout-derived cell lines, is the establishment of a cell line from the intestinal epithelium, RTgutGC (Kawano *et al.* 2011). By now, this cell line has undergone a basic characterization (Kawano *et al.* 2011), was used to establish the first fish intestinal barrier model (Geppert *et al.* 2016, Minghetti *et al.* 2017) and was recently applied in concert with rainbow trout gill and liver cells and a physiology-based model to accurately predict the bioconcentration of the polycyclic aromatic hydrocarbon, benzo(a)pyrene, in fish (Stadnicka-Michalak *et al.* 2018). It is this fish cell line which provided the impetus for the developments described in this thesis.

### 1.2.2 Key aspects of the fish intestine

The gastrointestinal tract (GIT) of fish is the location where ingested food and water is processed and absorbed through a single layer of specialized epithelial cells. The presence of microorganisms, with some being pathogenic, and natural or man-made, potentially toxic substances in the intestinal lumen pose a risk to fish health if these enter the circulation. The protective barrier of the intestinal epithelium, together with the associated immune system, acts as gate keeper by selectively allowing the trespass of water, nutrients and ions to maintain internal homeostasis and growth of the fish (Grosell *et al.* 2011, Jutfelt 2011).

In most fish, the GIT is organized in four main topographical regions with certain physiological functions: 1. Mouth and pharynx (headgut) represent the location for ingestion and mechanical processing of food; 2. Esophagus and stomach (foregut) are responsible for chemical digestion of food; 3. The intestine (midgut), accounting for the greatest proportion of the GIT due to its length, is involved in further chemical digestion and absorption of the nutrients; 4. Final section of the intestine including the rectum (hindgut) is mainly responsible for excretion of feces (Wilson and Castro 2010). A particular feature of fish compared to mammalian intestine is the pyloric caeca, which accounts for blind appendages attached to the anterior segments of the intestine to increase the total intestinal surface area (Figure 1.2 A) (Buddington and Diamond 1987). Further, the intestinal wall of fish is characterized by large, randomly shaped epithelial folds (Figure 1.2 B), which are proportionally larger than the finger-like intestinal villi of mammals (Wallace *et al.* 2005, Walton *et al.* 2018). Each fold is lined by a single layer of epithelial cells, called enterocytes (Figure 1.2 C). Stem cells are located at the base of each fold in the crypt region and allow the renewal of the intestinal epithelium. However, this process is much slower in fish compared to mammals, thus, fish enterocytes can remain on the intestinal fold for weeks compared to a few day lifespan of mammalian enterocytes (Buddington *et al.* 1997).

The intestinal epithelium marks the border between the outside (lumen) and inside (tissue) of the animal. On the intestinal lumen facing side (apical), enterocytes are exposed to rather rough conditions, including mechanical forces from fluid flow, bacterial colonization and osmotic changes. Their duty in absorbing nutrients while maintaining barrier function led to the evolution of distinct morphological and functional features. Enterocytes are long and narrow in shape and organized in a densely packed cell layer (Figure 1.2 D). On their apical side, they are characterized by microscopic membrane protrusions, called microvilli, which increase the cellular surface area to allow sufficient nutrient uptake. Further, barrier function is maintained by the formation of adhesive and tight junction proteins, which keep the cell membrane of adjacent cells in close contact and reduce the diffusion through the paracellular space (Figure 1.2 E) (Lokka *et al.* 2013). Despite this physical barrier, the epithelium allows the trespass of numerous substances and particles through active and passive transport mechanisms. Ions and hydrophilic nutrients are generally taken up by membrane-bound transporter proteins, larger molecules, particles, bacteria and virus are translocated via endocytosis at the apical membrane and exocytosis at the basolateral. In contrast, small hydrophilic molecules diffuse through tight junctions and the paracellular space. Lipophilic substances are thought to passively enter through cell membranes (Jutfelt 2011). On the organism facing side (basolateral), enterocytes are attached to the basement membrane, which is a thin layer (50 – 100 nm) of specialized extracellular matrix proteins. The basement membrane separates epithelial cells from the underlying connective tissue, which is composed of mainly fibroblasts secreting growth factors and extracellular matrix proteins (Figure 1.2 C) (Kalluri 2003, Kruegel and Miosge 2010). The interaction of these cell types is essential for fast wound healing after lesions in the intestinal epithelium and expected to be crucial for enterocyte polarization and differentiation (Simon-Assmann *et al.* 1988).

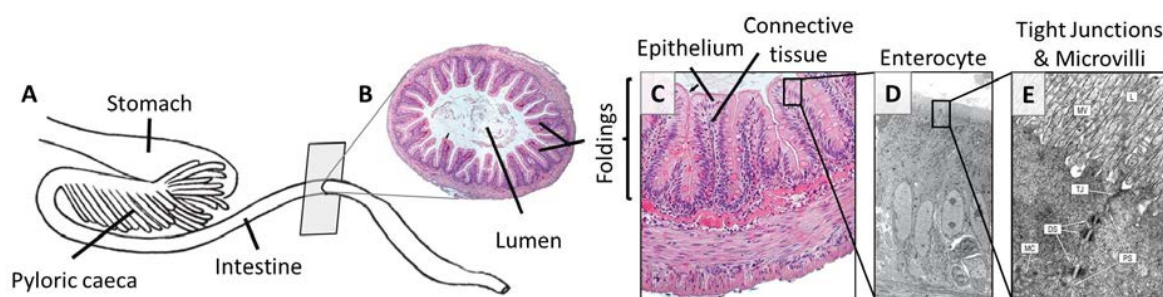


**Figure 1.2** General arrangement of the fish intestine.

(A) Schematic drawing of the gastrointestinal tract. (B) Eosin-hematoxylin staining of cross-section of the proximal intestine. (C) Eosin-hematoxylin staining of intestinal foldings. (D) Transmission electron microscopy of enterocytes and (E) enlargement of the apical part of the cell with lumen (L), intestinal microvilli (MV), tight junctions (TJ), desmosomes (DS), paracellular space (PS) and mitochondria (MC) (Modified from Lokka *et al.* (2013) and Jutfelt (2011)).

Research on the piscine intestinal epithelium has long been limited due to a lack of an adequate model system. In the following, models for the fish gut will be discussed in more detail with emphasis on rainbow trout (*Oncorhynchus mykiss*) as representative for freshwater fish in the Northern Hemisphere. Indeed, rainbow trout is widely used in science (fish physiology, pathology and ecology), regulation (ecotoxicology) and commerce (aquaculture, sport fishing).

### 1.2.3 Piscine intestinal models

Current intestinal barrier models of fish can be divided into *in vivo*, *ex vivo* and *in vitro* systems. These systems provide different levels of complexity and can be used to unravel the physiological and toxicological processes occurring within the intestine.

Experiments with fish (*in vivo*) can rely on fully developed and functional intestinal epithelia. However, accessibility of the fish intestine is rather restricted and these experiments involve resource intensive animal experiments that are often difficult to interpret and repeat because of the organism's complexity and inter-individual and species variability. Moreover, quantification of effects is definitive, i.e. the animal needs to be killed (James *et al.* 1997).

*Ex vivo* models are good alternatives, as they are characterized by their controlled environment. As such, isolated intestinal segments or gut-sac preparations have been adopted for various physiological and toxicological studies. In these isolated tissues, the original structure is largely maintained. However, preparations can only be used for short term experiments and only few experimental conditions can be tested per fish (Ojo and Wood 2007, Kwong and Niyogi 2008).

*In vitro* models are known for their simplicity and reproducibility, thereby enabling fast or even high-throughput studies. Experiments can be performed with either freshly isolated primary cells or established cell lines. Freshly isolated cells from the intestinal epithelium have been used for a variety of uptake (Kwong and Niyogi 2012), immunological (Komatsu *et al.* 2009) and molecular (Kwong *et al.* 2010) studies in order to characterize mechanisms and processes directly on the level of the cell without luminal or systemic inference. The isolated cells largely maintain cellular function e.g. active and passive transport processes despite the loss of their cell-to-cell structure. Notwithstanding, cells might be stressed from the isolation process. Moreover, their viability and longevity is a limiting factor that varies with different isolation methods; as well, animals are still required for each new batch of experiments.

The isolation and extended culture of rainbow trout intestinal epithelial cells from tissue sections of the hindgut finally resulted in the successful development of the RTgutGC (Rainbow Trout gut Germany Canada) cell line (Kawano *et al.* 2011). To date, RTgutGC is the best characterized and most studied piscine intestinal cell line for toxicological and dietary studies (Schmitt *et al.* 2015, Minghetti and Schirmer 2016, Langan *et al.* 2017). It can be assumed to be continuous, as it has been cryopreserved and passaged over several years (Kawano *et al.* 2011). Like enterocytes *in vivo*, the cells form confluent monolayers on the culture substrate and feature xenobiotic metabolism, indicated by the recently shown induction of the phase I biotransformation enzyme, cytochrome P<sub>450</sub> (Cyp1A) activity, by benzo(a)pyrene (Stadnicka-Michalak *et al.* 2018). Moreover, cells express multi-xenobiotic resistance transporters (Fischer *et al.* 2011) which function to efflux unmodified and/or biotransformed chemicals out of cells. These features are essential for a functional enterocyte model to follow the fate (uptake and detoxification) of hazardous substances present in the fish diet.

Based on this fish intestinal cell line, a protocol for culturing RTgutGC cells as monolayer in a two-compartment system using commercial cell culture inserts was established (Geppert *et al.* 2016, Minghetti *et al.* 2017) (Figure 1.3 A). The inserts are placed in common cell culture plates and allow the growth of cells on a permeable membrane, to face an upper (apical) and a lower (basolateral) compartment (Figure 1.3 B) (Geppert *et al.* 2016). The apical chamber mimics the gut lumen and can be filled with a physiological buffer, such as L-15/ex (Schirmer *et al.* 1997). The basolateral chamber represents the blood supply and is filled with culture medium supplemented with e.g. fetal bovine serum (FBS; L-15/FBS). Under these conditions, RTgutGC cells have been shown to form a polarized epithelial monolayer with apical expression of the tight junction protein Zonula Occludens-1 (ZO-1). Moreover, the trans-epithelial electrical resistance (TEER), a measure of barrier tightness (see section below) is comparable to values of freshly isolated gut segments of Atlantic Salmon (*Salmon salar*) (Sundell *et al.* 2003, Geppert *et al.* 2016, Minghetti *et al.* 2017). Further, Geppert *et al.* (2016) demonstrated the suitability of the RTgutGC barrier model for investigating nanoparticle transport across the intestinal epithelium.

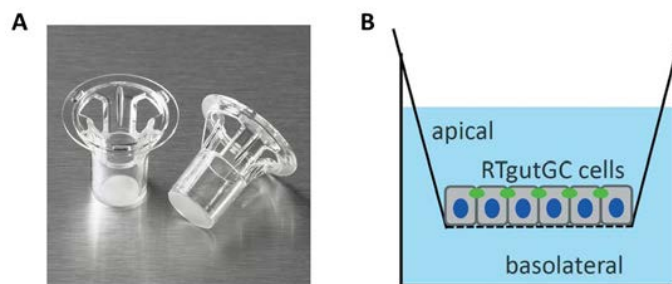


**Figure 1.3** The two-compartment model as applied for piscine intestinal cells.

(A) Photograph of commercial inserts. (From [www.sbtssl.com](http://www.sbtssl.com)). (B) Schematic drawing of an insert with RTgutGC cells cultured on the porous membrane. (Adopted from Geppert *et al.* (2016))

The static insert system with the commercially available permeable membranes constitutes the most frequently used cell culture system to mimic the natural environment of barrier forming cells, mainly from human origin, e.g. from intestine (Hubatsch *et al.* 2007), lung (Pariselli *et al.* 2009), or brain (Kenzaoui *et al.* 2012) tissue. However, these simplified models lack physiologically relevant features and mechanical stimulation, which are known to modulate cell morphology and function (van der Meer and van den Berg 2012).

#### 1.2.4 The pioneers: human gut-on-chip devices

A new type of cell-based *in vitro* models, called “organs-on-chips”, seems promising to solve at least some of the short-comings of the current *in vitro* systems by artificially engineering a more physiologically realistic microenvironment for cells (Esch *et al.* 2011, Huh *et al.* 2012b, van der Meer and van den Berg 2012). Herein, microfabrication, initially developed for the electronic industry, has created tremendous opportunities to restructure geometric aspects of the cells’ natural surrounding (Falconnet *et al.* 2006) and to apply instrumentation for precise cell manipulation (Dao *et al.* 2003) and surveillance (Curtis *et al.* 2009). The associated microfluidic technology enables unprecedented capabilities to control the cellular microenvironment with high spatial and temporal resolution, thus it can be used to expose cells to mechanical and biochemical signals in a physiologically relevant context (Griep *et al.* 2013). The combination of cells and engineering in organ-on-chip devices has led to the creation of functional human tissue units from lung (Huh *et al.* 2010), liver (van Midwoud *et al.* 2011), gut (Kim *et al.* 2012), brain (Kunze *et al.* 2011) and kidney (Jang and Suh 2010). Primary aims were to improve preclinical drug development and unravel underlying mechanisms of distinct diseases. Among those tissue models, recently developed human gut-on-chips are a great source of inspiration for further innovations and adaptations to other cell sources e.g. from fish, to broaden their application to research areas such as environmental toxicology, animal physiology and

aquaculture. Therefore, design parameters and innovations in the 3D recapitulation of this unique organ will be highlighted below.

The current gut-on-chip devices adopt the two-compartment principal of insert systems by introducing fluid filled micro-channels on each side of the membrane (Figure 1.4 A). Most commonly these types of chips are fabricated by fixing a semi-permeable plastic membrane composed of e.g. polyethylene terephthalate or polycarbonate between two pre-structured sheets of polydimethylsiloxane (PDMS) (Imura *et al.* 2009). One gut-on-chip device is additionally capable of generating peristalsis-like motions via a stretchable PDMS membrane as culture surface, thereby the motion is regulated by peripheral vacuum chambers (Kim *et al.* 2012) (Figure 1.4 B). The intestinal microbiota plays a pivotal role in human health and disease (von Martels *et al.* 2017); therefore, one design integrated an additional compartment for bacterial colonization (3-compartment system) in a microfluidic bioreactor, where bacteria are separated from intestinal cells by a nanoporous membrane (Shah *et al.* 2016) (Figure 1.4 C). The first artificial intestinal tract that can be opened for simplified analysis of the inner tube after drug exposure was developed by Konishi *et al.* (2015) (Figure 1.4 D). As well, the recreation of the 3D topography of the intestine is advancing (Yu *et al.* 2014). An example is a 3D membrane for intestinal villi recapitulation that might be integrated in microfluidic devices in the future (Figure 1.4 E) (Esch *et al.* 2012). The crypt region is the physiological counterpart to the villus. It shelters stem cells at its basis and is of great importance for cancer research (Zeuner *et al.* 2014). Microstructures composed of PDMS micro-wells and matrigel micropockets successfully guided isolated primary crypts to form a 2D/3D hybrid culture with distinct proliferative and non-proliferative zones (Figure 1.4 F) (Wang *et al.* 2014).

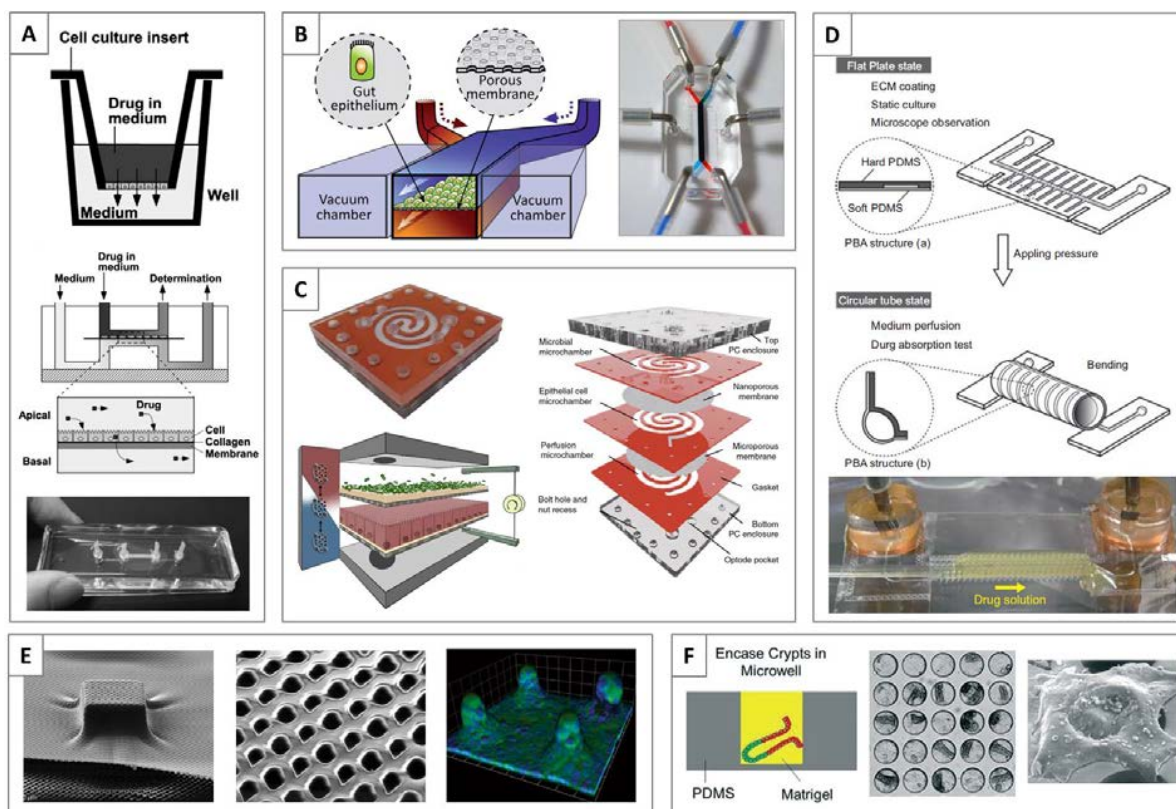


Figure 1.4 Examples of human *in vitro* gut models from literature (2009-2016).

(A) Microfluidic system to evaluate intestinal absorption (from Imura *et al.* (2009)). (B) Human-gut-on-chip that experiences intestinal peristalsis-like motions and flow (from Kim *et al.* (2012)). (C) Microfluidic-based model of the gastrointestinal human-microbe interface (from Shah *et al.* (2016)). (D) Openable artificial intestinal tract for drug evaluation (from Konishi *et al.* (2015)). (E) On chip 3D porous membrane to mimic intestinal villi (from Esch *et al.* (2012)). (F) Generation of colonic epithelium guided by microstructures (from Wang *et al.* (2014)).

All these models are pioneers for the recreation of a more physiological realistic intestinal microenvironment. However, further innovations are desirable to enhance their applicability for drug and toxicant absorption studies and physiological investigations. The first main improvement needs to occur with regard to the permeable culture surface, which currently represents a major limitation for permeation due to its relative thickness and low porosity (Jud *et al.* 2015, Geppert *et al.* 2016) (see following section, 1.2.5). Secondly, the measure of barrier tightness presents a fundamental parameter for epithelial barrier functionality and requires new concepts for the integration of adequate sensors into microfluidic channels and analysis of obtained data (see section 1.2.6).

### 1.2.5 Recreation of an artificial basement membrane

*In vivo*, epithelial cells are anchored to the basement membrane, a network of fibrous proteins that act as mechanical support without hampering cellular transport processes (Kalluri 2003). For cell

culture, the ideal membrane would feature basement membrane characteristics by being very thin and highly permeable to allow realistic transport phenomena. In addition, membranes should be robust for simplified handling, transparent to enable cell observation and cheap to fabricate. However, standard cell culture membranes can only compete with their robustness and established, low-cost manufacturing processes though being a rather poor reflection of the basement membrane (Figure 1.5 A). Progress in micro-technology led to the development of ultrathin membranes of  $1\ \mu\text{m}$  or less in thickness by conventional cleanroom fabrication processes (Kuiper *et al.* 1998, Striemer *et al.* 2007). Herein, silicon is the most commonly used substrate for membrane fabrication, because of its simple, highly controllable and scalable manufacturing. Two types of ultrathin permeable supports, realized in silicon chips, have been adopted for cell culture application.

The first type of membranes are composed of a thin layer of silicon nitride (SiN), which is deposited by low pressure chemical vapor deposition on silicon wafer. Pore patterning is achieved by photolithography to obtain pore sizes in the micrometer range (Kuiper *et al.* 1998). Thus far, SiN membranes have been successfully used for co-culture models to reconstruct the blood-brain barrier (Ma *et al.* 2005, Kenzaoui *et al.* 2012) and alveolar barrier (Jud *et al.* 2015) by culturing cells on opposite membrane sides (Figure 1.5 B). This membrane type is transparent with a golden glimmer from silicon nitride films and facilitates nanoparticle and cell translocation because pore sizes are appropriately large. Membranes are costly but already commercially available within the traditional insert format (<http://simplinext.com>). Fabrication of membranes with nanoscale pore diameters is possible but requires more elaborate techniques such as laser interference lithography (Kuiper *et al.* 1998) or focused ion beam drilling (Tong *et al.* 2004). Membrane thickness is typically 500 nm for a square membrane with an area of  $1\ \text{mm}^2$  (Jud *et al.* 2015). Size can be further tuned down but diminishes the stable membrane size.

The second type of membrane consists of nano-crystalline silicon. Membranes are fabricated by a rapid thermal annealing step of a three-layer film stack of  $\text{SiO}_2$  / amorphous silicon /  $\text{SiO}_2$  on silicon wafer, which results in the formation of porous nano-crystalline silicon (pnc-Si). The membranes are characterized by nanoscale pores with diameters from 5-100 nm, which allow size-dependent separation of biomolecules and but also nanoparticles of appropriate size (Striemer *et al.* 2007, Gaborski *et al.* 2010). Pnc-Si membranes have proven biocompatible (Agrawal *et al.* 2010) and able to support *in vivo* like behaviour of endothelial cells (Figure 1.5 C) (Nehilla *et al.* 2014). This transparent membrane has a fixed thickness of only  $\sim 15\ \text{nm}$ , but membrane area in turn is very limited to  $\sim 0.04\ \text{mm}^2$  for square membranes (Striemer *et al.* 2007).

A potential material for the creation of a third type of ultrathin membrane for barrier-forming cells is anodized aluminium oxide (AAO). The anodization process, which is an electrochemical reaction, leads to a self-ordering pore formation on the exposed metal surface. This is an inexpensive, highly controllable process. Pore sizes can be tuned in a range of 10-400 nm, depending on applied voltage and utilized electrolyte during anodization. Furthermore, AAO is characterized by regular pore distribution and small inter-pore distances of only 50-600 nm. For these reasons, AAO is a popular nanomaterial with applications in numerous areas including molecular separation, photonics and drug delivery (Poinern *et al.* 2011, Jani *et al.* 2013). Cell culture studies on AAO were conducted recently, proving its biocompatibility (Hoess *et al.* 2007, Parkinson *et al.* 2009, Hoess *et al.* 2010, Bruggemann 2013). Ultrathin AAO membranes are not yet established as cell culture interface. However, Wu *et al.* (2012) developed the fabrication process for an ultrathin AAO diode membrane to actively control the transport of ions (Figure 1.5 D), which can be further adapted to permit the reconstruction of an epithelial barrier on this type of membrane.

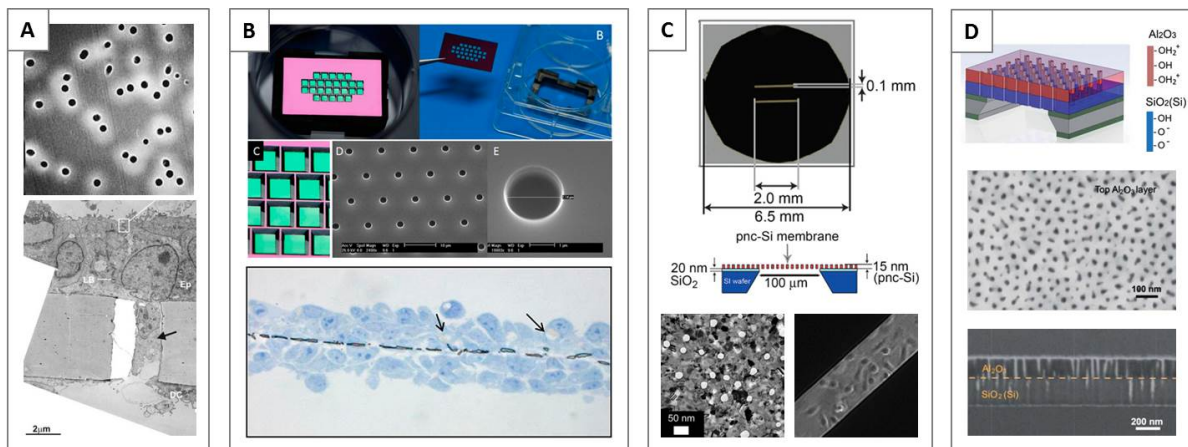


**Figure 1.5** Porous substrates for cell culture application.

(A) Commercial insert membrane composed of polycarbonate (from Angeloni Suter *et al.* (2011)). (B) Silicon nitride membrane (from Kenzaoui *et al.* (2012)). (C) Porous nanocrystalline silicon membrane (from Agrawal *et al.* (2010)). (D) Nanofluidic diode membrane composed of anodic aluminum oxide and  $\text{SiO}_2$  (from Wu *et al.* (2012)).

Aside from their great potential to generate realistic, cell-based barrier models, ultrathin membranes will also improve the evaluation of barrier functionality by microscopy of cells on these highly transparent substrates and by increasing measure sensitivity of the trans-epithelial electrical resistance (TEER) because the resistance of the permeable culture interface is decreased (see section 1.2.6).

### 1.2.6 Impedance based monitoring of barrier function

Evaluating barrier properties of *in vitro* models of the gut plays an essential role to define tightness and robustness of the intestinal epithelial layer (Le Ferrec *et al.* 2001). One frequently used method is the evaluation of trans-epithelial electrical resistance (TEER) to determine barrier tightness brought about by the formation of tight and adhesive junctions (Benson *et al.* 2013). It is a simple, non-invasive and real-time measurement, preferably used prior to more labor intensive permeability assays with fluorescently labelled molecules or endpoint-based methods such as immunocytochemical staining of tight junctions. TEER measurements are based on determining ohmic resistance or impedance by placing two electrodes on each side of a cell layer grown on a permeable membrane. For TEER measurements generally a direct current (DC) voltage ( $U$ ) is applied to the electrodes and the resulting current ( $I$ ) then allows to calculate the ohmic resistance ( $R$ ) based on Ohm's law ( $R = U / I$ ). However, DC currents can damage both the cells and electrodes. To avoid this issue, an alternating current (AC) voltage square wave with a frequency of 12.5 Hz is applied in the widely used Epithelial Voltmeter (EVOM) for TEER determination of cells cultured in inserts (www.wpi-europe.com). The resistance of the cell monolayer ( $R_{TISSUE}$ ) is obtained by subtracting the ohmic resistance of the blank (membrane without cells;  $R_{BLANK}$ ) from the resistance of the cell layer grown on the permeable membrane ( $R_{TOTAL}$ ). TEER values are typically normalized to  $\Omega * \text{cm}^2$  by multiplying the resistance of the cellular monolayer with the culture area ( $A$ ) (Equation 1.1). The obtained normalized TEER values are independent of the used porous membrane and culture area and can be compared across platforms (Srinivasan *et al.* 2015).

$$TEER = (R_{TOTAL} - R_{BLANK}) * A \quad \text{Equation 1.1}$$

For impedance based TEER evaluation, an applied AC signal is swept over a frequency range and the amplitude and phase response of the resulting current is measured. Impedance ( $Z$ ) is defined as the relation of a potential voltage drop ( $\Delta V$ ) to the applied current ( $I$ ) (Equation 1.2).

$$Z = \frac{\Delta V}{I} \quad \text{Equation 1.2}$$

The resulting impedance contains information not only about the resistive character of the cell layer (i.e., TEER) but the capacitive behavior of the cell membrane is also included (Figure 1.6).

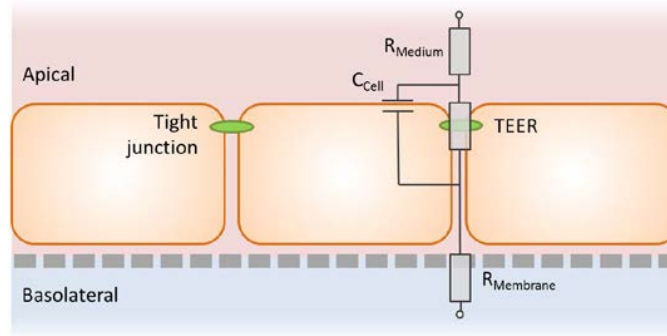


**Figure 1.6** Simplified equivalent circuit for impedance measurements.

This model accounts for an epithelial monolayer cultured on a permeable membrane. R represents resistors and C represents capacitors.

The complex quantity of resistive and capacitive contributions are frequency dependent. At low frequency, the lipid bilayer, forming the cell membrane, acts as insulator between the electrically conductive culture medium and cytoplasm and thus TEER can be retrieved from measured impedance values by applying Equation 1.1. The low frequency range is limited by the influence of the electrode-electrolyte interface at very low frequencies and by the membrane relaxation process, which takes place at higher frequencies (Heileman *et al.* 2013). Typically this range is below 100 kHz. At high frequencies, generally above 100 kHz, the lipid bilayer is short-circuited (cell membrane is relaxed) and cellular content has an effect on impedance (Günzel *et al.* 2012, Heileman *et al.* 2013, Xu *et al.* 2016). The contribution of the intracellular matter is less dominant, but measurable when cells are directly cultured on electrode containing solid substrate (Meissner *et al.* 2011). For cells cultured on permeable membranes and not being in direct contact with electrodes, the sensitivity of the measurement is too low and only the resistance of the culture medium is obtained (van der Helm 2018).

## 1.3 Research strategy

### 1.3.1 Problem definition

Summarizing the state of the art of cell-based intestinal barrier models of fish and human, it can be stated that recreation of the intestinal microenvironment *in vitro* is an essential undertaking to better mimic the functionality of the intestinal epithelium *in vivo* and thus enable reliability and accuracy of obtained experimental data e.g. for chemical risk assessment. However, the standard of current barrier models are conventional inserts, where a single cell type (such as enterocytes) is cultured on a several micrometer thick semi-permeable membrane under static conditions. Associated problems with this system include diminished or blocked transport between the lumen and blood constituting compartments and that cells may remain in a rather undifferentiated state due to a lack of physiological and mechanical stimulation. In light of this, the overall aim of the thesis was to apply the concept of organs-on-chips by combining key elements of piscine intestinal architecture and physiology within an artificially engineered microsystem housing rainbow trout intestinal cells. This system will be referred to as fish-gut-on-chip.

### 1.3.2 Research objectives

The development of the first fish-gut-on-chip was sub-divided into three main objectives. The first involved the creation of an artificial basement membrane analogue as physiologically realistic cell culture interface based on microfabrication technology. The second included the combination of epithelial cells and cells of a supporting lamina, namely fibroblasts, on the newly developed membranes to allow for cellular crosstalk. The third objective focused on the application of mechanical forces by fluid flow on the epithelial interface as found *in vivo*. The study was performed with the well-established epithelial intestinal cell line RTgutGC and recently initiated fibroblast intestinal cell cultures.

The conducted steps can be summarized as follows:

- Step 1.** Development of an ultrathin, highly permeable membrane
- Step 2.** Establishment and characterization of an intestinal fibroblast cell line
- Step 3.** Co-culture of epithelial cells and fibroblasts
- Step 4.** Engineering of a microfluidic bioreactor and shear stress application

### 1.3.3 Thesis structure

The results of the conducted research are presented in three experimental chapters and summarized and reflected in light of future research steps in a final chapter. A brief introduction to each experimental chapter is given below.

#### **Chapter 2 (Step 1): Ultrathin alumina membranes as scaffold for epithelial cell culture from the intestine of rainbow trout.**

Conventional cell culture membranes for initiation of *in vitro* barrier models hamper realistic permeation among compartments and visual inspection of cells by microscopy as well as sensitive TEER evaluation. This chapter describes the development of ultrathin and highly permeable membranes composed of nanoporous aluminium oxide and the interaction with epithelial RTgutGC cells. It was found that these membranes allow for fast diffusion of small molecules and encourage the formation of a polarized cell layer with apical tight junction formation and a measurable electrical resistance.

#### **Chapter 3 (Step 2 & 3): Reassembly of the epithelial-mesenchymal interface of the fish intestine *in vitro*.**

The interaction of epithelial cells with its underlying mesenchymal tissue, mainly composed of fibroblasts, is expected to be essential for a proper intestinal barrier development. In this chapter the establishment and characterization of a fibroblast cell line from the intestine of rainbow trout, and its interaction with epithelial RTgutGC cells, are described. The co-culture initiation on previously developed ultrathin nanoporous alumina membranes emphasized its utility in the recreation of a physiologically realistic intestinal barrier model and promoted improved barrier tightness, which was evaluated with TEER measurement.

#### **Chapter 4 (Step 1, 3 & 4): 'Fish-gut-on-chip': Development of a microfluidic bioreactor to study the role of the fish intestine as environment-organism barrier *in vitro*.**

In the intestinal microenvironment, epithelial cells lining the intestinal lumen, are exposed to fluid shear stress, which is known to alter barrier function. This chapter focused on the development of a microfluidic bioreactor with integrated ultrathin membranes composed of microporous silicon nitride membranes. Epithelial RTgutGC cells alone and in combination with supportive fibroblasts indeed adapted to realistic intestinal flow rates by increased barrier tightness as a measure of TEER.



## Chapter 2. Ultrathin alumina membranes as scaffold for epithelial cell culture from the intestine of rainbow trout (*Oncorhynchus mykiss*)

Permeable membranes are indispensable for *in vitro* epithelial barrier models. However, currently available polymer-based membranes are low in porosity and relatively thick, resulting in a limited permeability and unrealistic culture conditions. In this study, we developed an ultrathin, nanoporous alumina membrane as novel cell culture interface for vertebrate cells, with focus on the rainbow trout (*Oncorhynchus mykiss*) intestinal cell line RTgutGC. The new type of membrane is framed in a silicon chip for physical support and has a thickness of only 1  $\mu\text{m}$ , with a porosity of 15% and homogeneous nanopores ( $\text{\O} = 73 \pm 21 \text{ nm}$ ). Permeability rates for small molecules, namely Lucifer yellow, Dextran 40 and bovine serum albumin, exceeded those of standard polyethylene terephthalate (PET) membranes by up to 27 fold. With the final goal to establish a representative model of the fish intestine for environmental toxicology, we engineered a simple culture set-up, capable to test the cellular response towards chemical exposure. Herein, cells were cultured in a monolayer on the alumina membranes and formed a polarized epithelium with apical expression of the tight junction protein ZO-1 within 14 days. Impedance spectroscopy, a non-invasive and real time electrical measurement, was used to determine cellular resistance during epithelial layer formation and chemical exposure to evaluate barrier functionality. Resistance values during epithelial development revealed different stages of epithelial maturity and were comparable with the *in vivo* situation. During chemical exposure, cellular resistance changed immediately, when barrier tightness or cell viability was affected. Thus, our study demonstrates nanoporous alumina membranes as promising novel interface for alternative *in vitro* approaches, capable to allow cell culture in a physiologically realistic manner and to enable high quality microscopy and sensitive measurement of cellular resistance.

*Carolin Drieschner, Matteo Minghetti, Songmei Wu, Philippe Renaud, Kristin Schirmer*

This Chapter is mainly based on the paper:

Drieschner, C., Minghetti, M., Wu, S., Renaud, P. and Schirmer, K. (2017) 'Ultrathin Alumina Membranes as Scaffold for Epithelial Cell Culture from the Intestine of Rainbow Trout', ACS Appl Mater Interfaces, 9(11), 9496-9505.

## 2.1 Introduction

Fish play an important role in environmental toxicology to assess the risk of chemicals potentially released into the aquatic environment and to test the quality of effluent samples (Leeuwen 2007, Dempsey 2016). Alternative approaches to reduce the number of required fish and to prevent ethically questionable and expensive animal experimentation, include the use of primary cells and fish cell lines (Bols *et al.* 2005, Schirmer 2006, Minghetti *et al.* 2014). Like in human toxicology, a goal is to establish realistic tissue models in order to predict organ specific interactions of hazardous substances and to understand systemic effects (Marx 2012).

Organ-on-chip devices play a key role in the development of novel, physiologically realistic *in vitro* systems. Moreover, the connection of these miniaturized organ analogues on a microfluidic platform allows to combine different cell types to a human-on-a-chip bioreactor (Esch *et al.* 2011, Huh *et al.* 2012a, van der Meer and van den Berg 2012, Bhatia and Ingber 2014). In our research we envision a similar development to achieve a fish-on-a-chip.

The cornerstone of each organ-on-chip device is set by microtechnological innovations. In this paper we focus on the improvement of permeable membrane systems useful for epithelial cell cultures, such as the RTgutGC cell line, established from the intestine of rainbow trout (*Onchorynchus mykiss*) (Kawano *et al.* 2011). With the fish intestine being a major organ for chemical absorption from the diet and partially from water (Streit 1998, Kelly *et al.* 2004), an adequate *in vitro* system will allow to obtain insights in chemical uptake and defense mechanisms. Moreover, it will contribute to knowledge expansion for this hardly accessible organ, useful for fish physiology and aquaculture.

*In vivo*, epithelial cells are underlined by the delicate basement membrane, which separates them from the underlying tissue. The basement membrane is only a few hundred nanometer thick, elastic with a 3 dimensional shape and highly permeable (LeBleu *et al.* 2007). In contrast, conventionally used porous polyethylene terephthalate (PET) and polyester (PE) membranes for epithelial tissue models are stiff, several micrometer thick and low in porosity, certainly influencing cell behavior, translocation of soluble factors, particles and chemicals (Kenzaoui *et al.* 2012, Geppert *et al.* 2016). Fabrication of an ultrathin, highly permeable and formable artificial membrane was not yet demonstrated and remains a futuristic goal. Therefore, current customized membranes focus on the improvement of one or a combination of two features of natural basement membranes. For example, the first stretchable membrane, composed of polydimethylsiloxane (PDMS), was introduced by Huh *et al.* (2010) and incorporated in a human-lung-on-a-chip (Huh *et al.* 2010) and human-gut-on-a-chip (Kim *et al.* 2012, Kim and Ingber 2013) microfluidic bioreactor, allowing to

simulate breathing or peristaltic motions. Another outstanding innovation is the development of 3-dimensional membranes made of the photoresist SU-8, with the geometry of human intestinal villi, to mimic key aspects of the intestinal epithelium (Esch *et al.* 2012). However, both types of membranes cannot compete with the thinness and sponginess of the natural basement membrane.

Owing to the development of advanced micro- and nanotechnologies, several ultrathin porous membranes have recently been fabricated for cell culture applications. Typically, these membranes are integrated in silicon chips due to their fabrication process and for mechanical support. Until now, membrane materials include silicon nitride ( $\text{SiN}_x$ ) and porous nanocrystalline silicon (pnc-Si). Experiments with pnc-Si provide information on biocompatibility and cell behavior (Agrawal *et al.* 2010). With porous  $\text{SiN}_x$  membranes, complex tissue models of brain and lung have been established (Harris and Shuler 2003, Ma *et al.* 2005, Kenzaoui *et al.* 2013, Jud *et al.* 2015).

In search for novel, biocompatible materials and simple, inexpensive fabrication techniques for ultrathin membranes, we here present the development of nanoporous aluminum oxide as unique interface for epithelial intestinal cells from rainbow trout. The anodization of aluminum, resulting in a highly ordered, nanoporous structure, is a well-known, low-cost and reproducible process (Poinern *et al.* 2011). We applied this process to very thin aluminum layers, to obtain optically transparent and mechanically robust permeable membranes. The membranes are integrated in silicon chips and have a thickness of only  $1\ \mu\text{m}$  and pore sizes in the nanometer range. A customized set-up for standard cell culture multi-well plates was designed to facilitate culturing of RTgutGC cells on chip. Microscopic monitoring of the cells reinsured the materials biocompatibility and revealed an epithelial layer formation in a physiological manner. To further validate the system, we exposed the artificial intestinal epithelium to chemicals and examined barrier integrity using cell-based impedance spectroscopy (Brennan *et al.* 2012) as non-invasive and real time monitoring tool.

## 2.2 Material and methods

### Fabrication of nanoporous alumina membranes

Ultrathin alumina membranes were fabricated using standard microfabrication technology. The process flow is depicted in Figure S 2.1 (see supplemental material). Briefly, 200 nm of low stress silicon nitride (SiN<sub>x</sub>) was deposited on both sides of a 380 μm thick silicon wafer by low pressure chemical vapor deposition (LPCVD). The LPCVD was performed in a dedicated furnace, where the SiN<sub>x</sub> is formed by a gas flow of dichlorosilane (SiH<sub>2</sub>Cl<sub>2</sub>) in presence of ammonia (NH<sub>3</sub>), at a temperature of 820-850°C. Photolithography and reactive ion etching (RIE) were used to pattern free-standing silicon nitride membrane arrays. Therefore, 300 μm of silicon were etched vertically with RIE from the wafers backside, followed by pyramidal chemical etching in potassium hydroxide (KOH) solution, to release free-standing SiN<sub>x</sub> membranes with a final size of 800 μm x 800 μm. SiN<sub>x</sub> membranes serve as supportive layer for future alumina membranes. Next, a 1 μm layer of aluminum (Al) was deposited on the SiN<sub>x</sub> film on the wafer's front side and then anodized in 6 wt% phosphoric acid by applying 100 V. To subsequently remove phosphoric acid residue, the anodized wafer was rinsed extensively with deionized water and dried under laminar flow. Finally, nanoporous alumina membranes were released by selective dry etching of the SiN<sub>x</sub> supportive layer from the wafers backside. Individual Si-chips of 9 mm x 9 mm were obtained upon manual cleavage along cleavage lines. Each chip is composed of a micro-well array of 21 equal sized nanoporous alumina membranes (800 μm x 800 μm), with a total membrane area of 13.44 mm<sup>2</sup>.

For membrane inspection and pore size analysis, scanning electron microscopy (SEM) images were taken randomly from independent anodization bates, using a Zeiss LEO 1550 scanning electron microscope. In addition, spatial inspection of pore size (center, top-, bottom-, right- and left corner) of the anodized wafer surface revealed no significant spatial pore size variation. The pore size and density was analyzed with a MATLAB script ("pore-analyzer"), kindly provided by Stefano Varricchio from microsystems laboratory 4 (LMIS4) at EPFL, Lausanne, Switzerland.

### Experimental setup and chip preparation

Specifically designed plastic holders, made from 1 mm thick polymethyl methacrylate (PMMA) sheets (Jauslin Plexacryl sa, Switzerland), allowed the use of nanoporous alumina supports in standard 24-well cell culture plates (Greiner-bio-one, Germany) and ensured media availability from both membrane sides. In the following, this system is referred to as one-compartment system. It was used for cell culture establishment on alumina membranes and impedance based resistance

measurement of the epithelial cell layer. In addition, a second set-up was developed to perform permeability experiments in absence of cells for membrane characterization. For this set-up, Si-chips were glued (Loctite M-121HP Hysol Medical Device Epoxy Adhesive, Henkel, USA) to commercial inserts (ThinCert™ for 24 well plates, Greiner-bio-one, Germany) after PET membrane removal and placed in 24-well cell culture plates. This set-up creates an upper (apical) and lower (basolateral) compartment which are separated by the alumina membrane, creating a two-compartment system. Prior to usage, Si-chips, plastic holders and modified inserts were sterilized by incubation in 70° EtOH for 20 min and subsequent drying under a sterile bench.

### Permeability assay

Membrane permeability of cell-free nanoporous alumina membranes was assessed in the two-compartment system and compared to permeability of PET membranes (pore size = 0.4 µm; pore density =  $1 \times 10^6$  pores/cm<sup>2</sup>), which are integrated in the commercial insert system (ThinCert™ for 24 well plates, Greiner-bio-one, Germany). Two fluorescent dyes and one protein with different molecular sizes were used: Lucifer yellow (LY, molecular weight = 444.25 g/mol; Molecular Probes, Netherlands), dextran FD40 (FD40, molecular weight = 40 000 g/mol; Sigma Aldrich, Switzerland) and bovine serum albumin (BSA, molecular weight = 66 000 g/mol; Sigma Aldrich, Switzerland). Dyes or protein were dissolved in PBS to a final concentration of 50 µg/mL for LY, 1 mg/mL for FD40 and 200 µg/mL for BSA. Prior to experimentation, the chambers were filled with phosphate buffered saline (PBS) and incubated for two hours at 19°C. Working volumes were 400 µL for the apical chamber and 1.4 mL for the basolateral chamber. Thereafter, the apical (= donor) chamber was exchanged with the same volume of the previously prepared LY-, FD40- or BSA solutions and incubated for up to 24 hours at 19°C. For the fluorescent dyes LY and FD40, samples of 2x10 µL were withdrawn from the basolateral (= receiver) chamber after careful mixing at different time points during the 24 hours of the experiment. The aliquots were transferred to a 384 well plate (Greiner-bio-one, Germany) and the fluorescence was detected immediately using a multi-well plate reader (Tecan, Infinite M200, Switzerland) at the respective excitation and emission wavelengths (LY<sub>excitation/emission</sub> = 450/520 nm, FD40<sub>excitation/emission</sub> = 485/544 nm). After 24 hours (= end of experiment), a sample from the apical compartment was taken to verify the stability of the dye concentration in the apical compartment. The fluorescence data for LY, FD40 were transformed to the amount of permeated dye, based on appropriate standard curves. For BSA, 200 µL samples were only taken at the end of the experiment (24 hours) from the apical and basolateral chamber and protein content was analyzed by performing the modified Lowry protein assay (Thermo

Scientific, Switzerland). The apparent permeability  $P_{app}$  (cm/s) was calculated according to Equation 2.1 (Hubatsch *et al.* 2007).

$$P_{app} \left[ \frac{cm}{s} \right] = \frac{dQ}{dt} * \frac{1}{A * C_0} \quad \text{Equation 2.1}$$

With  $\frac{dQ}{dt}$  being the steady-state flux, A being the surface area of the membrane in  $cm^2$  and  $C_0$  being the initial concentration in the donor compartment.

### Cell culture

All experiments were performed with rainbow trout intestinal cells, RTgutGC (Kawano *et al.* 2011). For routine culture, RTgutGC cells were grown in complete medium (L-15/FBS), composed of Leibovitz L-15 medium (Invitrogen, Switzerland), supplemented with 5% fetal bovine serum (PAA; Switzerland) and 1% penicillin/streptomycin (GIBCO, Invitrogen, Switzerland). Cells were maintained at 19°C in the dark under normal atmosphere and culture medium was renewed once per week. Cells were split every one to two weeks, when reaching confluency of 80-90%, with trypsin (Sigma Aldrich, Switzerland) and sub-cultured in a 1:3 ratio in 75  $cm^2$  cell culture flasks (TPP, Switzerland). For experimentation, RTgutGC cells were grown on nanoporous alumina supports, which were integrated in a 24 well-plate on simple plastic holders (see above). For comparison, PET membranes, incorporated in commercially available transwell inserts (ThinCert™, 24-well, pore size 0.4  $\mu m$ , transparent; Greiner-bio-one, Germany), were used to represent a commonly used permeable cell culture interface. If not specified, the same protocols were applied to both, alumina and PET membranes. Prior to seeding, alumina and PET membranes were coated with 50  $\mu g/\mu L$  fibronectin (Roche, Germany) in PBS for two hours. Cells were seeded in L-15/FBS either at a low density of 20 000 cells/ $cm^2$  for individual cell observation or at a high density of 55 000 cells/ $cm^2$  for confluent cell layer formation. Two hours after cell seeding, media was changed to remove unattached cells in PET inserts. For alumina supports, the Si-chips were shortly washed in L-15/FBS and placed in a new well on top of the chip holder in fresh medium. Working volumes of cell culture medium were 1 mL for Si-chips on plastic holders, while transwell inserts were filled apically with 400  $\mu L$  and basolaterally with 1.4 mL. Cells were cultured for up to 28 days at 19°C and under normal atmosphere, with a media change every seven days.

### Scanning electron microscopy

Two preparation techniques were performed to obtain SEM images from the cell-alumina membrane interaction. For top-view images, RTgutGC cells were cultured on alumina membranes for 24 hours. Thereafter, cells were washed with PBS and fixed in 2.5% glutaraldehyde for one hour, followed by post fixation in 2% osmium tetroxide for one hour and block staining with 2% uranyl acetate for one hour with washing steps in between. Dehydration was performed in a graded series of 30, 50, 70, 90, and 100% ethanol, followed by twice water-free 100% ethanol, 30 min each. Then, alumina supports with cells were plunged into liquid nitrogen followed by freeze drying at -110°C, -100°C, -80°C, -70°C and +20°C for 30 min each step. The alumina supports with the dried cells were mounted on SEM aluminum stubs and sputter-coated with 5 nm of platinum. SEM images were recorded at 5 kV with a Zeiss Gemini 1530 FEG (Zeiss, Germany). For cross-section images, RTgutGC cells were cultured for two weeks on alumina supports. Sample preparation for fixation followed the same protocol as described for top-view images. After dehydration in increasing concentrations of ethanol, the alumina membrane with cells was impregnated first with 33% resin (EMbed 812, Electron Microscopy Science, USA) and then with 66% resin in water-free ethanol for one hour 30 min each. Thereafter, alumina support with cells was submerged in 100% resin twice for two hours each. All impregnation steps were performed at room temperature in small plastic dishes. The sample was completely submerged in the resin and then taken out of the resin bath. Excesses of resin was allowed to drain in an upright position for another one hour 30 min at room temperature. The sample was then transferred to the oven to be heated up slowly to 60 °C. Polymerization is allowed to take place for two days at 60 °C. The polymerized alumina support with cells was cooled to room temperature and directly mounted right-side-up onto SEM stubs with conductive carbon cement. The specimen was sputter coated with 6 nm platinum. In the focused ion beam (FIB)-SEM (FEI Helios 600i), the sample was screened with an electron beam at high accelerating voltage (30 kV) and imaged in the backscattered electron (BSE)-mode to select a region of interest. The sample was brought to a stage position, where electron beam and ion beam coincide (stage tilt at 52°) and a trench was milled with the FIB at 30 kV and 9.3 nA to open the sample. The resulting cross section was polished at an ion current of 2,5 nA and then imaged with an electron beam of 2 kV and 0,34 nA. Images were acquired in the BSE-mode at appropriate tilt correction and a dwell time of 30 μs. Neighboring images were merged to full panorama views.

### Light microscopy

Images were taken on a Nikon TMS inverted microscope with a Nikon Coolpix P6000 digital camera.

### Fluorescence microscopy

For immunohistochemical staining, cells were fixed with 3.7% paraformaldehyde (Invitrogen, Switzerland) in PBS for 10 min at room temperature. After washing in PBS, cells were permeabilized for 15 min with 0.2% Triton X-100 in PBS. After a further washing step with PBS containing 0.1% Triton X-100, cells were incubated in Image-iT (Invitrogen, Switzerland) for 30 min, rinsed with PBS and primary antibody for tight junction staining (Alexa Fluor-coupled ZO-1 antibody, Invitrogen, Switzerland) was applied overnight at 4°C at a concentration of 5 µg/ml in 0.5% goat serum and 0.05% Triton X-100 in PBS. The next day, cells were washed with 0.1% Triton X-100 in PBS. For f-actin staining, cells were incubated with FITC coupled phalloidin (1:100; Sigma-Aldrich, Switzerland) for one hour at room temperature. Subsequently, after washing in 0.1% Triton X-100 in PBS, samples were incubated with 10.9 µM DAPI (Invitrogen, Switzerland) in PBS for 5 min. After repeated washing in 0.1% Triton X-100 in PBS and PBS only, Si-chips were mounted on microscope slides using ProLong® Gold antifade reagent (Life Technology, United States) and analyzed on a Leica SP5 Laser Scanning Confocal Microscope (Leica, Switzerland).

### Impedance spectroscopy

Alumina membrane holding Si-chips and PET transwell inserts were placed in an Endohm-6-chamber (World Precision Instruments, Germany), which was connected to an impedance analyzer (Gamry Instruments, Germany). For Si-chips, a specific holder was designed to avoid direct contact of the chip with the basolateral electrode and to limit the sensing area to the region where cells were cultured on alumina membranes. This set-up resulted in 20% leakage of the electrical current. Impedance spectra were recorded from 1 to 300 000 Hz at an amplitude of 20 mV, with highest sensitivity at 1 500 Hz (see supplemental material, Figure S 2.2).

### Chemical exposure of epithelial cells

As proof of concept for the sensitivity of impedance measurements through alumina membranes, we performed two chemical exposure scenarios with RTgutGC formed epithelia. First, a short-term exposure of a barrier disrupting chemical and subsequent recovery was analyzed. Second, cells were continuously exposed to a barrier destructing chemical and monitored for 24 hours. Therefore, RTgutGC cells were cultured on nanoporous alumina supports until they reached impedance values of 60-70 ohms at 1500 Hz (minimum 14 days), as a qualify measure for barrier maturity. Prior to chemical treatment, cells were pre-equilibrated in L-15/ex for 30 min. L-15/ex is a simple buffer, preferably used for chemical exposure scenarios in fish cell lines (Dayeh *et al.* 2002, Tanneberger *et*

*al.* 2013). A schematic overview about the preparation of L15/ex has been shown elsewhere (Tanneberger *et al.* 2010). For the short-term exposure scenario, cells were treated for 5 min with 0.2 g/L ethylenediaminetetraacetic acid (EDTA, Sigma-Aldrich, Switzerland), known to effect tight junction tightness by sequestering  $\text{Ca}^{2+}$  via chelation. Thereafter, exposure medium was exchanged with L-15/ex to allow recovery. For the continuous exposure scenario, cells were treated with 20 mg/L sodium dodecyl sulphate (SDS, Sigma-Aldrich, Switzerland), an anionic surfactant used in many cleaning and hygiene products.

### **Atomic layer deposition of titanium**

We deposited a thin film of titanium on the Si-chips to prevent aluminum release from membranes. During the atomic layer deposition process,  $\text{TiCl}_4$  (precursor of  $\text{TiO}_2$ ) and  $\text{H}_2\text{O}$  were sequentially exposed as vapor at  $200^\circ\text{C}$ ; a final thickness of 2, 5 or 7 nm of  $\text{TiO}_2$  on the whole surface of the alumina membrane was obtained.

### **Metal analysis**

For determination of aluminum and titanium release from alumina and titanium coated (2, 5, or 7 nm) alumina membranes, we incubated the appropriate Si-chips in 1 mL L-15/FBS in the one-compartment system for seven days. Thereafter, medium was collected and diluted 1:10 in deionized water for high resolution inductively coupled plasma mass spectrometry (HR ICP MS, Element2, Thermo, Switzerland). The total aluminum mass was measured using isotope  $^{27}\text{Al}$ . The total titanium mass was measured using isotope  $^{47}\text{Ti}$  and  $^{49}\text{Ti}$ , due to calcium interference with the more sensitive and otherwise preferred isotope  $^{48}\text{Ti}$ . To control the reliability of quantification, water references (PlasmaCal 33 MS, SCP, Courtaboeuf, France) with a known aluminum and titanium content were measured. Aluminum speciation in L-15 medium was performed with visual MINTEQ version 3.0.

## 2.3 Results and discussion

The vast majority of current *in vitro* epithelial cell models relies on commercially available two-compartment insert systems, where epithelial cells are cultured on a polymer-based permeable membrane, dividing the system into an upper and a lower chamber. However, these membranes are several micrometer thick and often low in porosity. This almost certainly limits the translocation of molecules through the barrier system, affects epithelial architecture, influences microscopic imaging and restricts sensitive measurement of, e.g., changes in cellular resistance by trans-epithelial electrical resistance (TEER) or impedance monitoring.

### Characterization of alumina membranes

Ultrathin, nanoporous alumina membranes were developed with the aim to improve current epithelial barrier models, like that of the fish intestinal epithelium. The 1  $\mu\text{m}$  thick, transparent membranes are surrounded by a Si-chip for mechanical support (size: 9 mm x 9 mm) and arranged as array of 21 centered squares (Figure 2.1 A). Each membrane is 0.8 mm x 0.8 mm, yielding a total membrane area of 13.44 mm<sup>2</sup>. The silicon chip has a total thickness of 380  $\mu\text{m}$ . The membrane holding side (top side) is flat, while the bottom side is characterized by 21 micro wells, which were formed during the silicon etching process and terminate into the 21 free-standing membranes. For simple and reproducible cell culture application, the Si-chip is placed on top of specially designed plastic holders. These holders are compatible with common 24-well cell culture plates and allow for media availability from both sides of the alumina membranes (Figure 2.1 B). In this way, a one-compartment system is created, allowing to follow cell growth and epithelial barrier formation by microscopy and impedance spectroscopy. In addition, we generated a two-compartment system to perform permeability studies. For this purpose, the chip is attached to commercial insert holders (Figure 2.1 C) and placed in 24-well cell culture plates. For future applications, the chip could also be integrated in a different insert concept, which makes use e.g. of a clamping mechanism to facilitate mounting and unmounting of the chip (Jud *et al.* 2015). Moreover, chip design and membrane shape is flexible, and could be adapted for organ-on-chip applications. For example, a single elongated alumina membrane could build the permeable interface between an upper and a lower microfluidic channel within a PDMS based bioreactor.

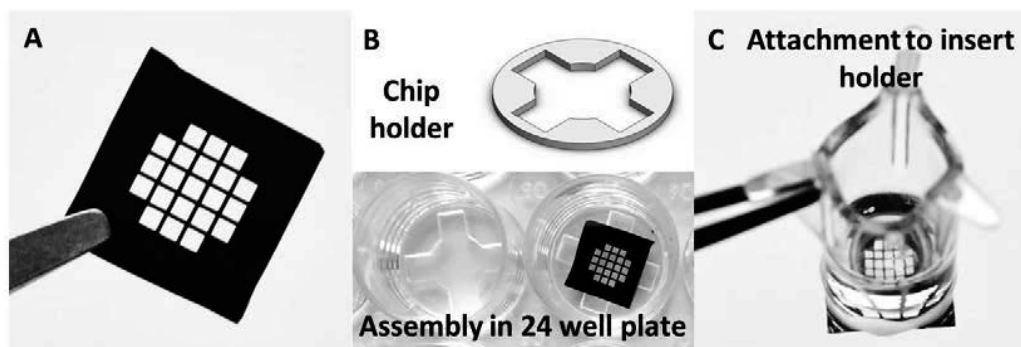


**Figure 2.1** Ultrathin nanoporous alumina supports.

(A) Silicon chip (Si-chip) holding 21 square and transparent alumina membranes (chip: 9 mm x 9 mm). (B) One-compartment cell culture set-up: Si-chip is placed on a simple holder within a 24 well plate to allow media supply from both sides of the membrane. (C) Two-compartment permeability set-up: Si-chip is glued onto commercially available 24 well cell culture inserts after PET-membrane removal.

The fabricated alumina membranes are characterized by densely packed nanopores, which span straight through the aluminum layer. Pore diameters range from 10 – 140 nm for the top (Figure 2.2 A) and bottom (Figure 2.2 B) side of the membrane. The mean diameter for the top side of the membrane is slightly bigger ( $82 \pm 26$  nm) compared to the bottom side ( $73 \pm 21$  nm). Moreover, marginally more pores were counted on the top side (top:  $43 \pm 2$  pores/ $\mu\text{m}^2$ ; bottom:  $36 \pm 1$  pores/ $\mu\text{m}^2$ ). This phenomenon is attributed to the anodization process, which creates the typical, highly-ordered nanoporous structure into the aluminum layer. During anodization, pores are propagated from the top to the bottom side (Poinern *et al.* 2011). For anodization of thin films of aluminum, it was observed that pore channels frequently evolve a branched shape and that not all initiated pores finally reach the bottom (Wu *et al.* 2012). According to these findings, a corresponding membrane porosity of 15% was calculated, based on bottom results. Compared to other fabrication techniques for ultrathin membranes, the anodization of thin aluminum films represents a fast and cost-efficient option to obtain a nanoporous material (Poinern *et al.* 2011). This is different from crafting of SiNx thin films with photolithography techniques, which rather yield microporous membranes with pore sizes starting from 1  $\mu\text{m}$  upward (Kenzaoui *et al.* 2013, Jud *et al.* 2015). On the other hand, fabrication of SiNx membranes with nanopores relies on time consuming and cost intensive techniques like e-beam lithography (Vlassioux *et al.* 2009). The choice of nanoporous or microporous membranes is strongly dependent on the final application and has to be considered in advance to experimentation.

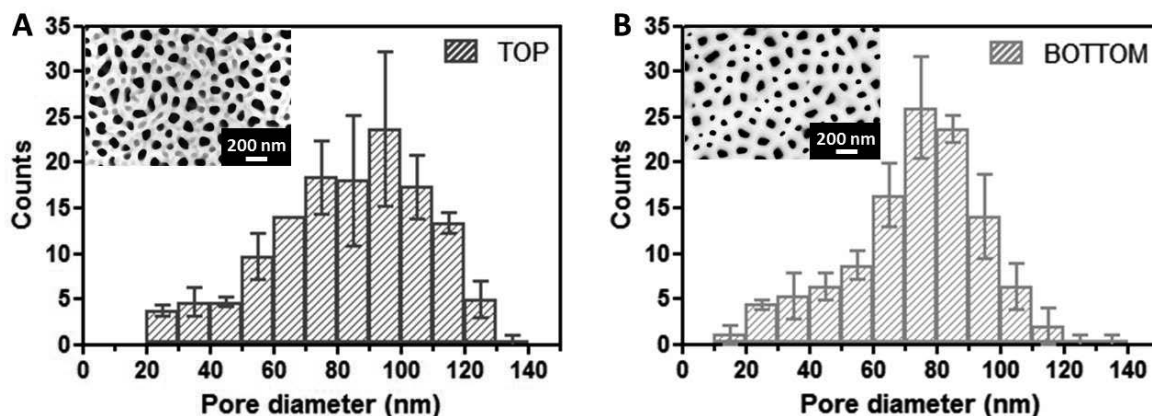


Figure 2.2 Pore size histograms of alumina membrane.

(A) From top side and (B) from bottom side of membranes. For each histogram, three representative scanning electron microscopy images from independent anodization batches, as depicted in the graph, were analyzed. Shown are the mean values and standard deviation.

Permeability of nanoporous alumina was evaluated in the two compartment insert system in absence of cells and compared to that of PET membranes (Figure 2.3 A). The absolute amount of permeated dye (Lucifer yellow or Dextran FD<sub>40</sub>) or protein (bovine serum albumin) from the apical to the basolateral chamber was evaluated over 24 hours and showed faster rates for the alumina membrane (Figure 2.3 B). For Lucifer yellow, the smallest molecule analyzed, an  $P_{app}(\text{alumina}) = 6.2 \cdot 10^{-5}$  cm/s and  $P_{app}(\text{PET}) = 7.5 \cdot 10^{-6}$  cm/s was calculated. For Dextran FD<sub>40</sub> we obtained the following values:  $P_{app}(\text{alumina}) = 2.3 \cdot 10^{-5}$  cm/s and  $P_{app}(\text{PET}) = 8.5 \cdot 10^{-7}$  cm/s. These values correspond to the linear section of the kinetic curves recorded for both dyes (see supplemental material, Figure S 2.3); the calculation incorporates membrane area, whereby permeable alumina membrane area is about half the size of PET membrane area. For bovine serum albumin, we estimated  $P_{app}(\text{alumina}) = 1.7 \cdot 10^{-5}$  cm/s and  $P_{app}(\text{PET}) = 3.2 \cdot 10^{-6}$  cm/s from the 24 hour time point. The  $P_{app}$  values for alumina membranes clearly show that membrane permeability decreases with molecule size, but is still much faster compared to PET membranes. These findings underline the great potential of alumina membranes in improving current *in vitro* epithelial barrier models for transport or co-culture studies, where the mechanical cell support is not supposed to act as barrier itself. At this point we would also like to add that alumina membranes are not suitable for nanoparticle transport studies. This type of research obviously requires bigger pore sizes, which are above the diameter of nanoparticles or nanoparticle agglomerates (Geppert *et al.* 2016).

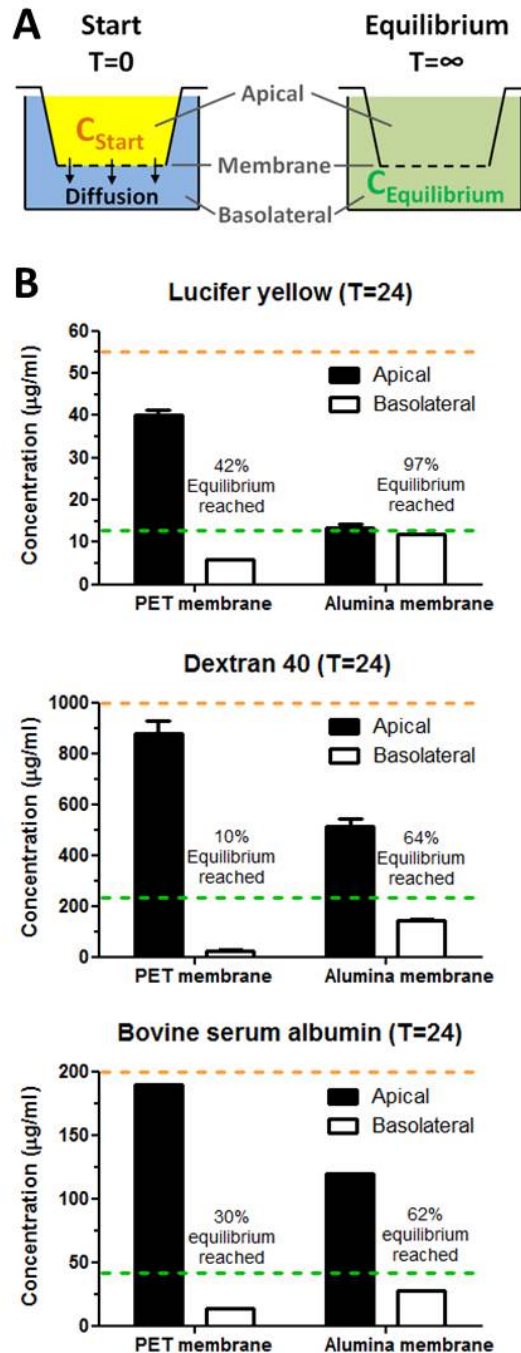
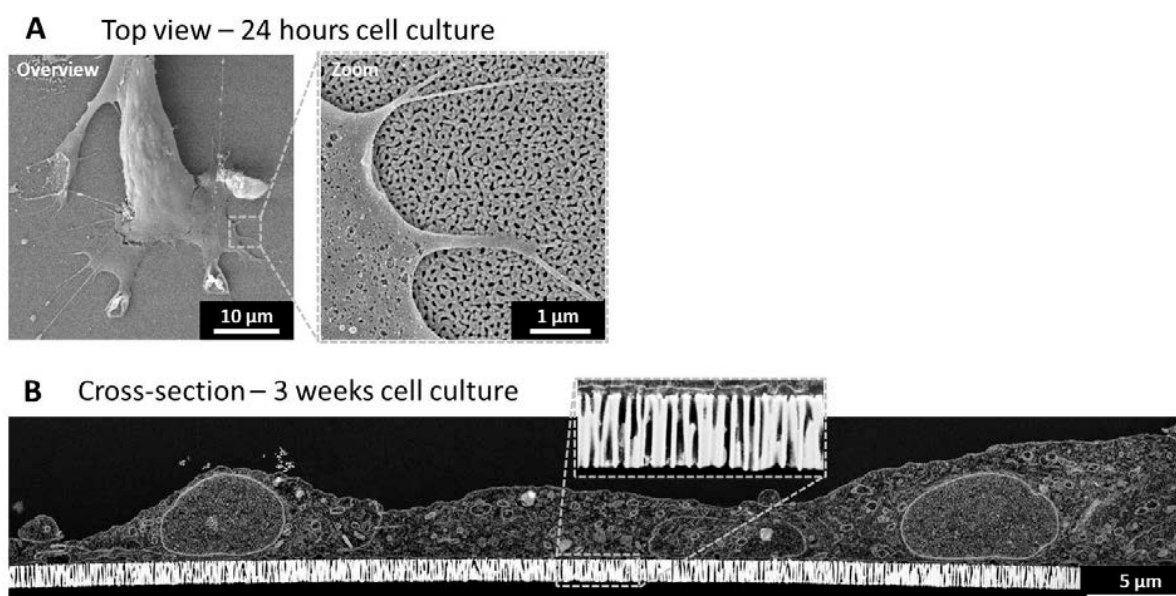


Figure 2.3 Comparison of membrane permeability between commercial PET and custom made alumina membranes in the absence of cells.

(A) Depiction of experimental set-up for both membranes: the apical chamber of the insert system was filled with 400  $\mu\text{l}$  of PBS containing either Lucifer yellow (LY), starting concentration ( $C_{\text{Start}}$ ) = 55  $\mu\text{g}/\text{mL}$ ; Dextran FD40 (FD40),  $C_{\text{Start}}$  = 1000  $\mu\text{g}/\text{mL}$ ; or bovine serum albumin (BSA),  $C_{\text{Start}}$  = 200  $\mu\text{g}/\text{mL}$ . The basolateral chamber was filled with 1.4 mL of PBS only. The experiment was started at time point 0 hours ( $T=0$ ). Over an unknown period of time ( $T=\infty$ ) the concentration between the apical and basolateral chamber reached an equilibrium due to diffusion. (B) After 24 hours ( $T=24$ ) concentrations of LY, FD40 and BSA were determined in the apical and basolateral chamber and the percentage of reached equilibrium was calculated for the basolateral chamber. The dark grey dashed line indicates  $C_{\text{Start}}$  and the light grey dotted line shows predicted  $C_{\text{Equilibrium}}$  based on complete diffusion between apical and basolateral chamber.

### Alumina membranes as cell culture interface

With regard to their application as culture interface for epithelial fish cells, alumina membranes were used to investigate the interaction of RTgutGC cells with the nanoporous surface. As shown by SEM investigations after one day of culture (Figure 2.4 A), cells are adherent to the substrate and exhibit a normal, flattened morphology. On the membrane, each cell is in contact with abundant, homogeneously distributed pores ( $\sim 36\,000$  pores/cell). Due to the small pore diameter, cells do not penetrate into the pores with their membrane protrusions (filopodia). Filopodia pore penetration has been observed for pore diameters of 240 nm and bigger (Hoess *et al.* 2012, Geppert *et al.* 2016). A cross-section TEM image of RTgutGC cells cultured for two weeks on alumina membranes (Figure 2.4 B) provides an impression of the ratio between epithelial layer thickness and permeable support, which is around 5:1. In addition, the magnified detail of the membrane highlights the straight pores, spanning through the aluminum layer and connecting the apically located cells with the basolateral media supply. These findings make the alumina membrane a physiologically realistic support for epithelial barrier systems, such as the fish intestine.



**Figure 2.4** Alumina membranes as cell culture interface for rainbow trout intestinal epithelial cells.

(A) Cells were seeded at a low density (20 000 cells/cm<sup>2</sup>) and cultured for 24 hours prior to scanning electron microscopy. (B) Cells were seeded at a high density (55 000 cells/cm<sup>2</sup>) and cultured for two weeks. Cross-sections were prepared with focused-ion-beam and images were taken with transmission electron microscopy.

Alumina membranes are optically transparent, allowing for routine monitoring of cell growth and morphology by light microscopy. As depicted in Figure 2.5 A, the cells show excellent cell-growth behavior on the membrane. Cells attach within two hours after seeding and start to spread. Already

after one day of culture, cells form a confluent monolayer when seeded at a high density of 55 000 cells/cm<sup>2</sup>. During the next 14 to 28 days, cells proliferate and become smaller and more homogeneous in size and morphology. Cellular polarization, which is a key feature of epithelial cells, was demonstrated by immunofluorescent imaging of cells stained against tight junction protein ZO-1, cytoskeleton (f-actin) and nuclei (DAPI) (Figure 2.5 B). At day one, cells showed a highly flattened morphology with actin stress fibers and weak tight junctions on the same optical plane. During a culture period of 14 days, tight junctions continuously move toward the apical cell boarder and staining intensity becomes stronger, while actin stress fibers remain located basolaterally. Cross-section analysis (z-stack assembly) revealed that long culture periods, i.e.,  $\geq 4$  weeks, resulted in undesired multilayer formation on the alumina supports due to continued cell proliferation. Thus, we conclude that RTgutGC cells form a mature epithelium, which is ready for experimentation within 14 days of culture. In addition, we could show that alumina membranes are suitable for confocal imaging through the ultrathin membrane (cells cultured on bottom side) with the same quality (see supplemental material, Figure S 2.4). This can be beneficial for imaging of co-cultured cells. Next, cell-based impedance spectroscopy was assessed to allow non-invasive monitoring of epithelial barrier formation over time (Figure 2.5 C). Therefore, cellular impedance of RTgutGC was measured every 3-4 days over the culture period of 28 days. During the first 24 hours, impedance values strongly increased to 16 ohms/cm<sup>2</sup>, due to cell attachment. Thereafter, values increased steadily to 26 ohms/cm<sup>2</sup> at day 28. These results are in accordance with trans-epithelial electrical resistance (TEER) measurements reported for RTgutGC cells cultured in commercial transwell inserts (Geppert *et al.* 2016). In addition, resistance values agree with the leaky nature of the fish intestinal epithelium *in vivo* (Sundell *et al.* 2003) and are thus quite different from the epithelial resistance of the frequently used human intestinal cell line Caco-2, where TEER values range from 500-1000 ohms/cm<sup>2</sup> (Liang *et al.* 2000). Low epithelial resistance can have a strong influence on measure accuracy. For RTgutGC cells cultured on PET membranes, we observed high variation among replicates (see supplemental material, Figure S 2.5). Alumina supports, in contrast, exhibit much lower background values due their thinness and high porosity, and thus offer low set-up related variation among samples, improving measure accuracy substantially (Figure 2.5 C). Finally, impedance values were compared with microscopical findings and additionally normalized to the resistance of day 14, where cells formed a mature epithelium (Figure 2.5 D). According to this evaluation, the epithelial barrier formation of RTgutGC cells can be divided in 4 stages: 1) cell attachment; 2) cell spreading and formation of a confluent monolayer; 3) polarization and 4) further proliferation and multilayer formation.

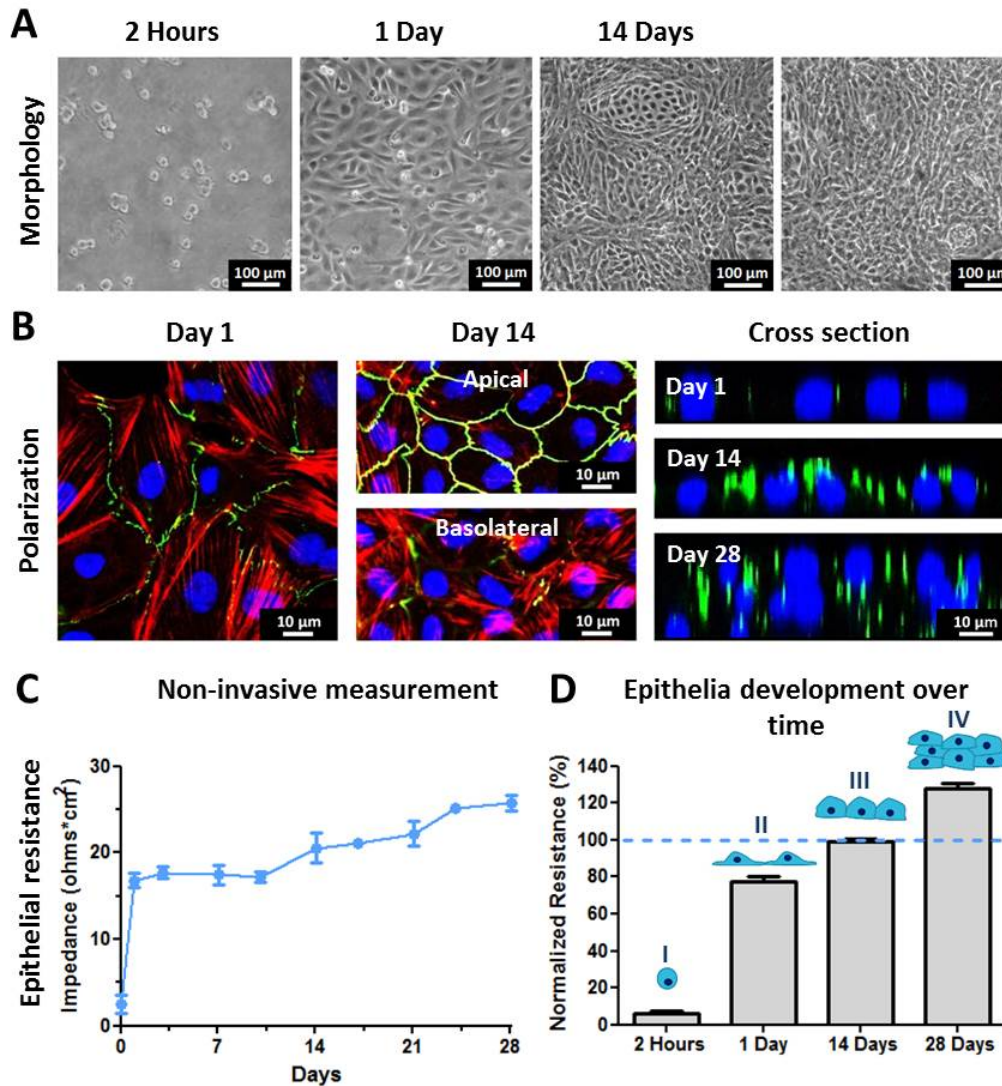


Figure 2.5 Cell growth, polarization and epithelial resistance of rainbow trout intestinal epithelial cells (RTgutGC) cultured on alumina membranes.

(A) Light microscopy of cells cultured for two hours, 1, 14 & 28 days. (B) Confocal microscopy of cells stained for tight junction protein ZO-1 (green), cytoskeleton f-actin (red) and nuclei (blue). Day 1: Tight junctions and actin stress fibers are found on the same optical plane. Day 14: Tight junctions migrate to the apical cell boarder while actin stress fibers remained basolateral (distance between apical and basolateral images was 4  $\mu\text{m}$ ). Cross-section: Assembly of z-stack images (staining for ZO-1 and nucleus) show unpolarized cells at day one, polarized monolayer at day 14 and multilayer formation at day 28. (C & D) Epithelial resistance was measured using impedance spectroscopy for 28 days at a frequency of 1500 Hz. (C) Ohmic resistance is depicted as function over time. Presented are the means of three biological replicates and standard deviation. (D) Resistance values are normalized to day 14, where cells formed a polarized epithelial monolayer. According to culture periods, the epithelial development can be arranged in four stages: Stage I (~0-5 hours): Cell seeding and attachment; Stage II (~5 hours – 3 days): Cell spreading and formation of a confluent monolayer; Stage III (~3 – 21 days): Cell growth and polarization; Stage IV (~21 – 28 days): Further cell division and multilayer formation.

### Impedance-based toxicity testing on piscine intestinal epithelia

Hazardous substances, taken up into the fish intestine, e.g., via diet, may influence the epithelium's role in acting as selective barrier towards food, pathogens and other toxins. We used impedance spectroscopy to monitor the RTgutGC epithelial resistance, while performing two chemical exposure scenarios. First, a short-term exposure of a barrier disrupting chemical, namely EDTA, was carried out and subsequent recovery was monitored (Figure 2.6 A). The cellular resistance rapidly declines during the exposure period, with normalized resistance values (normalized to control) dropping rapidly from 100% to 60%. Transfer of the epithelium to chemical-free medium resulted in total recovery of 100% within 50 min. For the second exposure scenario, cells were continuously exposed to the barrier destructing chemical SDS, and monitored for 24 hours (Figure 2.6 B, left graph). Normalized resistance values showed the greatest changes within the first four hours, where values dropped from 100% to 60%. Thereafter, normalized values declined gradually to 44%. Control and SDS exposed cells were stained after the 24 hours treatment, confirming a changed morphology of the actin cytoskeleton for exposed cells, which is likely induced by cellular apoptosis (Figure 2.6 B, right images). Impedance spectroscopy was shown previously to be a suitable sensing method for water quality analysis by using the rainbow trout gill cell line, RTgill-W<sub>1</sub>, cultured directly on electrodes (Brennan *et al.* 2012). With the conducted experiments, we demonstrate the applicability of the method for the RTgutGC epithelial barrier system, where measurement is conducted through the alumina membrane.

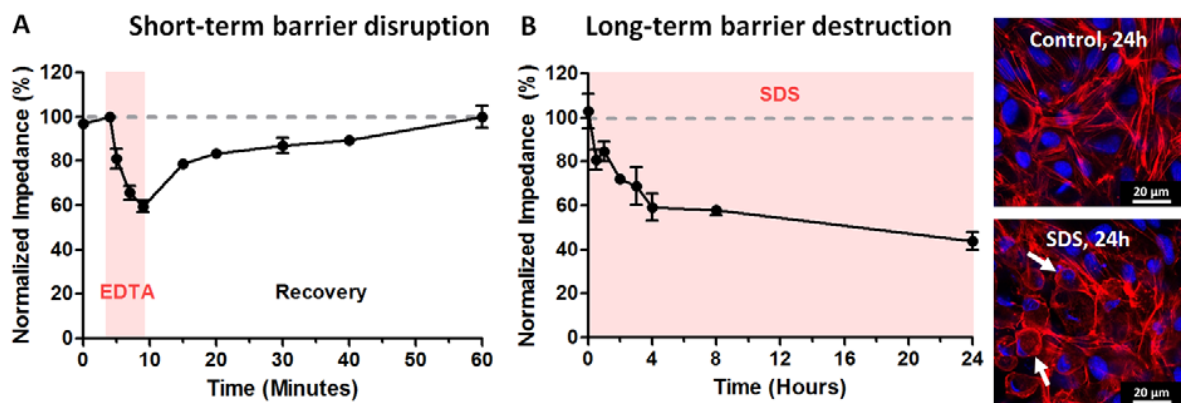


Figure 2.6 Impedance-based toxicity testing on mature epithelia.

(A) Normalized impedance during short-term exposure (5 min) to EDTA (Ethylenediaminetetraacetic acid) and subsequent recovery. (B) Long-term exposure (24 hours) to SDS (Sodium dodecyl sulfate). Left: Normalized impedance; Right: Cytoskeletal changes after 24 hours SDS exposure. Immunocytochemical staining of cytoskeleton f-actin (red) and nucleus (blue) revealed a fiber-like network of f-actin in untreated samples (control) and less organized f-actin fibers, dominantly present at the cell periphery, in SDS exposed samples. Normalized impedance of (A) & (B): Presented are the means of at least three biological replicates and standard deviation. Each value was normalized to control. Colored area indicates chemical exposure period.

### Surface modification of alumina membranes

Alumina ( $\text{Al}_2\text{O}_3$ ) is the oxidized form of aluminum, which is formed during the anodization process. We tested the release of aluminum ions from alumina membranes into fetal bovine serum containing cell culture medium, to verify unbiased usage of this metal surface for cell culture applications and toxicological studies. However, we found  $717 \mu\text{g/L}$  of aluminum released from a single Si-chip into  $1\text{mL}$  of cell culture medium during an incubation time of 7 days (Figure 2.7 A). Using visual MINTEQ we predicted aluminum to be present in the form of aluminum hydroxide (~90%) or bound to Glutamate & Glycine (~10%). In general, aluminum is classified as non-priority pollutant (US EPA) due to its low toxicological impact found in humans, mammals, *in vitro* cell cultures and bacteria (Organization 1998). For fish, aluminum can be extremely toxic when exposed under acidic ( $\text{pH} < 6$ ) or alkaline conditions ( $\text{pH} > 8$ ), by impairing the ion regulation of the gills, leading to a respiratory dysfunction (Wilson 2012). From these findings we conclude that alumina membranes can be used as cell culture interface without influencing cell viability and vitality, but care should be taken if pH shifts are to be expected. In addition, the released aluminum may interfere with metal exposure experiments, which are of interest in environmental toxicology (Ojo and Wood 2007, Minghetti *et al.* 2014). Thus, in order to prevent aluminum release from the membranes, we tested a surface modification by depositing a thin film of  $\text{TiO}_2$  with atomic layer deposition (ALD) on the total membrane surface. A deposition of 2 nm  $\text{TiO}_2$  decreased the aluminum release to  $89 \mu\text{g/L}$ . For 5 and 7 nm  $\text{TiO}_2$  films, the Al release was below  $5 \mu\text{g/L}$  (Figure 2.7 A). The ALD surface modification results in smaller pore sizes according to layer thickness, which might affect permeability. However, for frequently studies molecules, such as Lucifer yellow, Dextran 40 or bovine serum albumin, with diameters  $\leq 4\text{nm}$ , we would not expect a significant change in permeability due to the stable, high pore density. Figure 2.7 B demonstrates membrane morphology before and after ALD with 5 nm  $\text{TiO}_2$ . Release of titanium was not observed.

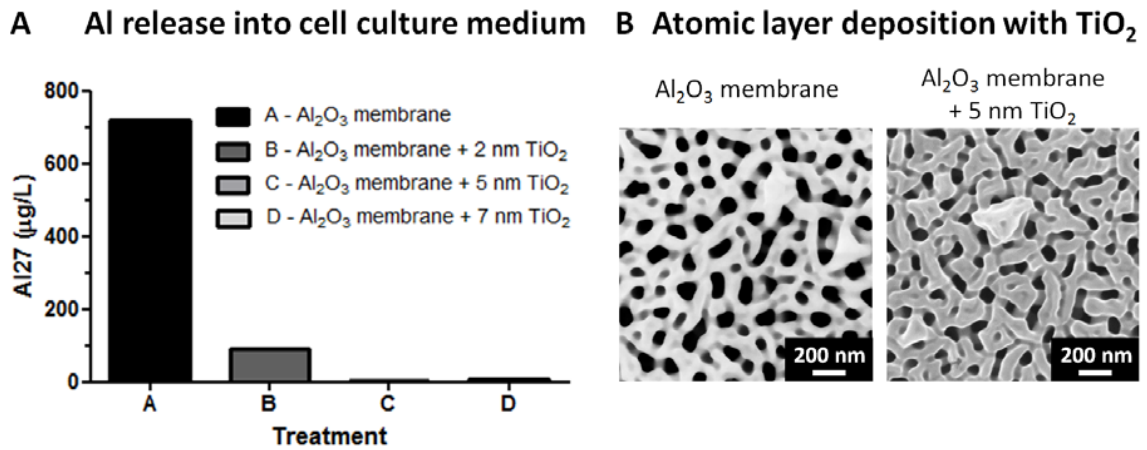


Figure 2.7 Al release from membranes and prevention.

(A) Al concentrations found in cell culture medium after incubation with alumina membranes for seven days at 19°C (1 mL/chip). Tested were untreated membranes (Al<sub>2</sub>O<sub>3</sub>) and membranes with an atomic layer deposition (ALD) of different TiO<sub>2</sub> thicknesses (2, 5 & 7 nm). (B) Changes in membrane morphology before and after ALD with 5 nm TiO<sub>2</sub>.

## 2.4 Conclusion

We developed a novel type of ultrathin alumina-based membrane to serve as permeable support for an *in vitro* tissue model, focusing on the fish intestine. Due to their unique nanoporous structure, the new membrane was found to overcome some issues of current polymer-based membranes, which are part of commercial transwell inserts. Unlike their commercial counterpart, alumina membranes closely mimic features of the basement membrane in terms of thinness, porosity and permeability. The established piscine intestinal barrier model, based on RTgutGC cell culture on alumina supports, has proved epithelial characteristics, such as the formation of a confluent polarized cell-monolayer. In future studies, it might be interesting to include a second cell type in the system. This could be a fibroblast or endothelial cell line grown on the opposite membrane side in order to mimic the physiological complexity of the intestinal barrier. In addition, the alumina supports could be adapted for microfluidic bioreactors, which would allow mechanical stimulation of intestinal cells as found *in vivo*. For optimal analysis of epithelial barrier function, we introduced cell-based impedance spectroscopy to measure changes in cellular resistance upon chemical exposure in real time. This bio-sensing method, in combination with alumina membranes, was found to be a sensitive endpoint for the *in vitro* piscine intestinal barrier, which naturally has a low resistance and therefore ideally mimics the leaky nature of the fish intestine. A limitation of alumina membranes can be seen in its release of aluminum ions. The released concentrations had no effect on cell growth or cellular behavior, but might interfere with metal exposure or other types of experiments. A solution to the problem was found by a surface modification with titanium dioxide, which drastically decreased the undesired release. Overall, we developed a novel and innovative culture system for barrier forming epithelial cells, which is applicable for physiological-, permeation- and toxicological studies, and not restricted to the RTgutGC cell line.

### Contributions

I performed all the experimental work and wrote the paper manuscript. Songmei Wu was involved in the development of ultrathin alumina membranes for cell culture application. Matteo Minghetti contributed to the experimental design of fish cell culture on alumina membranes. Kristin Schirmer and Philippe Renaud were supervising the project.

## 2.5 Supplemental material

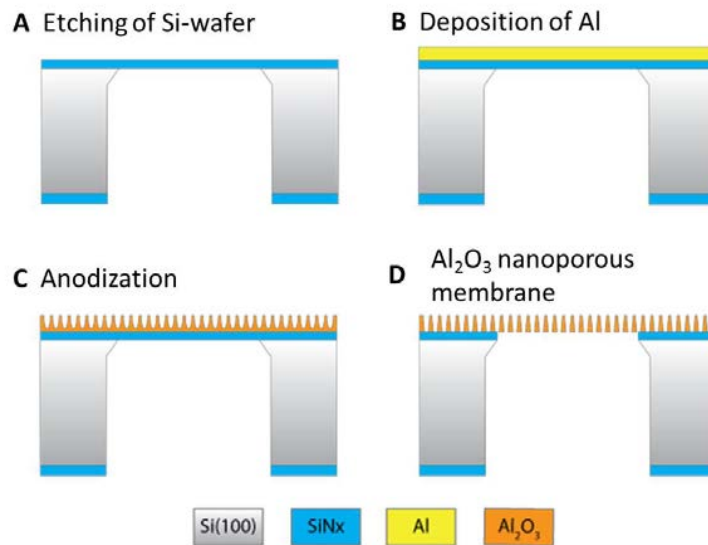


Figure S 2.1 Fabrication process of ultrathin anodic aluminum oxide membranes.

(A) Standard microfabrication tools are used to define the size of the free standing, low stress, silicon nitride ( $\text{SiN}_x$ ) membrane, which serves as support for further processing. (B) An Al layer of  $1\ \mu\text{m}$  is deposited on the  $\text{SiN}_x$  film. (C) Anodization of Al creates self-organized nanopore structures. (D) The alumina membrane is released from  $\text{SiN}_x$  by backside etching.

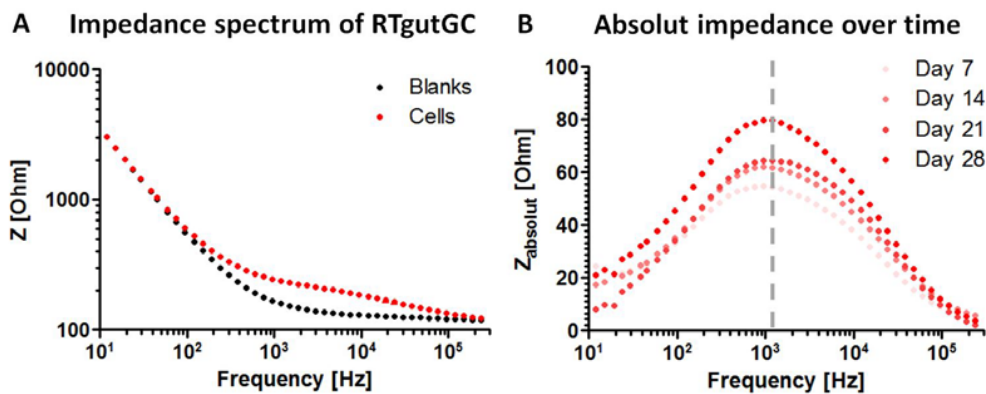


Figure S 2.2 Impedimetric characterization of RTgutGC cells grown on alumina supports.

(A) Frequency scan of cells cultured for 28 days. (B) Absolute impedance over the whole frequency range, demonstrating highest sensitivity at  $1500\ \text{Hz}$ , as indicated by the grey dashed line.

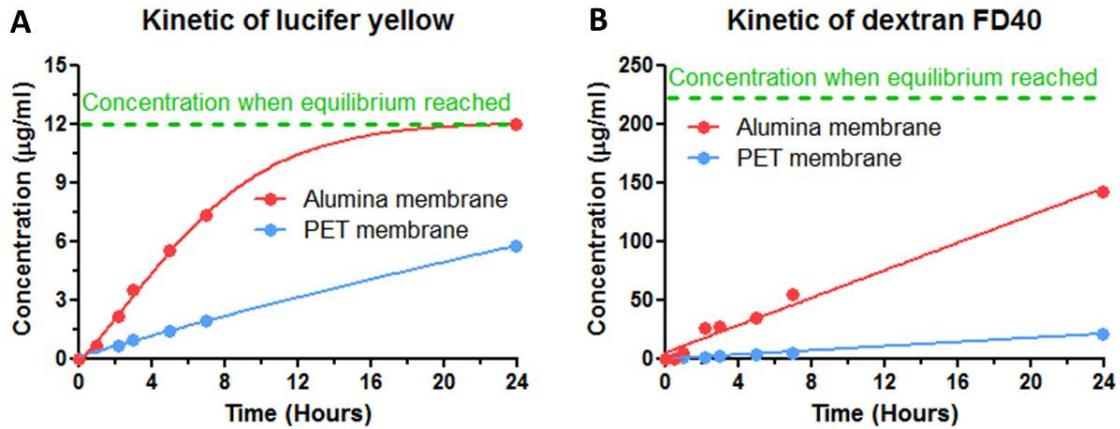


Figure S 2.3 Membrane permeability of alumina versus commercial PET membrane.

(A) For Lucifer yellow and (B) for Dextran 40. Depicted are measured concentrations in the basolateral chamber over time. Membrane area of alumina membrane was 13 mm<sup>2</sup> and of PET membrane 33.6 mm<sup>2</sup>.

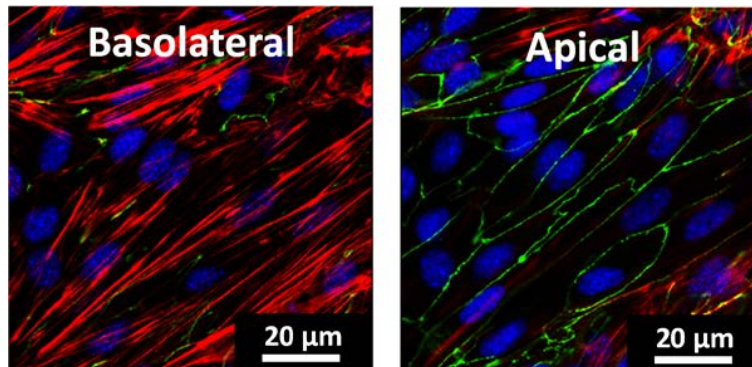
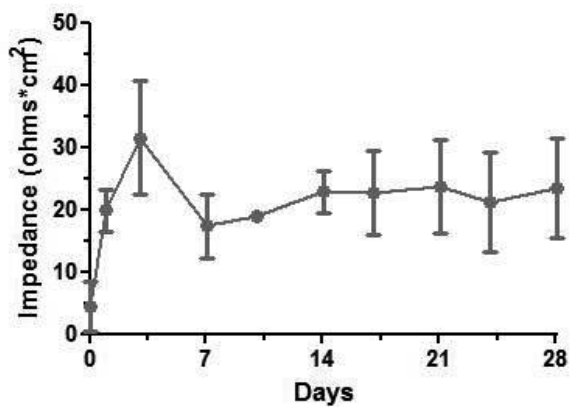


Figure S 2.4 Microscopy through alumina membrane.

Cells were seeded on the bottom side of the membrane, cultured for 14 days and stained for tight junction protein ZO-1 (green), cytoskeleton f-actin (red) and nucleus (blue). Confocal microscopy was performed from the top side of the membrane.



**Figure S 2.5 Epithelial resistance of RTgutGC.**

Cells were cultured for 28 days on commercial transwell inserts and resistance was determined by impedance spectroscopy at 1 500 Hz. Presented are the means of three biological replicates and standard deviation.



## Chapter 3. Characterization of a fibroblast-like cell line from the intestine of rainbow trout and its potential role in an advanced intestinal barrier model

An *in vitro* model of the fish intestine is of interest for research and application in diverse fields such as fish physiology, aquaculture and chemical risk assessment. The recently developed epithelial barrier model of the fish intestine relies on the RTgutGC cell line from rainbow trout (*Oncorhynchus mykiss*), cultured in inserts on permeable membranes. Our aim was to extend the current system by introducing intestinal fibroblasts as supportive layer in order to reconstruct the epithelial-mesenchymal interface as found *in vivo*. We therefore initiated and characterized the first fibroblast cell line from the intestine of rainbow trout, which was termed RTgutF. Co-culture studies of RTgutGC and RTgutF were performed on commercially available electric cell substrate for impedance sensing (ECIS) and on newly developed ultrathin, highly porous alumina membranes to imitate the cellular interaction with the basement membrane. Cellular events were examined with non-invasive impedance spectroscopy to distinguish between barrier tightness and cell density in the ECIS system and to determine trans-epithelial electrical resistance (TEER) for cells cultured on the alumina membranes. We highlight the relevance of the piscine intestinal fibroblasts for an advanced intestinal barrier model, particularly on ultrathin alumina membranes. These membranes enable rapid crosstalk of cells cultured on opposite sides, which led to increased barrier tightening in the fish cell line-based epithelial-mesenchymal model.

*Carolin Drieschner, Nguyen Vo, Hannah Schug, Michael Burkard, Niels Bols, Philippe Renaud, Kristin Schirmer*

### 3.1 Introduction

Rainbow trout (*Oncorhynchus mykiss*) cell lines have been established from a variety of different tissues and organs and are indispensable for mechanistic investigations in fish based research (Bols and Lee 1991, Castano *et al.* 2003, Bols *et al.* 2005, Bols *et al.* 2017). Great success was achieved in the past years in demonstrating the potential of fish cell lines as alternatives for the replacement of animal testing in environmental risk assessment (Schirmer 2006, Tanneberger *et al.* 2012). The attractiveness of rainbow trout cell lines as economic and easy to handle source for reliable and reproducible output is further increasing with the development of functional tissue analogues (Malhão *et al.* 2013, Geppert *et al.* 2016, Minghetti *et al.* 2017), technical innovations in label free bio sensing (Brennan *et al.* 2012, Curtis *et al.* 2013, Widder *et al.* 2015, Tan and Schirmer 2017) and computational modelling (Stadnicka *et al.* 2012, Stadnicka-Michalak *et al.* 2014, Stadnicka-Michalak *et al.* 2015).

An organ of manifold interest is the fish intestine. It takes up nutrients from the diet while attenuating the trespass of pathogens and potentially hazardous chemical substances. Moreover, it regulates ion homeostasis of the whole organism and quickly mobilizes immune reactions if required (Grosell *et al.* 2011). The main interest in this unique organ is easily discernible for three branches: fish physiology, aquaculture and environmental risk assessment. However, accessibility of the gut is limited to short-lived and difficult to prepare *in vivo* or *ex vivo* gut sac preparations. Yet, such preparations have been used, for example, to study the uptake of contaminants, such as hydrophobic chemicals (Sandvik *et al.* 1998, Kelly *et al.* 2004), metals (Hoyle and Handy 2005, Kwong and Niyogi 2009, Leonard *et al.* 2009) and nanoparticles (Handy *et al.* 2008); understand mechanisms of seawater adaptation (Sundell and Sundh 2012, Whittamore 2012); and refine fish culture conditions and fish feeds (Brunt and Austin 2005, Merrifield *et al.* 2009).

A novel *in vitro* model of the fish intestine is based on the epithelial-like cell line RTgutGC (Kawano *et al.* 2011). Herein, the cells are cultured in commercial transwell inserts on a permeable membrane and form a barrier between two compartments, representing the intestinal lumen on one side and the inner of the organism on the other (Geppert *et al.* 2016, Minghetti *et al.* 2017). Sophisticated inventiveness has led to the creation of the “transfer chamber”, a lockable reactor for inserts with permeable membranes, to trace intestinal permeation and bioaccumulation of very hydrophobic substances (Schug *et al.* in preparation). Furthermore, our research has led to the development of ultrathin alumina membranes as novel scaffold for RTgutGC cells. By being at least 10 times thinner and more porous and thus much better permeable, these membranes indeed overcome some of the shortcomings of conventional membranes (Drieschner *et al.* 2017)(Chapter 2).

Given these advances, a next step for the development towards a representative organ analogue of the fish intestine is to improve the creation of a physiologically realistic microenvironment. Hence, the tissue composition and interplay of various cell types needs to be considered. *In vivo*, the intestinal epithelium is underlined by fibroblasts as supportive layer (Powell *et al.* 2011). Fibroblasts originate from the mesenchyme and have diverse functions in the organism, including production of extracellular matrix, immune stimulation and wound healing (Sorrell and Caplan 2009, Ingerslev *et al.* 2010). Notwithstanding, prior to our research, a fibroblast counterpart to the epithelial RTgutGC cell line did not exist.

The crosstalk between epithelial cells and fibroblasts is expected to be essential for epithelial barrier development and functionality (Yasugi 1993, Simon-Assmann *et al.* 2007, Shaker and Rubin 2010). Lately, 2D and 3D *in vitro* models of the human intestine have been developed with the aim to remodel the epithelial-mesenchymal interface. These examinations report improved wound healing (Seltana *et al.* 2010), induced differentiation and proliferation of epithelial cells (Visco *et al.* 2009), changed sensitivity patterns towards drug exposure (Hoffmann *et al.* 2015) and more *in vivo* like TEER values (Pereira *et al.* 2015).

Thus, to initiate further development of an increasingly realistic *in vitro* analogue of the fish intestinal microenvironment, we developed and characterized the first fibroblast-like cell line from the intestine of rainbow trout. Furthermore, we established co-cultures with the epithelial-like cell line RTgutGC on commercial, planar electrode containing solid supports and on the recently developed ultrathin, highly porous alumina membranes. Cellular behaviour was monitored for both systems using impedance spectroscopy and frequency dependent analysis.

## 3.2 Material and methods

### Cell culture

The initiation and characterization of the intestinal fibroblast cell line, RTgutF, is described in detail below. The rainbow trout intestinal epithelial cell line, RTgutGC (Kawano *et al.* 2011), was routinely cultured in Leibovitz's L-15 medium (Invitrogen, Switzerland), supplemented with 5% fetal bovine serum (FBS; PAA, Switzerland) and 1% gentamycin (GIBCO, Invitrogen, Switzerland) at  $19\pm 1^\circ\text{C}$  under normal atmosphere in the dark.

### Establishment of the RTgutF cell line

#### *Initiation*

The RTgutF cell line was developed from tissue fragment cultures of the anterior intestine of a sexually mature male rainbow trout in Dr. Bols' laboratory in the Department of Biology at the University of Waterloo (Waterloo, ON, Canada). After euthanizing the fish with an overdose of the anaesthetic MS222 (Syndel, Canada), the anterior part of the intestinal tract was removed and placed in a petri dish. The exterior surface of the excised tissue was gently rinsed with the rinsing solution:  $\text{Mg}^{2+}$  and  $\text{Ca}^{2+}$ -free Dulbecco's phosphate-buffered saline (DPBS; Lonza, Canada) with 300 U/mL penicillin and 300  $\mu\text{g}/\text{mL}$  streptomycin. A bulb transfer pipette filled with the rinsing solution was inserted into one open end of the intestinal tube to flush the lumen content; this cycle was repeated ten times. Then, the gut was cut open longitudinally and rinsed with the rinsing solution for five more times, as previously done to establish the RTgutGC cell line (Kawano *et al.* 2011). A scalpel blade was used to scrape off the internal intestinal folds to mechanically remove as much epithelial cell mass as possible. The tissue was then immersed sequentially in several petri dishes filled with the rinsing solution to clean the tissue. The resulting tissue was minced into small pieces of about  $1\text{ mm}^2$ . The tissue fragments were rinsed again for three more times and then placed in  $25\text{ cm}^2$  tissue culture flasks (Falcon, Canada) in L-15 medium with 10% FBS (Sigma Aldrich, Canada), 200 U/mL penicillin, and 200  $\mu\text{g}/\text{mL}$  streptomycin at  $20^\circ\text{C}\pm 1^\circ\text{C}$  under normal atmosphere in the dark.

#### *Propagation*

Medium was renewed daily during the first week and then every three days afterwards during the two following weeks. Primary cultures that had epithelial cells were discarded. The original flask that eventually gave rise to the RTgutF cell line had extensive networks of fibroblastic cells outgrowing from the explanted gut tissues. The fibroblastic cells were sub-cultured with trypsin/EDTA solution

(Lonza, Canada) for the first time after two months in culture. The passaged cells were transferred into a new cell culture vessel and kept in L-15 medium with 15% FBS with antibiotics to expand the cell progeny population. Subcultures were initiated by rinsing with trypsin/EDTA solution and splitting into new flasks every two weeks gave rise to the RTgutF cell line.

RTgutF cultures at passage 6 were sent to Dr. Schirmer's laboratory in the Department of Environmental Toxicology at Eawag, the Swiss Federal Institute of Aquatic Science and Technology (Dübendorf, Switzerland), where cellular characteristics and functional properties of the cell line were studied.

#### *Growth characteristics*

At Dr. Schirmer laboratory, RTgutF cells were routinely maintained in L-15 medium, supplemented with 15% FBS and 1% gentamycin at  $19\pm 1^\circ\text{C}$  under normal atmosphere in the dark. Culture medium was renewed once per week and cells were split every one to two weeks, when reaching confluency of 80-90%, in a 1:3 ratio in  $75\text{ cm}^2$  cell culture flasks (TPP, Switzerland). For the proliferation assay, RTgutF cells at passage 22-25 were seeded at a density of  $15'000\text{ cells/cm}^2$  in L-15 medium supplemented with different serum concentrations and 1% gentamycin in 12-well plates (Greiner-bio-one, Switzerland). Plates were incubated for 5 hours at  $19\pm 1^\circ\text{C}$  in the dark to assure cell attachment. Thereafter, medium was aspirated and replaced with 2 mL of L-15 containing 0, 5, 10 or 20% of FBS and the antibiotics. The cell number was determined at day 1, 3, 7, 10, 14 and 17 after seeding.

On the respective day, three wells per FBS concentration were washed twice with Versene followed by trypsinization. Cells were resuspended in the trypsin solution and trypsin reaction was stopped by adding L-15/FBS (15%). The cell number was determined using a Casy TTC cell counter. The doubling time was determined by fitting an exponential growth equation (Equation 3.1) and calculating the rate constant (Equation 3.2), where  $k$  is the rate constant expressed in reciprocal of the  $x$  axis time units.

$$\textit{Cell number} = \textit{cell number}_{t_0} * e^{(k*time)} \quad \text{Equation 3.1}$$

$$\textit{Doubling time} = \frac{\ln(2)}{k} \quad \text{Equation 3.2}$$

#### *Cryopreservation*

RTgutF cell cultures have been successfully cryopreserved in L-15/FBS (10%), supplemented with 10% (v/v) dimethyl sulphoxide (DMSO; Sigma Aldrich, Switzerland) in liquid nitrogen. Success was judged by the straight forward recovery of the cell cultures upon thawing at different passages (13, 26, 52).

#### *Telomerase activity*

As an indicator of cell culture longevity, telomerase activity was assessed using Telo TAGGG Telomerase PCR ELISA (Roche, Germany) following manufacturer's protocols. In brief, RTgutF cells ( $2 \times 10^5$  cells) were harvested at different passages, lysed and telomeric repeat amplification was performed with provided substrate primers (20 minutes elongation, 5 minutes inactivation and 30 x amplification cycles). Products were denatured and hybridised with Digoxigenin (DIG), followed by immobilisation with biotin and streptavidin coating. Samples were semi-quantitatively assessed using the internal standard and horseradish peroxidase (Anti-DIG-HRP), which is sensitive to Tetramethylbenzidine. The limit of detection was considered as the two-fold background activity. Protein content was assessed by bicinchoninic acid protein assay kit (Pierce, USA) following the instructions of the manufacturer. Relative telomerase activity was normalized to 1 mg/mL total protein.

#### **RTgutF and RTgutGC cell cultures on solid support with integrated electrodes**

RTgutF and RTgutGC cells were cultured either as mono- or as co-cultures directly on electric cell substrate for impedance sensing (ECIS), specifically on 8-well chips, each with 20 inter-digitated finger electrodes (8W20idf PET, Applied BioPhysics, ibidi, Germany) to measure the electrical properties of approximately 4'000 to 8'000 cells. For monitoring growth kinetics, RTgutF or RTgutGC cells were seeded at a density of 25'000 cells/cm<sup>2</sup> each. For monitoring barrier formation, cells were seeded at a concentration of 55'000 cells/cm<sup>2</sup> each. For co-culture initiation, RTgutF seeding was performed three days prior to RTgutGC seeding on top. During experimentation, the medium was fully changed every one to two days.

#### **RTgutF and RTgutGC cell cultures on ultrathin permeable alumina membranes**

Ultrathin alumina membranes were fabricated, prepared and used as previously described (Drieschner *et al.* 2017) (Chapter 2). According to the fabrication process, the membranes are realized within a silicon frame for support, the entire unit will be referred as alumina chip. Alumina chips feature a flat side (top) and a micro-structured side (bottom) with a microwell array to access

the nanoporous membrane. For preparation, alumina chips were sterilized in 70% ethanol for 20 min and membranes were coated with 50  $\mu\text{g}/\mu\text{L}$  fibronectin (Roche, Germany) in distilled autoclaved water for two hours on each membrane side and placed in L-15/FBS (5%) for one day prior to cell seeding. For monocultures, either RTgutGC cells were seeded on top of the membrane or RTgutF cells on the bottom side, each with a density of 55'000 cells/cm<sup>2</sup>. Co-cultures were established in two ways: 1) RTgutGC cells were seeded on top of RTgutF cells and 2) RTgutF and RTgutGC cells were seeded on opposite sides of the membrane. For 1) RTgutF cells were pre-cultured on the top side of the membrane for three days, followed by seeding of RTgutGC, each at a density of 55'000 cells/cm<sup>2</sup>. For 2) RTgutF cells were pre-cultured on the bottom side for three days, followed by seeding of RTgutGC on the top side, each with a seeding density of 55'000 cells/cm<sup>2</sup>. After cell attachment, which occurred within two hours after seeding, the alumina chips were placed on specifically designed polycarbonate holders (Drieschner *et al.* 2017) (Chapter 2) in 24 well plates to allow media supply from both sides of the membrane and media was exchanged every one to two days.

### Impedance spectroscopy

Impedance (Z) spectroscopy involved two steps: determining the baseline in the absence of cells and determining the signal in the presence of cells. For baseline analysis, both types of chips (commercial ECIS and self-made alumina chips) were first pre-equilibrated in L-15/5% FBS for one day. The ECIS chip was then directly connected to the impedance analyser (Gamry Instruments, Germany). The alumina chip was placed in an Endohm-6 chamber (World Precision Instruments, Germany), which was then connected to the impedance analyser. Impedance spectra were recorded from 75 to 300 kHz and an amplitude of 10 mV for ECIS chips and from 6 to 300 kHz and an amplitude of 20 mV for alumina chips. Impedance profile and corresponding phase angle were analysed for each system to select optimal frequencies for further analysis as described below.

For ECIS chips, cells are directly cultured on the interdigitated finger electrodes, which provides very high measure sensitivity. This arrangement allows to adapt the principal of low and high frequency analysis, as characterized and applied by Meissner *et al.* (2011) and Benson *et al.* (2013), to distinguish between paracellular and transcellular resistance. In brief, at low frequency (LF), the cell membrane acts as insulator and the ionic current predominantly flows paracellular. Thus, measured resistance values provide information on cell-substrate / cell-cell adhesion. At high frequency (HF), the cell membrane capacitor is short-circuited and resistance of intracellular matter has the main effect on impedance. Figure 3.1 A demonstrates selection criteria for LF and HF. At the lower end of

the frequency range, the impedance spectrum is dominated by the capacitance of the electrodes (top graph). Hence, the region of interest starts at around 1 kHz. Further, the phase angle (bottom graph), indicating if a system behaves like a resistor ( $\rightarrow 0^\circ$ ) or capacitor ( $\rightarrow 90^\circ$ ), is used to determine LF and HF. The highest measurement sensitivity for LF is achieved at the maximal phase angle difference ( $P_{max}$ ) within the low frequency range ( $< 12$  kHz; crossing curves). Thus, a LF of 3 kHz for ECIS was chosen. HF is selected where the phase angle is close to  $0^\circ$  ( $P$  close to  $0^\circ$ ) and the membrane capacitor is short-circuited (end of spectra). Therefore, we have chosen 300 kHz. It is important to keep in mind that neither LF or HF-based resistance values are purely indicative for paracellular or transcellular events (phase angle profile). Yet, for simplification, we refer to LF obtained values as paracellular resistance and to HF obtained values as transcellular resistance.

Impedance measurement for cells cultured on permeable membranes is less sensitive because counter electrodes are located on opposite membrane sides and resistance of the culture membrane and the media have a dominating effect at the higher frequency range and thus do not allow to retrieve information about the transcellular resistance (Figure 3.1 B). In this set-up the region of interest is limited by the capacitance of the electrodes at the LF end and by stray capacitance at the HF end (top graph). Resistance values to calculate trans-epithelial electrical resistance (TEER) are obtained at the frequency with the greatest difference of impedance between the presence and absence of cells (van der Helm *et al.* 2017). In the phase-angle plot (bottom graph) this frequency often correlates with the crossing of curves from cell and blank measurements. This resistance was determined at 3 kHz. For TEER calculation, resistance values were multiplied with the membrane area.

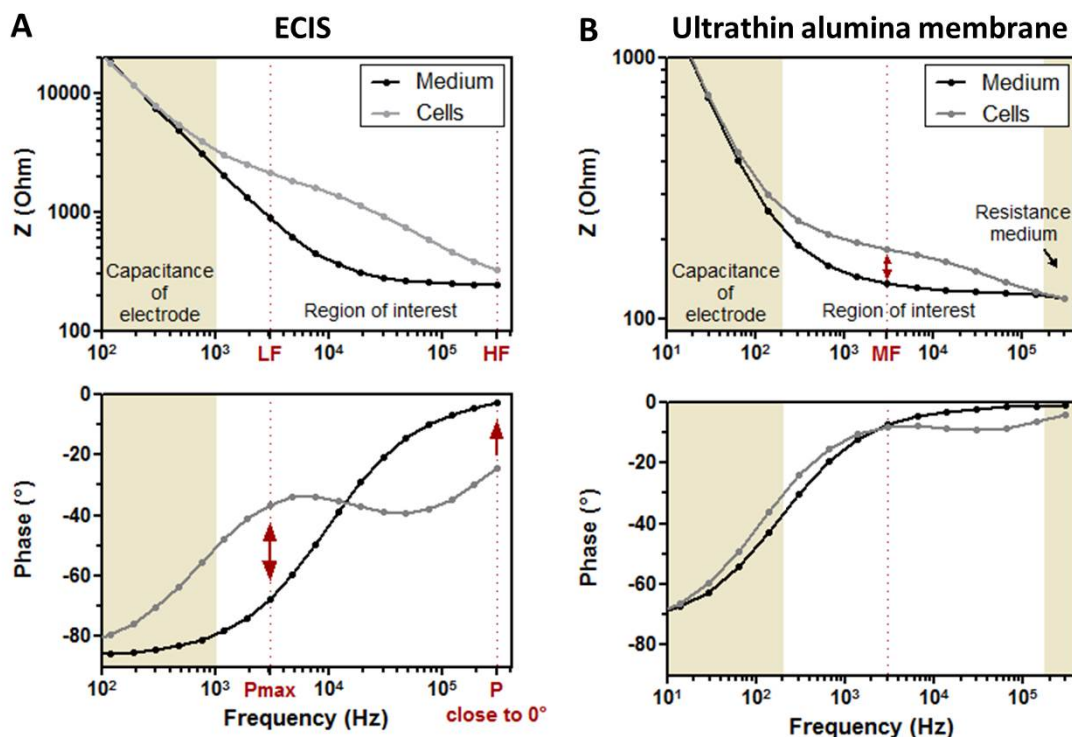


Figure 3.1. Impedance spectra and corresponding phase angle analysis.

RTgutGC cells were grown as high density cultures on solid, electrode containing supports (ECIS) (A) and on ultrathin permeable alumina membranes (B).

## Microscopy

### Light microscopy

Phase-contrast images were obtained with cells cultured in 24 well plates (Greiner-bio-one, Switzerland) using Leica DMI600 inverted microscope.

### Fluorescence microscopy

Immunocytochemical staining was applied to visualize collagen and vimentin as fibroblast markers, ZO-1 as indication of tight junction formation, and cell nuclei. To initiate staining, cells were cultured on coverslips (Thermanox, Thermo Fisher, Switzerland) or four-chamber tissue culture Lab-Tek slides (Nunc, Thermo Fisher, Canada) and left to attach and spread out overnight.

For collagen (type I, alpha 1; COL1A1, antikörper-online.de, Switzerland) immunostaining, cells were fixed with 3.7% paraformaldehyde (Invitrogen, Switzerland) in PBS for 10 min at room temperature. After washing in PBS, cells were permeabilized for 15 min with 0.2% Triton X-100 in PBS. After a further washing step with PBS containing 0.1% Triton X-100, cells were incubated in Image-iT (Invitrogen, Switzerland) for 30 min, rinsed with PBS and primary antibody (diluted 1:40 in 0.5% goat

serum and 0.05% Triton X-100 in PBS) for COL1A1 was applied overnight at  $4\pm 1^{\circ}\text{C}$ . The next day, cells were washed with 0.1% Triton X-100 in PBS and the secondary antibody, Alexa Fluor 488<sup>®</sup>-conjugated goat-anti-rabbit IgG (Invitrogen, Switzerland), was applied at a dilution of 1:1000 for one hour at room temperature. Samples were washed in 0.1% Triton X-100 in PBS and incubated with 10.9  $\mu\text{M}$  DAPI (Invitrogen, Switzerland) in PBS for 5 min. After repeated washing in 0.1% Triton X-100 in PBS and PBS only, coverslips were mounted on microscope slides using ProLong<sup>®</sup> Gold antifade reagent (Life Technology, United States). Imaging and analysis was performed on a Leica SP5 Laser Scanning Confocal Microscope (Leica, Switzerland) using the LAS AF Lite 2014 software.

The vimentin immunostaining followed the same procedure as previously described (Bloch *et al.* 2016). Briefly, cells were fixed in 100% ice-cold methanol for 15 minutes at  $4\pm 1^{\circ}\text{C}$ , followed by a quick wash in PBS to rehydrate cells. Fixed cells were incubated for one hour in a blocking buffer containing 10% goat serum, 3% bovine serum albumin, and 0.1% Triton X-100 in PBS and then probed with mouse monoclonal anti-vimentin antibody (Sigma Aldrich, Canada) diluted at 1:200 in blocking buffer for one hour at room temperature. The secondary antibody was Alexa Fluor 488<sup>®</sup>-conjugated goat anti-mouse IgG used at 1:1000 dilution in PBS for one hour. Cells were then washed five times with PBS, allowed to dry and mounted in Fluoroshield medium containing DAPI (Abcam, Canada). Fluorescence images were taken with a Zeiss LSM510 laser-scanning microscope and confocal images were acquired and analyzed using the ZEN lite 2011 software.

#### *Scanning electron microscopy*

For cross-section images, RTgutF and RTgutGC cells were cultured on opposite sides of alumina membranes for 10 days. Thereafter, cells were washed with PBS and fixed in 2.5% glutardialdehyde for one hour, followed by postfixation in 2% osmium tetroxide for one hour and block staining with 2% uranyl acetate for one hour with washing steps in between. Dehydration was performed in a graded series of 30, 50, 70, 90, and 100% ethanol, followed by twice water-free 100% ethanol, 30 min each. Subsequently, alumina membranes with cells were impregnated, first with 33% resin (EMbed 812, Electron Microscopy Science, USA) and then with 66% resin in water-free ethanol for 1.5 hours each. Thereafter, alumina chips with cells were submerged in 100% resin twice for two hours each. All impregnation steps were performed at room temperature in small plastic dishes. The sample was completely submerged in the resin and then taken out of the resin bath. Excess of resin was allowed to drain in an upright position for another 1.5 hours at room temperature. The sample was then transferred to the oven heated up to  $60^{\circ}\text{C}$ , where polymerization of the resin proceeded for two days. The polymerized alumina chip with cells was cooled to room temperature and directly mounted right-side-up onto SEM stubs with conductive carbon cement. The specimen was sputter

coated with 6 nm platinum. In the focused ion beam (FIB)-SEM (FEI Helios 600i), the sample was screened with an electron beam at high accelerating voltage (30 kV) and imaged in the backscattered electron (BSE)-mode to select a region of interest. The sample was brought to a stage position, where electron beam and ion beam coincide (stage tilt at  $52^\circ$ ) and a trench was milled with the FIB at 30 kV and 9.3 nA to open the sample. The resulting cross section was polished at an ion current of 2.5 nA and then imaged with an electron beam of 2 kV and 0.34 nA. Images were acquired in the BSE-mode at appropriate tilt correction and a dwell time of 30  $\mu$ s. Neighbouring images were merged to full panorama view.

### 3.3 Results and discussion

Focusing on the recreation of basic intestinal architecture, the aim of this study was to combine absorptive epithelial cells, which face the intestinal lumen *in vivo*, and supportive fibroblasts, which are the main cell type in the underlying connective tissue. In order to achieve this, we followed three lines of investigation. First, a novel fibroblast cell line from rainbow trout, RTgutF, was initiated and characterized. Second, this cell line was used alone or in combination with the intestinal epithelial cell line RTgutGC on solid, non-porous supports to evaluate their electrical properties. Third, ultrathin nanoporous alumina membranes were used as basement membrane analogue to allow separation of the two cell types on one hand, while still promoting cellular cross-talk on the other.

#### The RTgutF cell line

Based on the explant outgrowth technique, which was previously applied for the establishment of cell lines from various organs and tissues of different teleost species (Kawano *et al.* 2011, Vo *et al.* 2015, Semple *et al.* 2017), we succeeded in establishing the first intestinal fibroblast cell line from rainbow trout. Cells have been passaged more than 60 times with effective cryopreservation.

Primary cultures initially generated fibroblastic and epithelial cell populations; however, fibroblastic cells were successfully separated. Early passages (< 6) of RTgutF cells showed heterogeneous cell morphology, with a majority of thin elongated cells forming a network like structure and a minority of plump outspread cells (see supplemental material, Figure S 3.1). From passage 6 onwards, RTgutF cell populations changed to a uniform morphology. At low densities cell bodies are spread out (Figure 3.2 A top) while at high densities the cell shape becomes elongated with centred nuclei. If left to grow upon confluency, cells start to form multiple cell layers (Figure 3.2 A bottom - inset) and detach within 14 to 21 days after reaching confluency. In contrast, RTgutGC cells remain in monolayer for up to several month after reaching confluency. This reflects a specific behaviour of the individual cell types, and is coherent with the fact that close contact among *in vitro* normal epithelial cells leads to contact inhibition and cell cycle arrest (Puliafito *et al.* 2012). Fibroblasts, on the other hand, are known to freely move within the 3D arrangement of connective tissue and are thus less strongly adherent to their culture surface *in vitro* (Hay 1995).

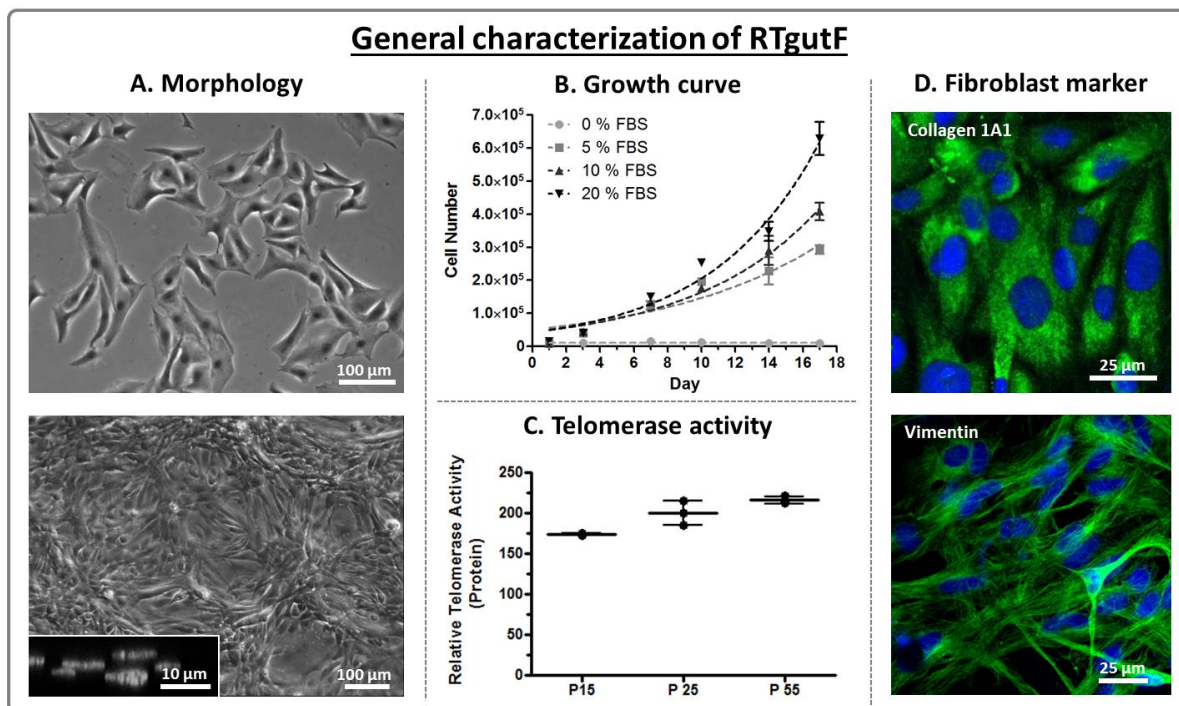


**Figure 3.2** General characterization of RTgutF cultured on conventional support.

(A) Phase contrast image of cells at low density (top) cultured for 1 day and cells at high density (bottom) cultured for 14 days. At high densities, RTgutF cells partially formed multiple layers (inlay, bottom image). (B) Growth kinetics of RTgutF cultured in L-15 supplemented with different FBS concentrations. Depicted are mean values of three biological replicates and SD. (C) Relative telomerase activity at different passages. Represented is the mean of three biological replicates and SD. (D) Confocal images demonstrate positive staining of RTgutF cells for collagen 1A1 (top image, green staining) and vimentin (bottom image, green staining). Cell nuclei were counterstained with DAPI (blue).

RTgutF cells respond to increased concentrations of serum by an acceleration of proliferation (Figure 3.2 B). Doubling times calculated from the growth curves ranged from 6 ½ days for 5% to 5 days for 10%, to 4 ½ days for 20% FBS. In contrast, in the absence of serum, no cell proliferation occurred; yet, RTgutF cells remained attached to the culture surface. For routine cell culture, a reduced FBS concentration of 10% can be recommended. This concentration supports normal fibroblast morphology and optimal proliferation rates, which are comparable to the proliferation profile of RTgutGC cells (Kawano *et al.* 2011).

The RTgutF cell line appears to be infinite based on the number of passages achieved today. In support of this observation, cells express stable levels of telomerase (Figure 3.2 C), an enzyme known to extend cell longevity by extending the chromosome termini, which are otherwise shortened with each cell cycle (Dey and Chakrabarti 2018). In some species, including rainbow trout, telomerase activity is not limited to stem cells, but was detected in all somatic cells (Klapper *et al.* 1998). Indeed, telomerase activity in RTgutF cells was comparable to that of other normal fish cell lines and one telomerase transfected mammalian cell line (see supplemental material, Figure S 3.2).

Further evidence that supports the notion that RTgutF cells are fibroblasts was provided by immunocytochemical staining of collagen 1 (Col1A1) and vimentin. Both proteins are abundantly expressed throughout the cell body of RTgutF cells (Figure 3.2 D). In mammalian cell culture, these proteins are frequently used markers of fibroblasts (Franke *et al.* 1982, Burkard *et al.* 2015). In rainbow trout, no finite biochemical markers are defined yet for cell type identification (Bols *et al.* 2005). However, fibroblast specific expression of collagen 1 has been verified for rainbow trout dermal skin cell cultures and tissue samples (Rakers *et al.* 2011), which supports the potential use of collagen 1 expression as marker for rainbow trout cell line classification. Vimentin expression in rainbow trout is less clear and expression patterns have been described as significantly different from mammals (Herrmann *et al.* 1996). Thus, the information of positive vimentin expression in RTgutF cells should be rather seen as an enrichment of the literature of the notoriously complex expression patterns of vimentin in fish than as a definite fibroblast marker.

With the establishment of RTgutF, the first intestinal fibroblast-like cell line from rainbow trout, it was possible to extend the current RTgutGC model. The supportive function of fibroblasts was analyzed by co-culture initiation on solid substrate and on porous supports, respectively.

### **Impedimetric characterization of intestinal cells on solid support**

In a first approach, epithelial RTgutGC and fibroblastic RTgutF cells were cultured on electric cell substrate for impedance sensing (ECIS), which provides a solid, non-porous cell culture interface and allows evaluation of electrical properties of cells. The electrical properties were examined by non-invasive impedance measurements and permitted to evaluate paracellular resistance at low frequency, which is indicative of cell connections and cell adhesion, and transcellular resistance at high frequency, providing information on cell viability.

In the process of forming a confluent monolayer, RTgutF and RTgutGC cells revealed starkly different paracellular resistance profiles (Figure 3.3 A). RTgutGC presented a gradual increase in resistance values, which was at all times greater compared to RTgutF, with the maximum difference in resistance being about four-fold. Distinctly different profiles were also observed for RTgutF and RTgutGC cells seeded as densely packed monolayer with a confluency of 100% (Figure 3.3 B). Here, the paracellular resistance of RTgutGC was about two-fold higher than of RTgutF, which indicates stronger cell-cell and cell-substrate connections of RTgutGC and is typical for epithelial cells (Hay 1995). Indeed, the formation of tight junctions between adjacent cells has a strong effect on the paracellular resistance profile (Benson *et al.* 2013) and was previously verified for RTgutGC cells by

staining of ZO-1, a protein of the tight junction complex (Geppert *et al.* 2016, Drieschner *et al.* 2017, Minghetti *et al.* 2017) (Chapter 2) and transmission electron microscopy (Minghetti *et al.* 2017). In comparison, RTgutF do not form a continuous line of ZO-1 around the cell boarder when in contact with each other (see supplemental material, Figure S 3.3), which is typical for the movable fibroblasts (Sorrell and Caplan 2009). For co-culture initiation, RTgutGC was seeded directly on top of RTgutF. The paracellular resistance of co-cultures was above that of RTgutF monolayer, but below that of RTgutGC monolayer (Figure 3.3 B). This result is explainable by the likely mixture of the two cell lines, resulting in non-continuous tight junction formation between epithelial cells and fibroblasts. Thus, the formation of a natural basement membrane between the two cell types, as demonstrated in a co-culture model of primary rat intestinal endodermal cells and fibroblasts (Simon-Assmann *et al.* 2007), is unlikely and makes the physical separation of RTgutGC and RTgutF, e.g. through a permeable membrane, necessary.

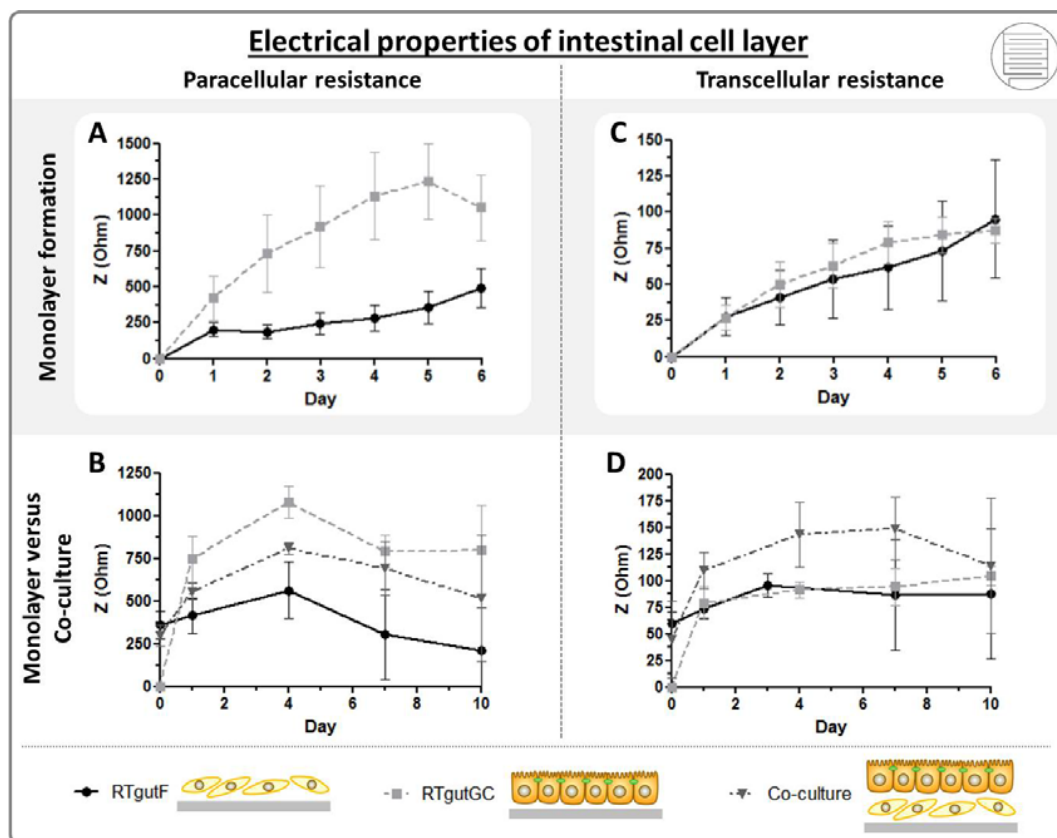


Figure 3.3 Frequency dependent impedimetric monitoring for cultures on electric cell-substrate for impedance sensing (ECIS).

(A & C) Monolayer formation of fibroblasts (RTgutF) versus epithelial cells (RTgutGC) seeded at a moderate density ( $25'000 \text{ cells/cm}^2$ ; confluency 50%). (B & D) Monitoring of tightly packed monolayer of individual cell types and co-cultures seeded at high density ( $55'000 \text{ cells/cm}^2$ ; confluency 100%). Paracellular resistance (A & B) was determined at a low frequency and reflects cell adhesion and formation of cell-cell contacts. Transcellular resistance (C & D) was measured at high frequency and represents intracellular matter, overall indicative of cell viability and in this specific case of cell density. Data represent the mean of four biological replicates and the error bars represent the SD.

Following the transcellular resistance profile during monolayer formation (Figure 3.3 C) it was found that RTgutF and RTgutGC exhibit almost identical resistance values with a steady increase over the culture period. The increase correlated with the doubling time of 4-5 days for both cell lines. Further, the transcellular resistance of co-cultured cells (Figure 3.3 D), which comprises two cell layers, is almost double compared to the confluent monolayers of RTgutF and RTgutGC. For all three approaches, transcellular resistance values remained stable between day 1 till day 7 of culture, reflecting the stagnant or slow cell growth of high density cultures. Thus, the transcellular resistance is not only capable to inform about cell viability and cell death as shown by Meissner *et al.* (2011), but also about cell proliferation and cell density. Notwithstanding, the decline of transcellular resistance for co-cultures at day 10 may indicate the start of a critical shortage of nutrients accompanied with decreasing cell viability due to nutrient undersupply and hypoxia for the lower cell layer.

The comparison of electrical properties of RTgutF and RTgutGC provided further evidence of the fibroblast nature of RTgutF. Co-culture initiation on solid support was not beneficial for the overall resistance of the epithelial-fibroblast cell arrangement, which was used as quality control for a functional co-culture model. Therefore, the next step comprised the culture of epithelial cells and fibroblasts on permeable membrane supports.

### **Reconstruction of the intestinal barrier on ultrathin, porous membranes**

Previous established ultrathin and highly permeable alumina membranes (Drieschner *et al.* 2017) (Chapter 2) were used as artificial basement membrane analogue to support co-culture of epithelial RTgutGC and fibroblastic RTgutF cells in a physiologically realistic manner.

Cells were either cultured as monolayer or in two distinct configurations, with RTgutF and RTgutGC in direct contact (co-culture contact) or separated via the alumina membrane (co-culture separate). Trans-epithelial electrical resistance (TEER) analysis was used to determine the effect on barrier tightness (Figure 3.4 A). RTgutF monocultures developed the lowest resistance with  $\sim 13 \Omega \cdot \text{cm}^2$  during the whole culture period. RTgutGC and co-cultures with RTgutGC seeded on top of RTgutF (contact) exhibited slightly higher resistance values of  $15\text{-}18 \Omega \cdot \text{cm}^2$ , which remained stable from day 1 to day 10 of culture. These values are equivalent with previously reported resistance values of RTgutGC monolayer cultured on alumina membranes (Drieschner *et al.* 2017) (Chapter 2). Only when RTgutGC and RTgutF cells were cultured on opposite sides of the membrane (separate) a

positive effect on barrier tightness with an almost two-fold increase in TEER, compared to RTgutGC monolayer, was observed. This supports two ideas: i) physical separation of epithelial cells and fibroblasts *in vitro* is beneficial for maintaining the functional architecture of the intestine as found *in vivo*; ii) the cellular cross-talk at the epithelial-mesenchymal interface improves barrier function by enhancing barrier tightness. The role of the permeable support, to act as artificial basement membrane analogue, is clearly fundamental for the success of this model. Ultrathin alumina membranes can thus be seen as superior interface for co-culture initiation by supporting fast communication of different cell types through the straight and abundant nanopores. In addition, these membranes allow for sensitive evaluation of TEER, even in the lower resistance range with changes of a few  $\Omega$ , which is not possible with conventional cell culture membranes (Drieschner *et al.* 2017) (Chapter 2).

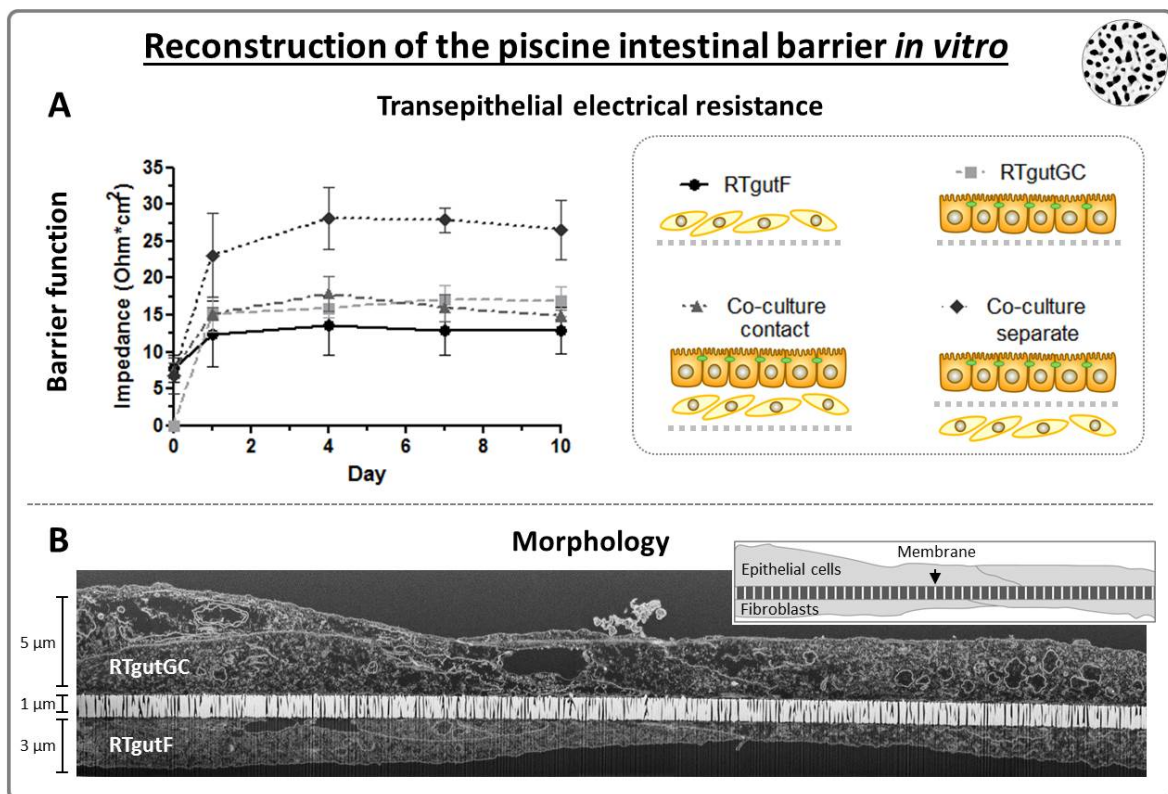


Figure 3.4 Mono- and co-cultures on ultrathin alumina membranes.

(A) Impedimetric monitoring of barrier function of single cultures of RTgutF or RTgutGC, Co-culture with RTgutGC being seeded on top of RTgutF (contact), Co-cultures with RTgutF and RTgutGC being cultured on opposite sides of the membrane (separate). Depicted are resistance values at a low frequency (paracellular resistance) and at a high frequency (transcellular resistance). Data represent the mean of at least four biological replicates and the error bars represent the SD. (B) Cross section of a co-culture where cells are separated via membrane (10 days). The sample was prepared with focused-ion-beam and imaged with transmission electron microscopy. The inset is a simplified drawing of the cross section.

For further investigation of cellular morphology of separate co-cultures of RTgutF and RTgutGC cells, a transmission electron microscopy image of a cross-section of 10 day old cultures was prepared (Figure 3.4 B). The image demonstrates cellular monolayer on both sides of the highly porous membrane. Moreover, cells exhibit a flattened morphology, with a cell height of ~ 5  $\mu\text{m}$  for RTgutGC and ~3  $\mu\text{m}$  for RTgutF. The difference in cell height among the two cell lines, even when being small, is an additional hint for their origin from different tissues. Fibroblasts are typically thin and elongated in shape (Ossum *et al.* 2004), while absorptive epithelial cells, lining the intestinal lumen, have a columnar shape with a height of up to ~30  $\mu\text{m}$  (Merrifield *et al.* 2009). The flattened shape of RTgutGC cells, however, is a typical adaptation of *in vitro* cell cultures, because cells lack important physiological stimulation, such as mechanical forces from fluid flow occurring on the apical surface of epithelial intestinal cells (Kim *et al.* 2012).

The developed co-culture model of intestinal epithelial cells and fibroblasts on ultrathin alumina membranes opens new possibilities to study the physiological function of the fish intestine *in vitro*. One interesting application of this model is the investigation of immunological defence mechanisms of the fish intestine because fibroblasts represent an immune competent cell type (Sorrell and Caplan 2009). Further refinement of the model could be achieved by exposing epithelial RTgutGC cells to realistic flow conditions by implementing ultrathin membrane chips into a microfluidic bioreactor. Eventually, the novel barrier model of the fish intestine is attractive for its physiological realism and opens new doors for fundamental piscine intestinal research.

### 3.4 Conclusion

In conclusion, we established the first intestinal fibroblast cell line from rainbow trout to initiate research on the role of epithelial-mesenchymal interaction in the fish intestine. It is important to note that cell lines offer plethora of biological research material on an economic and ethical justifiable basis and thus help to overcome the current restricted research on the fish intestine due to difficult and limited access. With the extension of the current epithelial barrier model to a deeper layer of the intestinal wall – the connective tissue, we found a positive effect on barrier tightness when individual cell types were separated by newly developed ultrathin alumina membranes. This reflects the importance of the active role of fibroblasts in modulating epithelial barrier functionality by producing and releasing extracellular matrix proteins and growth hormones. Further, it demonstrates the great potential of microtechnological innovations for the rearrangement of the cellular microenvironment *in vitro*, which plays a central role for the recreation of true organ analogues that are capable to offer reliable insights in physiological functions. Thus, the newly developed intestinal barrier model, accommodating epithelial and mesenchymal cells, is a first approach to mimic fish gut complexity and further narrow the gap between *in vitro* and *in vivo* models.

#### Contributions

The RTgutF cell line was initiated and cultured till passage 6 by Nguyen Vo, in the laboratory of Niels Bols at University of Waterloo in Canada. RTgutF characterization was performed by Hannah Schug (growth curve), Michael Burkard (telomerase activity), Nguyen Vo (vimentin staining) and me (morphology & collagen 1A1 staining). All experimental work completed on ECIS and alumina membranes was performed by me. I wrote the manuscript of this chapter with help in the material and methods section from Nguyen, Hannah and Michael for their experimental work. Kristin Schirmer and Philippe Renaud were supervising the project.

### 3.5 Supplemental material

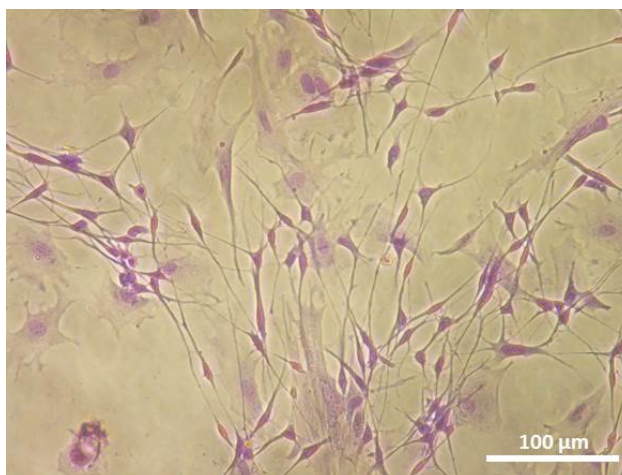


**Figure S 3.1. Morphology of RTgutF cells at passage 3.**

Cells were stained with May-Grunward/Giemsa.

#### **Method applied: May-Grunward/Giemsa Staining**

Cells were stained with May-Grunward/Giemsa to help visualize their organization and shapes in culture as previously demonstrated by Bloch *et al.* (2016).

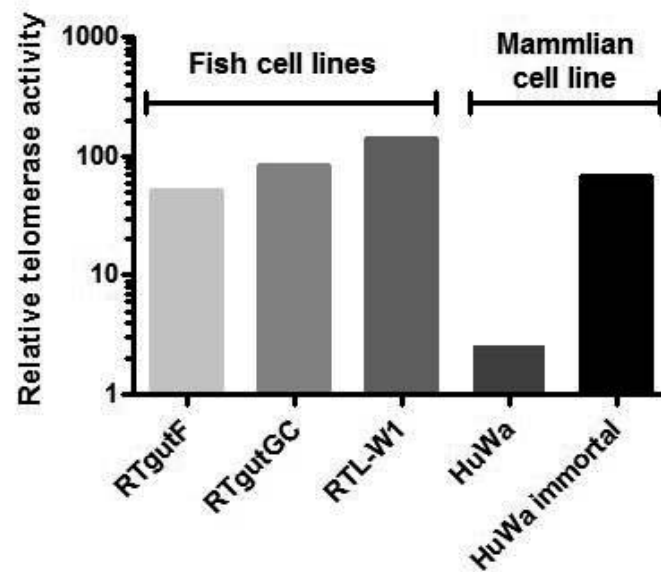


Figure S 3.2 Relative telomerase activity of three fish- and one mammalian cell line.

Fish cell lines were established from rainbow trout and include RTgutF (intestinal fibroblasts), RTgutGC (intestinal epithelial cells) and RTL-W1 (liver cells). The mammalian cell line was analyzed before and after immortalization with TERT.

**Method applied: Telomerase activity**

Telomerase activity was assessed as described for RTgutF in material and methods.

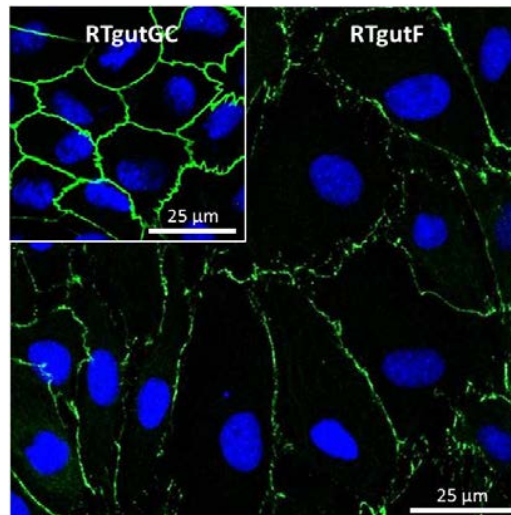


Figure S 3.3 Expression of tight junction protein ZO-1 in RTgutF and RTgutGC cells.

ZO-1 is stained in green and nuclei in blue.

For RTgutF cells ZO-1 is scattered around the cell, while for RTgutGC ZO-1 form a solid line around the cell.

**Method applied: Fluorescence Microscopy**

RTgutF and RTgutGC cells were cultured on coverslips (Thermanox, Thermo Fisher, Switzerland) and stained as described in Drieschner *et al.* (2017)(Chapter 2).

## Chapter 4. 'Fish-gut-on-chip': Development of a microfluidic bioreactor to study the role of the fish intestine as environment-organism barrier *in vitro*

Intestinal barrier function is brought about by specialized epithelial cells that regulate complex and dynamic processes including nutrient uptake, ion regulation, immune system stimulation and defense against pathogens. Mimicry of the intestinal microenvironment in gut-on-chip devices has primarily been explored with human cells to better predict drug absorption and understand pathophysiological diseases. In this study, we present the first fish-gut-on-chip microfluidic bioreactor, to shed light on the role and function of the fish intestine as environment-organism barrier. *In vitro* piscine intestinal barrier models are in great need to study basic fish physiology, for the refinement of fish feed in aquaculture and for predicting chemical uptake and bioaccumulation in fish for risk assessment. The newly developed fish gut analogue combines intestinal cell cultures from rainbow trout (*Oncorhynchus mykiss*), namely the epithelial-like cell line, RTgutGC, and the fibroblast-like cell line, RTgutF, on ultrathin, porous silicon nitride membranes within a user-friendly micro-well plate based reactor, that is equipped with an open microfluidic perfusion system. Epithelial barrier function was confirmed with positive staining of the tight junction protein ZO-1 and trans-epithelial electrical resistance (TEER) measurements using impedance spectroscopy. Imitating intestinal passage on the luminal side by applying a physiological flow rate (200  $\mu\text{L/h}$ ) produced moderate shear stress (0.02  $\text{dyne/cm}^2$ ) that resulted in doubling of TEER values from  $\sim 30$  to  $\sim 60 \Omega \cdot \text{cm}^2$ . This functional adaptation better mimics the intestinal epithelium *in vivo* than cells cultured under static conditions. Thus, the fish-gut-on-chip recapitulates basic intestinal architecture and physiology of the living piscine intestine within a controlled microfluidic environment and hence has the potential to bridge traditional 2D cell culture models and *in vivo* animal experiments.

*Carolin Drieschner, Sarah Könemann, Kristin Schirmer, Philippe Renaud*

## 4.1 Introduction

Fish intestinal epithelia are important gatekeepers and communicators between fish and the surrounding environment. They regulate the interaction with fresh- or saltwater milieus, food, microorganisms and xenobiotics (Grosell *et al.* 2011). As fish are early indicators for aquatic ecosystem health (Harris 1995), understanding compromised intestinal barrier function has significant implications for the field of environmental toxicology and aquaculture industry (Jutfelt 2011).

Our current knowledge of the fish intestine largely originates from *in vivo* experiments (James *et al.* 1997) or *ex vivo* gut sac preparations to study e.g. intestinal absorption of iron as essential metal (Kwong and Niyogi 2009). However, difficult accessibility and the trend towards ethically justifiable, low cost and simplified *in vitro* systems (Schirmer 2006) call for the development of fish cell line based intestinal barrier models.

The RTgutGC cell line, derived from the epithelium of the intestine of rainbow trout (Kawano *et al.* 2011), has previously been implemented in commercial trans-well inserts. This allows to study the physiological and toxicological response of the cells e.g. during simulated seawater adaptation and silver exposure (Minghetti *et al.* 2017), as well as intestinal uptake of potential hazardous nanomaterial (Geppert *et al.* 2016) and hydrophobic chemicals (Schug *et al.* in preparation).

Yet, commercial inserts have limitations, such as low permeability of the polymeric cell culture membrane and reduced visibility of cells (Kenzaoui *et al.* 2012, Jud *et al.* 2015). This has led to the development of ultrathin nanoporous alumina membranes (Drieschner *et al.* 2017)(Chapter 2), which provided impetus for the establishment of an intestinal co-culture model of epithelial RTgutGC and newly developed fibroblastic RTgutF cell lines to partially reconstruct the complexity of the intestinal wall for improved barrier functionality (Chapter 3). However, culture conditions are stagnant which is not reflective of *in vivo*.

Here, we report on the development of the first prototype fish-gut-on-chip device that provides *in vivo* like culture conditions for rainbow trout intestinal cells. The open-microfluidic platform combines established culture ware with an engineered microsystem to enable facilitated handling on one side and a controllable microenvironment for cells on the other side. Our study explored the potential of ultrathin silicon nitride membranes for epithelial-barrier-remodeling under flow conditions. Barrier function of RTgutGC monolayer or RTgutGC/RTgutF co-cultures were verified with staining of the tight junction protein ZO-1. Flow shear stress associated modulation of cell

proliferation and cell height were assessed with cell nuclei and cell membrane staining. Changes in barrier tightness were monitored with trans-epithelial electrical resistance (TEER), measured through device integrated platinum electrodes. Overall, the fish-gut-on-chip platform incorporates several innovations compared to previously described gut-on-chip designs and provides a novel system for investigating the role and function of the fish intestine.

## 4.2 Material and methods

### Reactor design and fabrication

The fish-gut-on-chip device consists of a number of different components. Their fabrication and integration is described below. The final design is presented in the results.

*Silicon nitride (SiN) porous supports* were manufactured for microfluidic applications and are the centerpiece of the fish-gut-on-chip device. In the following they will be termed SiN<sub>FLOW</sub> chips. SiN<sub>FLOW</sub> chips were fabricated by applying the procedure outlined by Kuiper *et al.* (1998). Briefly, a 500 nm thick layer of low stress SiN was thermally grown by low pressure chemical vapor deposition on both sides of standard ( $\varnothing$  100 mm, 380  $\mu$ m thick, <100> oriented, double side polished) silicon wafers. Standard photolithography and reactive ion etching were used to pattern silicon nitride films on both sides of the wafer. The pattern on the bottom side defined the pore size ( $\varnothing$  1.2  $\mu$ m) and pore arrangement on the permeable membrane. The structures on the top side specified the chip size by formation of cleavage lines and openings to form an etch mask for the membrane formation process. In a subsequent step, anisotropic chemical etching in potassium hydroxide (KOH) solution was used to release free-standing SiN membranes from silicon. Individual chips (24 per wafer, dimensions: 22.5 mm x 9 mm) were obtained by manual cleavage along the cleavage lines. Each chip contains two parallel rectangular cavities that culminate into the porous SiN membrane (10 mm x 1 mm) and serve as future upper microfluidic channels with a pyramidal geometry that resulted from KOH etching. A square opening, culminating into a non-porous SiN membrane (1 mm x 1 mm), is located at each end of the channels. The non-porous SiN membranes are removed with scotch tape, thus the openings clear the path for microfluidic connection to the bottom side of the chip. Membrane images were taken using a Zeiss LEO 1550 scanning electron microscope.

*Polydimethylsiloxane (PDMS) sheets* are attached on both sides of SiN<sub>FLOW</sub> chips to confine microfluidic channels. The sheets were fabricated by spin coating of PDMS. Therefore, PDMS based agent and curing agent (Sylgard 184, Sigma Aldrich, Switzerland) were mixed in a 10:1 weight ratio. After degassing, this mixture was spin coated onto a silanized silicon wafer ( $\varnothing$  100 mm, single side polished) at 100 rpm for 60 sec. Silanization was performed by evaporation of chlorotrimethylsilane (TMCS, Sigma Aldrich, Switzerland) to form a passivation layer on the wafer surface that allows simple PDMS detachment. Subsequently, PDMS was cured for at least 2 h at 80°C. A thickness of 1 mm of the PDMS layer was determined with a digital measuring slide. The PDMS sheets were cut to shape by using pre-manufactured aluminum templates, a scalpel and a puncher. The top PDMS sheet is characterized by 10 holes: 4 for inlets, 4 for outlets and 2 for electrode access. This sheet

was used to define the upper microfluidic channel, which is integrated in the SiN<sub>FLOW</sub> chip (dimensions: height: 0.38 mm, base area: 10 x 1 mm, wall angle from pyramidal KOH etching: 35.26°, volume: 5 µL). The bottom PDMS sheet contains two rectangular openings to serve as lower microfluidic channels (dimensions: height: 1 mm, width: 1.5 mm, length: 20 mm, volume: 30 µL).

*A modified micro-well plate* was used as platform for reactor assembly on the plates bottom and perfusion from top micro-wells. A 384 well polystyrene microplate and associated lid (Greiner Bio-One, Switzerland) were adapted by hole drilling for microfluidic and electrode connections and for sampling of microchannel eluates. Milling of micro-well walls, to connect individual wells, was performed to create a down-grade slope from in- to outlets to allow for an open microfluidic circuit and to generate a drainage. In detail, outlet well and adjacent drainage well were connected via partial milling (6 mm) of the well wall and drainage wells were interconnected by total milling (9 mm) of connecting well walls. The drain was integrated in the side wall of the microplate by hole drilling and gluing of a shortened flow connector (Ø 8 mm, NORMAPLAST, Tecalto, Switzerland) with two-component epoxy adhesive (Loctite M-21HP Hysol, Henkel). A tubing (Ø 7.5 mm, silicone, Fisher Scientific, Switzerland) was fixed to the drain connector on one side and to a collection reservoir (50 mL falcon tube, TPP, Switzerland) on the other. For open microfluidics, tubings (PTFE, inner Ø: 1.06 mm; Fischer Scientific, Switzerland) were fixed into appropriate holes within the lid using short pieces of flexible tygon tubing (Sigma Aldrich, Switzerland) as adapters. For perfusion, the micro-well plate was closed with the lid and tubings were connected to medium filled syringes (Once/Codan, Huber, Switzerland), which were installed on a microfluidic pump (NE-1000, SyringePump, Switzerland).

*Electrodes* for impedance sensing were integrated in the fish-gut-on-chip device. The top electrode was created by implementing a platinum (Pt) wire Ø 0.3 mm (Advent research material, England) in the center of the upper microfluidic channel via a hole in the bottom of the micro-well plate. The wire was glued (Adhesive silicone CAF<sub>3</sub>, Bluestar Silicones, Silitech, Switzerland) into the appropriate well of the microplate to avoid leakage and wire dislocation during measurements. The bottom electrode was manufactured using standard photolithography lift-off technique to obtain a planar Pt electrode (1 mm x 8 mm) on glass substrate. Electrodes composed of a 20 nm thick titanium adhesion layer and a 200 nm thick Pt layer were sequentially evaporated on a float glass wafer (Ø100 mm, 525 µm thick) (LAB 600H evaporator, Leybold Optics). Individual electrode platelets (18 mm x 22 mm) were obtained by dicing of the wafer. The active electrode sensing area (1.5 mm<sup>2</sup>) was determined by attaching the glass platelet to the bottom PDMS sheet, which forms the lower microfluidic channel. Electrode connection for impedance sensing was realized with spring

contacts (3A 24.64 mm Round Head and 90° Concave, Distrelec, Switzerland) mounted from the top of the micro-well plate.

*Polycarbonate (PC) platelets* (3.4 mm x 4.9 mm x 2 mm) were obtained by trimming of PC plates (Röhmi, Switzerland) and hole drilling for screw connection.

Prior to *reactor assembly*, PDMS sheets were cleaned from dust using Scotch tape and all reactor parts were sterilized with ethanol (70%) for 10 min, dried under a sterile bench, and exposed to UV light for 30 min. Microfluidic tubings and syringe connectors (Rotilabo, Roth, Switzerland) were autoclaved. For reactor assembly, all parts were aligned to the modified bottom of the microplate in the following order: upper PDMS sheet – SiN<sub>FLOW</sub> chip – lower PDMS sheet – electrode platelet – PC platelet. Individual parts, besides PC platelet, stuck together by the adhesive nature of PDMS. The installation of the PC platelets was done to avoid leakage and to strengthen assembly of the whole composition.

## Cell culture

*Cell lines and culture conditions:* Experiments were performed with the epithelial cell line RTgutGC(A. Kawano *et al.* 2011) and the fibroblast cell line RTgutF (Chapter 3), both established from the intestine of rainbow trout. Cells were routinely grown in Leibovitz's L-15 medium (Invitrogen, Switzerland), supplemented with 5% fetal bovine serum (FBS; PAA, Switzerland) for RTgutGC and 10% FBS for RTgutF, and 1% gentamycin (GIBCO, Invitrogen, Switzerland). Cells were maintained at 19±1°C under normal atmosphere in the dark.

Prior to *cell seeding in the fish-gut-on-chip device*, microfluidic channels were filled with ethanol (70%), incubated for 5 min and replaced stepwise by sterile milliQ water to avoid the formation of air bubbles. Then, the upper channel was flushed thrice with 100 µL of coating solution, containing 50 µg/µL fibronectin in sterile water and incubated for 4 h. Thereafter, coating solution in the channel was replaced by L-15/FBS (5%). For the co-culture setting, the lower channel was coated subsequently with the same procedure, but during coating the in- and outlet wells were closed with a sterile sealing foil (Fisher Scientific, Switzerland) and the whole fish-gut-on-chip assembly was placed upside down. It is important that solutions are never removed from microfluidic channels but that liquids are gently replaced by adding the new solution through inlet wells, which results in flushing of the channels.

Cell seeding of monocultures of RTgutGC was obtained by flushing the upper channel with 2 x 100  $\mu\text{L}$  of cell suspension containing  $1.4 \times 10^6$  cell/mL in L-15/FBS (5%). After cell attachment, occurring within 30 min, the upper channel was flushed thrice with 100  $\mu\text{L}$  of L-15/FBS (5%) to remove unattached cells. For co-culture establishment, RTgutF cells were seeded first in the lower channel by filling the channel with cell suspension containing 55'000 cell/mL in L-15/FBS (10%), closing the in- and outlet wells with foil, and placing the reactor upside down to allow cell settling on the membrane. After 30 min, the reactor was turned back, the lower channel flushed thrice with 100  $\mu\text{L}$  of L-15/FBS (10%) and RTgutGC cells were seeded as described above. After the mono- or co-culture seeding procedure, cells were incubated at  $19 \pm 1^\circ\text{C}$  under normal atmosphere in the dark for two days prior to flow application.

For *flow application*, the upper channel was perfused at various flow rates (20  $\mu\text{L}/\text{h}$ , 200  $\mu\text{L}/\text{h}$ , 600  $\mu\text{L}/\text{h}$ ), resulting in very low to moderate shear stress of, respectively, 0.002  $\text{dyne}/\text{cm}^2$ , 0.02  $\text{dyne}/\text{cm}^2$  and 0.06  $\text{dyne}/\text{cm}^2$ , on the apical surface of RTgutGC cells. Perfusion of the lower channel (200  $\mu\text{L}/\text{h}$ ) ensured fresh media supply from the basolateral side of RTgutGC cells and, if present, sustained cell viability of RTgutF cells, while creating only minimal, unavoidable shear stress (0.002  $\text{dyne}/\text{cm}^2$ ). For static cultures, serving as control, channels were flushed with new medium (2 x 100  $\mu\text{L}$ ) on a daily base.

### **Epithelial barrier measurements**

*Impedance spectroscopy* was performed to determine trans-epithelial electrical resistance (TEER) of RTgutGC monolayer and co-cultures with RTgutF. Baseline resistance (membrane without cells) was obtained prior to cell seeding and subtracted from the resistance generated by cells cultured on the membrane prior to calculation of TEER (in  $\Omega \cdot \text{cm}^2$ ). Impedance spectra were recorded from 100 Hz – 5 MHz at an amplitude of 20 mV using an impedance analyser (MFIA, Zurich Instruments, Switzerland).

#### *Triton exposure*

A proof-of-principal experiment for detecting changes in impedance due to chemical stress was performed on two days old RTgutGC cultures which were kept under static conditions in the fish-gut-on-chip device. To accomplish this, cells were exposed to different concentrations of Triton X-100 (Sigma Aldrich, Switzerland) in L-15/FBS (5%) ranging from 0.125% - 0.2%.

### Characterization of cellular features

*Phase-contrast images* of cells cultured on silicon nitride membranes were taken with Leica DMI600 inverted microscope.

*Immunocytochemical staining* of plasma membrane (cell mask) and cell nuclei (DAPI stain) of live cells was applied to determine cell density and cell height after exposure to various shear stress conditions. Cellular polarization was analyzed by staining of the tight junction protein ZO-1, cytoskeletal f-actin (phalloidin) and cell nuclei (DAPI stain) on fixed cells. Prior to staining, SiN<sub>FLOW</sub> chips accommodating cultured cells on SiN membranes were disassembled from the microfluidic reactor.

For live staining, cells were washed thrice in phosphate buffered saline (PBS) and cell mask deep red plasma membrane stain (7.5 µg/mL in PBS, ThermoFisher, Switzerland) was applied together with DAPI stain for 8 min at room temperature. Subsequently, cells were washed thrice in PBS and SiN<sub>FLOW</sub> chips were mounted onto microscope slides.

Fixed staining of ZO-1, f-actin and DAPI followed the same procedure as described previously (Drieschner *et al.* 2017). Briefly, cells were fixed in 3.7% paraformaldehyde (Invitrogen, Switzerland) in PBS for 10 min, followed by a quick washing step and permeabilization with 0.2% Triton X-100 in PBS for 15 min. After a further washing step with PBS, containing 0.1% Triton X-100, cells were incubated in Image-iT (Invitrogen, Switzerland) for 30 min, washed with PBS and primary antibody for tight junction staining (5 µg/mL, Alexa Fluor-coupled ZO-1 antibody, Invitrogen, Switzerland) was applied together with FITC coupled phalloidin (1:100; Sigma-Aldrich, Switzerland) in 0.5% goat serum and 0.05% Triton X-100 in PBS overnight at 4 °C. The next day, cells were washed with 0.1% Triton X-100 in PBS and subsequently incubated with 10.9 µM DAPI (Invitrogen, Switzerland) in PBS for 5 min. After repeated washing in 0.1% Triton X-100 in PBS and PBS only, SiN<sub>FLOW</sub> chips were mounted on microscope slides using ProLong Gold antifade reagent (Life Technology, United States).

Imaging and analysis was performed on a Leica SP5 Laser Scanning Confocal Microscope (Leica, Switzerland) using the LAS AF Lite 2014 software.

## **Statistics**

Statistical analysis was performed for TEER measurements on normal distributed data using two-way ANOVA.

## 4.3 Results and discussion

### Design and characterization of the fish-gut-on-chip model

The fish-gut-on-chip device was designed to recapitulate the microenvironment of the piscine intestine by mimicking flow phenomena within the lumen and rapid crosstalk between absorptive epithelial cells lining the intestinal wall and supportive fibroblasts present in the underlying connective tissue. The device has the typical "epithelium-on-chip" geometry, which consists of two parallel microfluidic channels separated by a permeable membrane.

In contrast to many microfluidic barrier models, which use non-physiological, several micron thick permeable membranes as support for cell growth (Kim *et al.* 2012, Griep *et al.* 2013, Ramadan *et al.* 2013, Shah *et al.* 2016), we developed the fish-gut-on-chip device by integrating an ultrathin, highly permeable silicon nitride (SiN) membrane (Figure 4.1). The membranes are framed in silicon chips and fabricated as array on silicon wafers. Individual chips are termed SiN<sub>Flow</sub> chip and comprise two experimental units for separate handling, where each unit incorporates a rectangular SiN membrane for cell culture and two square openings for perfusion of the bottom channel. The SiN membranes feature a thickness of only 500 nm, a pore size of ~1.2  $\mu\text{m}$  diameter and a porosity of 24%. This makes SiN membranes more comparable to the highly permeable basement membrane, which is found *in vivo* between different biological compartments, such as epithelium and underlying connective tissue in the intestine (Kalluri 2003). Moreover, SiN membranes are optically transparent and allow perfect visibility of cells during phase contrast imaging and fluorescence microscopy, even when imaging is performed through the membrane. Previous studies demonstrated the utility of thin SiN porous supports for nanoparticle translocation studies on static *in vitro* models of the human blood-brain-barrier (Kenzaoui *et al.* 2013) and human alveolar barrier (Jud *et al.* 2015), which is problematic with conventional permeable cell culture membranes due to their thickness ( $\geq 10 \mu\text{m}$ ) (Kenzaoui *et al.* 2012, Jud *et al.* 2015). Indeed, the production of SiN membranes, requiring clean room fabrication processes, is more expensive than production of PDMS (Le-The *et al.* 2018) or conventional polymeric culture membranes composed of e.g. polyethylene terephthalate (PET) or polycarbonate (PC). However, SiN porous supports are very robust and can be reused several times by applying the cleaning method outlined by (Kenzaoui *et al.* 2013).

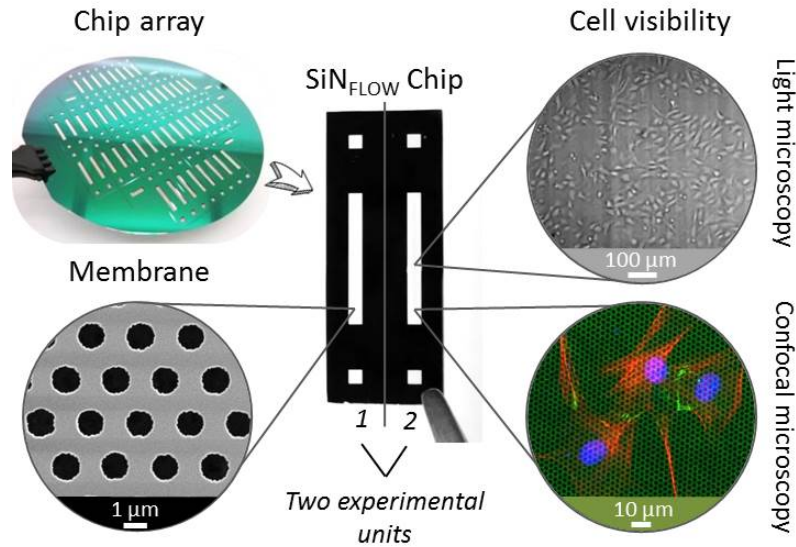


**Figure 4.1** Silicon nitride porous supports.

Silicon nitride (SiN) membranes are fabricated within individual chips (SiN<sub>Flow</sub> chip) in silicon wafers. Each chip is composed of two experimental units. Membranes are characterized by high porosity (scanning electron microscopy image, bottom left), transparency for cell monitoring (light microscopy, top right) and a thickness of only 500 nm that allows fluorescence microscopy of cells through the membrane (bottom right, membrane in green from laser reflection, cells are stained for cell nucleus in blue, cytoskeleton in red and tight junction protein ZO-1 in green).

Cell culture and flow application on the newly developed SiN<sub>Flow</sub> chips is achieved by integration of the chip within the fish-gut-on-chip device. The device combines several novelties; an overview of its assembly and working principal are depicted in Figure 4.2. Conceptually, the fish-gut-on-chip system is assembled on the bottom of a modified micro-well plate to allow for simplified reactor handling through the micro-wells from the top, which includes coating, cell seeding, microfluidic and electrode connection and sampling of microchannel outflow (Figure 4.2 A). Microfluidic channels are defined by sandwiching the SiN<sub>Flow</sub> chip between two sheets of patterned PDMS. From the bottom side the assembly is closed by a glass platelet with integrated planar electrodes for TEER evaluation and a polycarbonate platelet for fixation to the micro-well plate. The thickness of the modular stack on the bottom of the micro-well plate is less than 5 mm and allows for microscopic investigation of cells cultured on the SiN membrane from the bottom. For rearrangement of the piscine intestinal mucosal architecture, epithelial RTgutGC and fibroblastic RTgutF cells can be cultured on opposite membrane sides. This allows to create asymmetric exposure conditions: one channel simulates realistic flow rates and a medium composition as found in the intestinal lumen; and the other mimics the steady renewal of nutrients from the blood circulation.

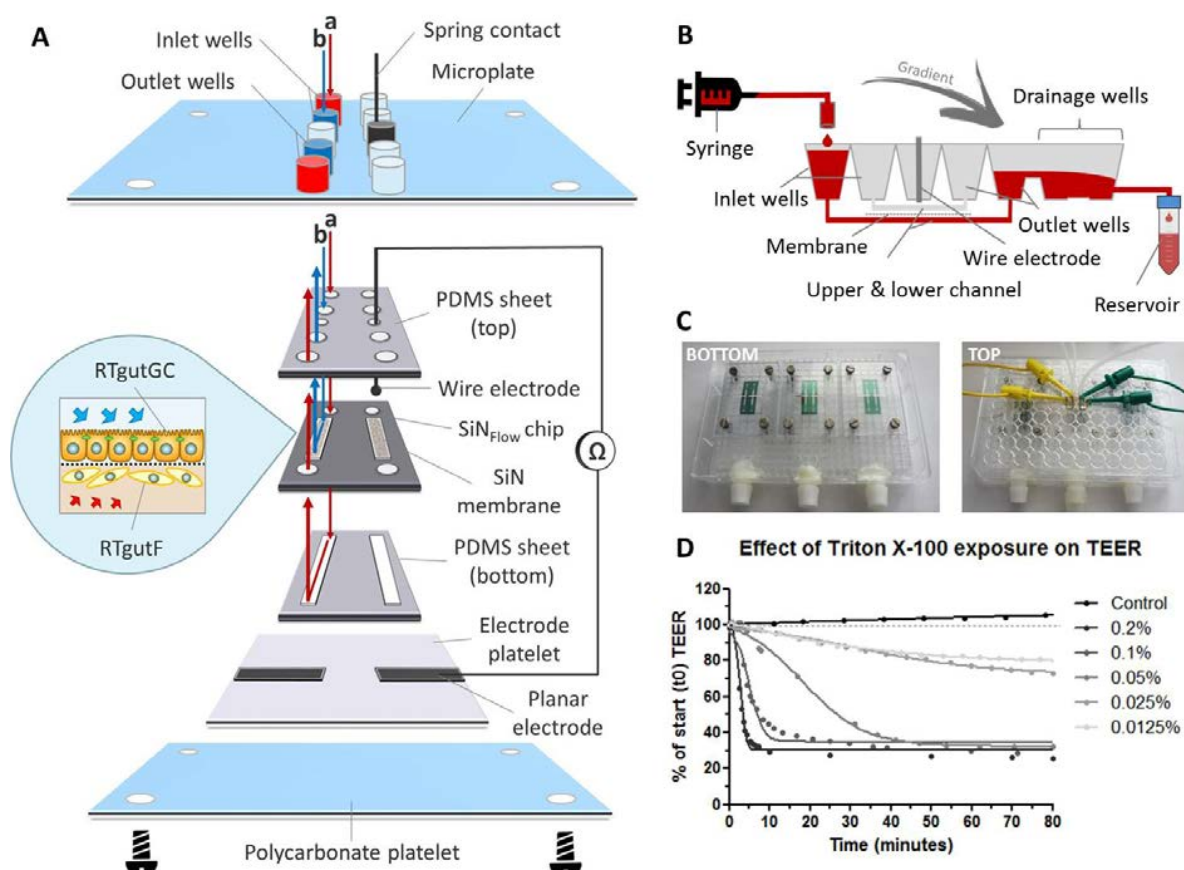


Figure 4.2. The fish-gut-on-chip model.

(A) The device is composed of a modular stacked assembly of the SiN<sub>Flow</sub> chip sandwiched between two sheets of PDMS and an electrode platelet from the bottom. This arrangement is screwed to the bottom of a modified 384 well plate using a polycarbonate platelet. The micro-well plate format allows for simplified perfusion of the upper and lower microfluidic channels from the top micro-wells and connection to reactor integrated electrodes with spring contacts. Membrane magnification depicts conceptual cell culture of epithelial RTgutGC and fibroblastic RTgutF cells on opposite membrane sides. (B) Working principle of open microfluidic circuit sketched for the lower microfluidic channel on a partial cross-section of the micro-well plate. (C) Photographs of bottom and top side of the reactor. Bottom view: 3 SiN<sub>Flow</sub> chips are assembled on the well plate. Top view: The middle chip is connected with tubing's for perfusion and cables for impedance spectroscopy. (D) Effect of varying concentrations of Triton X-100 on barrier tightness of RTgutGC monolayer.

For flow application, an open microfluidic circuit was implemented in the fish-gut-on-chip device (Figure 4.2 B). The drop-wise filling of the inlet wells from syringe-connected tubings results in perfusion of the upper and/or lower channel. Subsequently, the outlet wells are filled with liquid, which flows over to the drainage wells due to gradient driven forces along the down-grade slope of interconnected micro-wells. The outflow is finally collected in an installed reservoir. This perfusion strategy prevented air bubble formation in the microfluidic channels, which is a serious obstacle for long-term cell-culture in microfluidic systems (Sung and Shuler 2009, Zheng *et al.* 2010). Open microfluidics can be applied for low- to midrange flow rates, as required to simulate fluid flow in the intestine (Kim *et al.* 2012). Very high flow rates, as applied for *in vitro* blood vessel models (Morigi *et*

*al.* 1995), might not be possible because the pressure to force fluids through the microfluidic channels is limited.

For parallelization of experiments, which is a major goal for facilitated organ-on-chip application (Rogal *et al.* 2017), each microplate was equipped with three SiN<sub>FLOW</sub> chips, with each being composed of two experimental units (Figure 4.2 C). Thus, a total of six experimental conditions can be tested simultaneously. Connection to microfluidic tubings and electrodes for impedance-based TEER measurements were established through the micro-plate lid (Figure 4.2 C), which can be removed during experimentation. This facilitates manipulation of individual chips, e.g. for microscopy of samples at different time points.

The functional formation of an epithelial barrier by RTgutGC cells within the fish-gut-on-chip device was verified with TEER measurements. Impairment of the cellular barrier through exposure to different concentrations of Triton X-100, a non-ionic surfactant known to permeabilize the cell membrane (Schnaitman 1971), was performed as proof-of-principal to test the reliability of measurements obtained through reactor integrated platinum electrodes (Figure 4.2 D). During Triton X-100 exposure, RTgutGC cells showed a concentration dependent decline in TEER, expressed in percent of the resistance prior exposure. Effects for concentrations between 0.05-0.2% were observed immediately within the first minutes of exposure and resulted in a rapid decline of resistance within 5-40 minutes down to ~30%. The 30% threshold most likely represents the resistance of dead cells, which remained attached to the culture surface. Indeed, Triton X-100 concentrations of 0.1% and 0.2% are used for cell membrane permeabilization within 15 minutes during immunocytochemical staining (see protocol in materials and methods). The excessive membrane permeabilization at these concentrations, in turn, results in cell death (Dayeh *et al.* 2004). Lower concentrations of 0.0125 and 0.025% showed a steady but less steep decline to 70-80% within the exposure time of 80 min. These values are in the same range as previously reported EC<sub>50</sub> values for 2 h exposure of fish and mammalian cells obtained from viability assays (Dayeh *et al.* 2004). Hence, we demonstrated the successful application of on-line TEER evaluation by impedance spectroscopy in order to monitor barrier tightness of the RTgutGC epithelial cell layer. Further improvement of TEER recording might be obtained by the 4-point impedance measurement approach, which requires the integration of four electrodes, two on each side of the permeable membrane. This could be wire electrodes inserted in channel in- and outlets (van der Helm *et al.* 2016) or micro-fabricated, planar and preferentially semi-transparent electrodes on solid support (Henry *et al.* 2017) to still allow for visual inspection of cells. The 4-point technique makes TEER evaluation more robust by reducing variations of non-biological origin, e.g. from small changes in

temperature or medium composition (van der Helm *et al.* 2016). In addition, a more accurate representation of TEER would be obtained upon application of a fitting algorithm according to equivalent circuit modeling (Douville *et al.* 2010).

### **Response of the gut-on-chip to shear stress and supportive fibroblasts**

To explore the physiological relevance of mimicking shear stress, epithelial RTgutGC cells were grown at first as monocultures under different flow conditions, followed by initiation of co-culture with fibroblastic RTgutF cells at one selected flow rate. For experimentation, the upper channel was lined by RTgutGC intestinal epithelial cells and culture medium was perfused at 20, 200 or 600  $\mu\text{L}/\text{h}$ , resulting in a shear stress of 0.002, 0.02 or 0.06  $\text{dyne}/\text{cm}^2$  respectively, after two days of pre-culture under static conditions. These shear rates have been selected to simulate the broad range of physiological flow occurring in the intestine (Kim *et al.* 2012). Perfusion of the lower channel mimicked the basolateral supply with nutrients from the blood stream. The applied constant flow caused very low shear stress of 0.002  $\text{dyne}/\text{cm}^2$  on intestinal RTgutF fibroblasts, if present. The response of the epithelial cells was compared to cells cultured under static conditions within the fish-gut-on-chip device and was evaluated by measuring TEER, a common marker for tight junction integrity (Srinivasan *et al.* 2015), by microscopic analysis of (i) cell density by nuclei staining, and (ii) cell height by cell membrane staining (Figure 4.3).

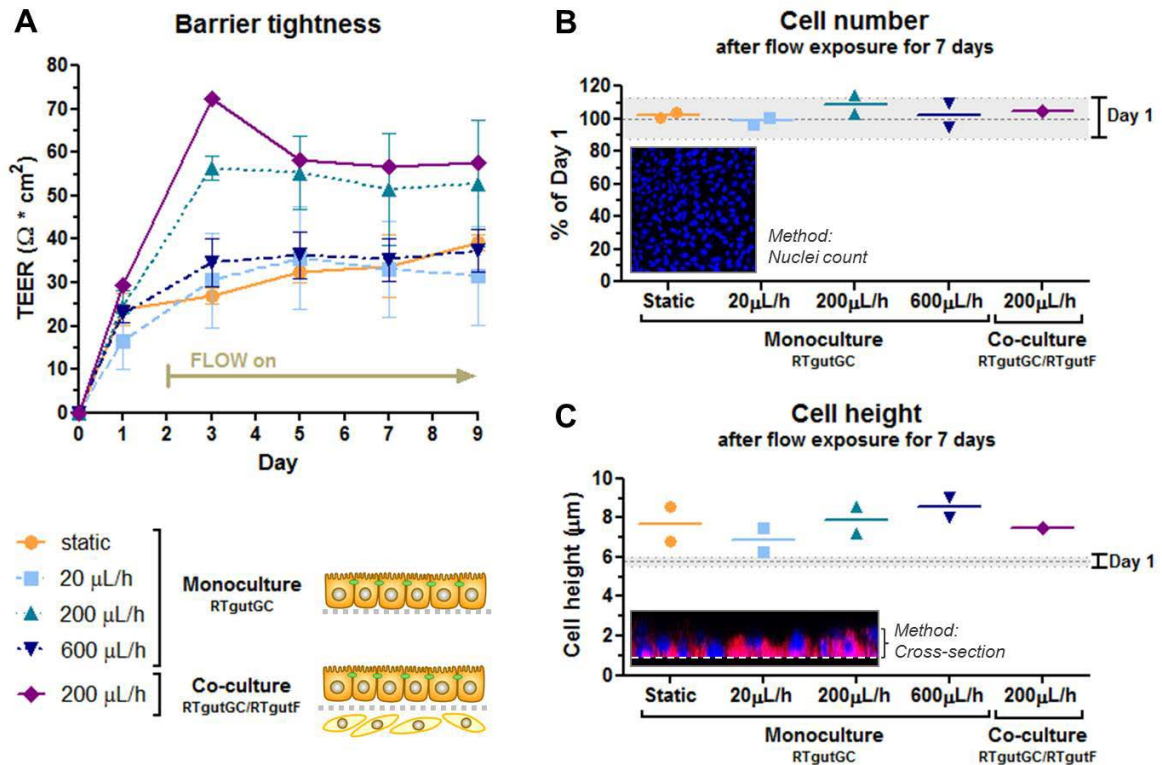


Figure 4.3. Impact of shear stress on epithelial barrier organization.

Effect of shear stress on the artificial fish gut was evaluated with TEER analysis (A), proliferation assessment (B) and cell height determination (C). Flow rates of 20 – 600  $\mu\text{L/h}$  were tested, resulting in shear stress of 0.002 – 0.06  $\text{dyne/cm}^2$  on the apical surface of RTgutGC cells. Experiments with RTgutGC monocultures were performed with 3 biological replicates for TEER and 2 biological replicates for cell number and cell height determination. Co-culture experiments were performed once.

TEER analysis of RTgutGC monolayer revealed a significant increase from  $\sim 30 \Omega \cdot \text{cm}^2$  for static cultures to  $\sim 55 \Omega \cdot \text{cm}^2$  for cultures under a flow of 200  $\mu\text{L/h}$  already after day 3 of culture (Figure 4.3 A). The resistance of flow-exposed cells (200  $\mu\text{L/h}$ ) remained stable until the end of the culture period of 9 days. Resistances for flow rates of 20  $\mu\text{L/h}$  and 600  $\mu\text{L/h}$  were comparable with static conditions. Co-cultures exposed to 200  $\mu\text{L/h}$  had resistance values similar to RTgutGC monocultures at the same flow rate. The resistance values of RTgutGC monolayer cultured under static conditions in the microfluidic bioreactor are in accordance with previously reported values obtained in cell culture inserts (Geppert *et al.* 2016, Minghetti *et al.* 2017) and on ultrathin alumina membranes (Drieschner *et al.* 2017). For freshwater adapted Atlantic salmon (*Salmo salar*), TEER values between 30 and 150  $\Omega \cdot \text{cm}^2$  have been reported (Sundell *et al.* 2003); thus RTgutGC cell cultures under static and flow conditions generally closely reflect the *in vivo* TEER in salmonids. Notwithstanding, RTgutGC cells exposed to moderate flow (0.02  $\text{dyne/cm}^2$ ) seem to adapt to that flow rate by an increase in barrier tightness. Likewise, an increase in TEER upon the same shear stress of 0.02  $\text{dyne/cm}^2$  has been reported for human intestinal cells, suggesting that mechanical distortion might

alter the formation of tight junctions (Kim *et al.* 2012). The effect of a supportive lamina of fibroblasts in the co-culture composition was less evident under flow conditions when compared to the static co-culture system established on ultrathin alumina membranes (Chapter 3). Further investigation would be required to single out if this is an artefact or if the difference originates from the changed culture substrate to silicon nitride membranes or if the combination of flow and co-culture has simply no additive effect on barrier tightness.

For cell seeding of RTgutGC we chose a density that allowed formation of a tightly packed monolayer. This leads to contact inhibition and cell cycle arrest in normal epithelial cells (Puliafito *et al.* 2012). Indeed, RTgutGC cells showed no or very low proliferative activity when compared to day one of the static system (Figure 4.3 B). In addition, proliferation was not modulated by any of the treatments, which makes the system more robust for further experimentation during the test period. These results are consistent with previous studies demonstrating that RTgutGC remain in monolayer for at least 14 days when seeded at a similar density on permeable membranes (Drieschner *et al.* 2017, Minghetti *et al.* 2017)(Chapter 2).

In the fish-gut-on-chip device, RTgutGC cells possessed a height of ~6  $\mu\text{m}$  at day 1. During the culture period of 9 days, cells increased only marginally in height to 7-9  $\mu\text{m}$ , which was independent of flow and co-culturing (Figure 4.3 C). The flattened morphology is a typical adaptation of static *in vitro* cell cultures, however, introduction of physiological stimuli, i.e. though fluid flow, is considered to promote cellular re-adaptation to their original morphology (van der Meer and van den Berg 2012). In the fish intestine *in vivo*, enterocytes possess a columnar shape and a height of ~30  $\mu\text{m}$  (Ostaszewska *et al.* 2005). In the human-gut-on-chip model by Kim *et al.* (2012), the mechanical stimulation of human intestinal epithelial (Caco-2) cells with fluid shear stress of 0.02 dyne/cm<sup>2</sup> was sufficient to increase cell height from 6  $\mu\text{m}$  to 30  $\mu\text{m}$ . The continued flattened morphology of RTgutGC cells during exposure to the same shear stress conditions might indicate a general lower potential to differentiate into functional enterocytes, at least under the thus far explored conditions. Caco-2 cells, in contrast, were found to express strong tight junctions and to form microvilli for apical surface enlargement, even when cultured under static conditions, for an extended culture period of 21 days (Press and Di Grandi 2008).

The co-culture of epithelial RTgutGC and fibroblastic RTgutF cells is an advanced approach to better mimic the complexity of the intestinal wall (Chapter 3). Having established fluid flow now allowed to examine the expression of the tight junction protein ZO-1, orientation of cytoskeletal f-actin and general cellular organization under realistic shear flow conditions (0.02 dyne/cm<sup>2</sup> on RTgutGC cells)

(Figure 4.4). As demonstrated previously, RTgutGC cells express ZO-1 as continuous line on the apical cell boarder already at day 1 (Drieschner *et al.* 2017, Minghetti *et al.* 2017) (Chapter 2) and expression remains stable until day 9. In contrast, RTgutF cells exhibit only scattered ZO-1 patterns, which is coherent with the basic characterization of the RTgutF cell line (Chapter 3) and the fact that fibroblasts do not form functional tight junctions (Sorrell and Caplan 2009). Clear differences were found in actin skeleton organization in RTgutF over time under flow: while actin fibers formed an unorganized network at day 1, they were found to be aligned and tightly packed at day 9. Furthermore, RTgutGC cells remained in a monolayer over the culture period, whereas RTgutF cells, originally seeded as monolayer (day 1), proliferated and formed a multilayer of 2-3 levels (day 9) (Figure 4.4, cross-section, DAPI stain).

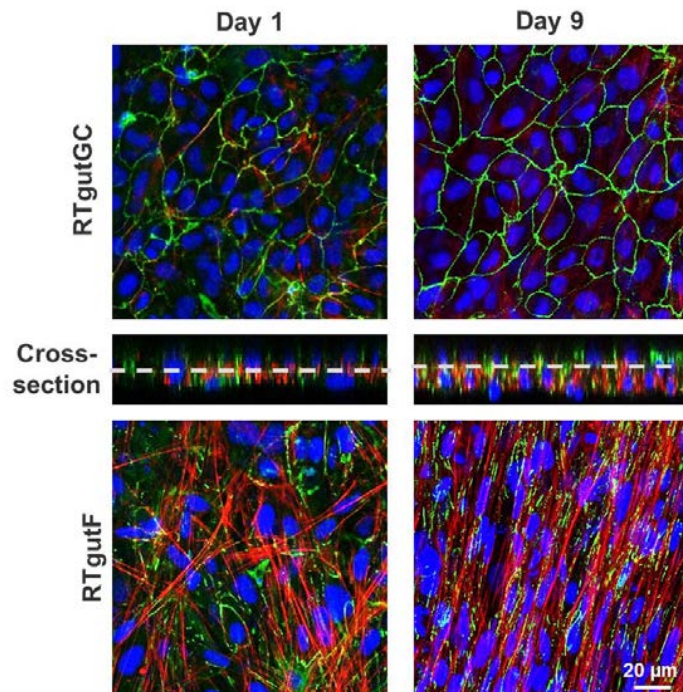


**Figure 4.4.** Co-culture of piscine intestinal epithelial (RTgutGC) and fibroblast (RTgutF) cell lines.

Cells were cultured for 9 days in the fish-gut-on-chip device, with RTgutGC exposure to a shear stress of  $0.02 \text{ dyne/cm}^2$ . Cells were stained for the tight junction protein ZO-1 (green), cytoskeletal f-actin (red) and nuclei (blue) and analyzed with confocal microscopy.

The fact that the fibroblasts proliferate while the epithelial cells do not, adds a dynamic component that needs to be considered when doing time-resolved analysis. The established co-culture model is particularly valuable for understanding the role of the fish intestine as immunological barrier. Herein, fibroblasts present an immune competent cell type, which releases cytokines to attract other cell types of the intrinsic immune system e.g. upon stimulation through bacterial toxins (Sorrell and Caplan 2009).

## 4.4 Conclusion

The fish-gut-on-chip device provides a controllable innovative microfluidic platform to study critical barrier functions in the presence of relevant physiological cues, including fluid flow and coexistence of supporting fibroblasts. Characterization of the model revealed that physiological realistic fluid flow and shear stress, as experienced in the living intestine, is sufficient to promote stable intestinal epithelial tightening, which is enhanced compared to static piscine intestinal barrier models. The co-culture of epithelial cells and fibroblasts in order to reconstruct basic intestinal architecture, is supported particularly through the ultrathin and porous silicon nitride membrane, which serves as cell culture interface. The fish-gut-on-chip device may therefore facilitate studies of, e.g., xenobiotic uptake or immunological defense mechanisms. Given the modularity of the device and the flexibility of its set-up, other epithelial barrier systems of fish or other organisms, including humans, might also be modelled with this device.

### Contributions

I designed and fabricated the SiN<sub>FLOW</sub> chip and the microfluidic bioreactor. Cell culture, immunocytochemical staining and confocal microscopy was performed by Sarah Könemann. I accomplished the impedance measurements, analyzed all data and wrote the manuscript of this chapter. Kristin Schirmer and Philippe Renaud were supervising the whole project.

## Chapter 5. Conclusion and future perspective

This thesis gathered information on the behavior of fish intestinal cells in an artificial, engineered microenvironment. It lays the ground for new strategies of reconstructing and monitoring *in vitro* epithelial barrier function using the organ-on-chips principal. The main conclusions from this dissertation can be summarized as follows:

- Ultrathin aluminum oxide and silicon nitride membranes are superior in their great permeability and thinness, which makes them an excellent culture substrates for barrier-forming cells
- Co-culture of piscine intestinal epithelial cells (RTgutGC) and fibroblasts (RTgutF) has a positive effect on barrier function
- Moderate shear stress enhances barrier tightness of RTgutGC cells

In the following part, these outcomes are discussed and set into perspective for future research.

### 5.1 Ultrathin permeable membranes as novel culture interface

The first part of this dissertation (Chapter 2) focused on the development of a new type of ultrathin membrane composed of anodized aluminum oxide as culture interface for barrier forming cells which closely mimics the highly permeable basement membrane. The anodization of aluminum is a low-cost and well characterized process and its application to thin alumina films resulted in self-formation of densely packed nanopores. The thus created membranes were demonstrated as favorable porous substrates for piscine intestinal cell culture by supporting epithelial monolayer formation, polarization and barrier tightening. Further, these membranes facilitate the initiation of co-cultures of epithelial and fibroblast cells by adopting the role of the basement membrane that acts as physical support for epithelial cell anchoring and separation from underlying fibroblasts in a physiological realistic manner. Not reported previously for cell culture application was the release of aluminum ions, which might limit their application range for physiological and toxicological studies. The deposition of a passivation layer of titanium dioxide on the membranes, in turn, prevented the aluminum ion release, but also diminished pore size. Another method to improve thermal stability and resistance against acid, base, and other corrosive chemicals of the AAO surface could be a high

temperature treatment (Lee and Park 2014). In conclusion, this membrane type is an interesting alternative to conventional, several micrometer thick cell culture membranes, when a transparent and highly permeable substrate with pores in the nanometer range is beneficial. Given the extraordinary permeability of AAO membranes, specifically for small molecules, a future application is the mechanistic investigation of intestinal transport mechanisms during acclimation of the piscine intestinal epithelium to increasing concentrations of salinity, which would mimic the journey of rainbow trout from fresh- to seawater. A first approach in this direction was already performed for RTgutGC cells cultured in commercial inserts, supporting the notion that epithelial cells acclimatize by barrier tightening, as verified with TEER measurements (Minghetti *et al.* 2017). In a follow-up approach, with the physiologically more relevant AAO membranes, the barrier tightening could be further examined with transport studies of small fluorescent molecules, such as Lucifer yellow and Dextran of different sizes. A model of seawater acclimatized piscine intestinal epithelia would indeed be useful to understand e.g. chemical uptake mechanisms not only for fresh- but also for saltwater adapted fish.

To create of the fish-gut-on-chip microfluidic bioreactor (Chapter 4), a second type of ultrathin membranes, composed of silicon nitride, was explored. These membranes were fabricated according to established protocols with pore sizes in the micrometer range, but also fabrication with nanopores is possible (Kuiper *et al.* 1998). Characteristic epithelial features of piscine intestinal cells were supported equally as when cultured on commercial insert- or ultrathin aluminum oxide membranes. In addition, membranes can be re-used and were fabricated thinner and with a higher porosity than aluminum oxide membranes because of better stability. Thus, this type of membrane, even when fabrication is still associated with high costs, has enormous potential to replace conventional cell culture membranes to enable realistic permeation studies. As such, nanoparticle translocation, which is often hampered by commercial membranes (Kenzaoui *et al.* 2012), can now be performed without limitations for epithelial and endothelial *in vitro* barrier models. Another application area are specific microscopy techniques, such as X-ray, scanning and transmission electron microscopy, where investigations of cells, cultured on thin, non-porous silicon nitride membranes is already established, and in favor because it can be coupled to correlative light microscopy (Finney *et al.* 2007, Nishiyama *et al.* 2010, Ring *et al.* 2011). As such, these microscopy techniques could be applied to barrier forming cells on porous silicon nitride membranes to unravel physiological and toxicological mechanisms.

Ultrathin permeable membranes provide an innovative new cell culture substrate for biomimetic epithelial tissue models. This thesis for the first time explored their potential to fish cells and is the

first work, to our knowledge, that integrated ultrathin membranes within a microfluidic device for creation of an optimal physiological environment through the inclusion of flow. This approach offers a unique opportunity to improve current *in vitro* barrier models of fish or other organisms, including humans.

## **5.2 Role of cellular complexity of the intestinal barrier *in vitro***

The attempt to reconstruct basic intestinal architecture comprised the combination of piscine intestinal epithelial cells and fibroblasts on ultrathin membrane chips (Chapter 3 & 4). The resulting increase in barrier resistance, compared to epithelial monolayers, can be interpreted as enhanced barrier tightness, which indicates better mimicry of the *in vivo* counterpart. The inclusion of a second cell type in the barrier model, on the other hand, decreased simplicity because the system now consists of more 'parts', which in turn diminishes robustness and throughput. As example, the continuous proliferation of fibroblasts adds a dynamic component to the intestinal barrier model, which needs to be considered well during experimentation to obtain reliable and repeatable results. Consequently, the simpler one-cell-type approach, using only absorptive epithelial cells, might be preferable for conventional uptake studies e.g. of chemicals. On the contrary, specific research questions, e.g. on the immune responsiveness of the intestinal barrier, would clearly benefit from the co-culture system because fibroblasts are an immune competent cell type (Sorrell and Caplan 2009) and are thus involved in immunological defense mechanisms of the intestinal barrier (Dezfuli *et al.* 2008). Further investigations in this direction would require the confirmation of established piscine intestinal fibroblasts (RTgutF) as immune active cell type, as done for a rainbow trout fibroblast cell line from the hypodermis (Ingerslev *et al.* 2010). Other important cellular protagonists involved in intestinal barrier function are mucus secreting goblet cells scattered within the epithelium, immune cells such as macrophages and lymphocytes, and endothelial cells lining blood vessels that supply the intestine (Grosell *et al.* 2011). Replicating the entire architecture as occurring in the living tissue *in vitro* may not be desirable or even feasible as discussed above, but understanding the role of each single 'part' is essential for a better *in vitro* to *in vivo* extrapolation and can be performed in a step wise manner.

## **5.3 Potential of the perfused fish-gut-on-chip**

The developed fish-gut-on-chip device mimics physiological realistic fluid shear stress on the epithelial-lumen interface and continuously supplies nutrients from the mimicked blood compartment. A positive effect on epithelial resistance was found when cells were exposed to

moderate shear rates. This effect needs to be further investigated by permeation studies with fluorescent marker molecules as done by (Minghetti *et al.* 2017). The continuous perfusion of the microfluidic channels within the fish-gut-on-chip is beneficial for physiological and toxicological investigations. Bacterial – epithelial co-culture models are now possible, because an overgrowth of bacteria and associated epithelial cell death, as found under static conditions, is prevented because bacterial numbers are diminished on a regular base (Kim *et al.* 2012). Xenobiotic exposure scenarios benefit from the continuous supply of the exposure medium, which will facilitate to maintain constant chemical concentrations, which is difficult for hydrophobic and/or volatile compounds under static conditions (Tanneberger *et al.* 2010). As a vision, the development and combination of further miniaturized organ analogues, represented by rainbow trout derived cell lines, could be combined to a whole fish-on-chip microfluidic platform, to study systemic effects of chemical pollutants.

In conclusion, this thesis offers a strategy for the reconstruction of the piscine intestinal microenvironment *in vitro* by combining rainbow trout derived cell cultures with engineered and perfused microsystems. It provides fundamental information on the interaction of intestinal epithelial RTgutGC cells with novel permeable substrates, a supportive cell layer of fibroblasts and fluid shear stress. The newly developed models and methods, including protocols for ultrathin porous membrane fabrication in microchip format, a fibroblast cell line from the intestine of rainbow trout (RTgutF) specifically established and characterized in this study, and design parameters for fabrication of a microfluidic bioreactor are useful advances and can be applied to future investigations on the role and function of the fish intestinal barrier.

## Bibliography

- Agrawal, A. A., Nehilla, B. J., Reisig, K. V., Gaborski, T. R., Fang, D. Z., Striemer, C. C., Fauchet, P. M. and McGrath, J. L. (2010) 'Porous nanocrystalline silicon membranes as highly permeable and molecularly thin substrates for cell culture', *Biomaterials*, 31(20), 5408-17.
- Angeloni Suter, S., Favre, M., Ahmed, S., Giazzon, M., Matthey, N. and Liley, M. (2011) *Ultrathin porous support for nanoparticle translocation in vitro assay* Bio-MEMS, Nanotechnology & Life Sciences, CSEM, SA, Neuchâtel-Switzerland.
- Benson, K., Cramer, S. and Galla, H. J. (2013) 'Impedance-based cell monitoring: barrier properties and beyond', *Fluids Barriers CNS*, 10(1), 5.
- Bhatia, S. N. and Ingber, D. E. (2014) 'Microfluidic organs-on-chips', *Nature Biotechnology*, 32(8), 760-772.
- Bloch, S. R., Vo, N. T., Walsh, S. K., Chen, C., Lee, L. E., Hodson, P. V. and Bols, N. C. (2016) 'Development of a cell line from the American eel brain expressing endothelial cell properties', *In Vitro Cellular & Developmental Biology-Animal*, 52(4), 395-409.
- Bols, N. C., Dayeh, V. R., Lee, L. E. J. and Schirmer, K. (2005) 'Use of fish cell lines in the toxicology and ecotoxicology of fish. Piscine cell lines in environmental toxicology' in *Biochemistry and Molecular Biology of Fishes* Elsevier, 43-85.
- Bols, N. C. and Lee, L. E. (1991) 'Technology and uses of cell cultures from the tissues and organs of bony fish', *Cytotechnology*, 6(3), 163-87.
- Bols, N. C., Pham, P. H., Dayeh, V. R. and Lee, L. E. (2017) 'Invitromatics, invitrome, and invitroomics: introduction of three new terms for in vitro biology and illustration of their use with the cell lines from rainbow trout', *In Vitro Cellular & Developmental Biology-Animal*, 53(5), 383-405.
- Brennan, L. M., Widder, M. W., Lee, L. E. and van der Schalie, W. H. (2012) 'Long-term storage and impedance-based water toxicity testing capabilities of fluidic biochips seeded with RTgill-W1 cells', *Toxicol In Vitro*, 26(5), 736-45.
- Bruggemann, D. (2013) 'Nanoporous Aluminium Oxide Membranes as Cell Interfaces', *Journal of Nanomaterials*.
- Brunt, J. and Austin, B. (2005) 'Use of a probiotic to control lactococcosis and streptococcosis in rainbow trout, *Oncorhynchus mykiss* (Walbaum)', *Journal of Fish Diseases*, 28(12), 693-701.

- Buddington, R. K. and Diamond, J. M. (1987) 'Pyloric ceca of fish: a "new" absorptive organ', *Am J Physiol*, 252(1 Pt 1), G65-76.
- Buddington, R. K., Krogdahl, A. and Bakke-Mckellep, A. M. (1997) 'The intestines of carnivorous fish: structure and functions and the relations with diet', *Acta Physiol Scand Suppl*, 638, 67-80.
- Burkard, M., Whitworth, D., Schirmer, K. and Nash, S. B. (2015) 'Establishment of the first humpback whale fibroblast cell lines and their application in chemical risk assessment', *Aquat Toxicol*, 167, 240-247.
- Castano, A., Bols, N., Braunbeck, T., Dierickx, P., Halder, M., Isomaa, B., Kawahara, K., Lee, L. E. J., Mothersill, C., Part, P., Repetto, G., Sintes, J. R., Rufli, H., Smith, R., Wood, C. and Segner, H. (2003) 'The use of fish cells in ecotoxicology - The report and recommendations of ECVAM workshop 47', *Atla-Alternatives to Laboratory Animals*, 31(3), 317-351.
- Curtis, T. M., Collins, A., Gerlach, B., Brennan, L. M., Widder, M. W., Van der Schalie, W., Vo, N. and Bols, N. (2013) 'Suitability of invertebrate and vertebrate cells in a portable impedance-based toxicity sensor: temperature mediated impacts on long-term survival', *Toxicology in vitro*, 27(7), 2061-2066.
- Curtis, T. M., Widder, M. W., Brennan, L. M., Schwager, S. J., van der Schalie, W. H., Fey, J. and Salazar, N. (2009) 'A portable cell-based impedance sensor for toxicity testing of drinking water', *Lab on a Chip*, 9(15), 2176-83.
- Dao, M., Lim, C. T. and Suresh, S. (2003) 'Mechanics of the human red blood cell deformed by optical tweezers', *Journal of the Mechanics and Physics of Solids*, 51(11-12), 2259-2280.
- Dayeh, V. R., Chow, S. L., Schirmer, K., Lynn, D. H. and Bols, N. C. (2004) 'Evaluating the toxicity of Triton X-100 to protozoan, fish, and mammalian cells using fluorescent dyes as indicators of cell viability', *Ecotoxicology and Environmental Safety*, 57(3), 375-382.
- Dayeh, V. R., Schirmer, K. and Bols, N. C. (2002) 'Applying whole-water samples directly to fish cell cultures in order to evaluate the toxicity of industrial effluent', *Water Res*, 36(15), 3727-38.
- Dempsey, N. (2016) *Animal Experiment Statistics*, <http://researchbriefings.parliament.uk: July 2017>].
- Dey, A. and Chakrabarti, K. (2018) 'Current Perspectives of Telomerase Structure and Function in Eukaryotes with Emerging Views on Telomerase in Human Parasites', *International journal of molecular sciences*, 19(2), 333.

- Dezfuli, B. S., Giovinazzo, G., Lui, A. and Giari, L. (2008) 'Inflammatory response to *Dentitruncus truttae* (Acanthocephala) in the intestine of brown trout', *Fish & shellfish immunology*, 24(6), 726-733.
- Douville, N. J., Tung, Y.-C., Li, R., Wang, J. D., El-Sayed, M. E. and Takayama, S. (2010) 'Fabrication of two-layered channel system with embedded electrodes to measure resistance across epithelial and endothelial barriers', *Analytical chemistry*, 82(6), 2505-2511.
- Drieschner, C., Minghetti, M., Wu, S., Renaud, P. and Schirmer, K. (2017) 'Ultrathin Alumina Membranes as Scaffold for Epithelial Cell Culture from the Intestine of Rainbow Trout', *ACS Appl Mater Interfaces*, 9(11), 9496-9505.
- Esch, M. B., King, T. L. and Shuler, M. L. (2011) 'The role of body-on-a-chip devices in drug and toxicity studies', *Annu Rev Biomed Eng*, 13, 55-72.
- Esch, M. B., Sung, J. H., Yang, J., Yu, C., Yu, J., March, J. C. and Shuler, M. L. (2012) 'On chip porous polymer membranes for integration of gastrointestinal tract epithelium with microfluidic 'body-on-a-chip' devices', *Biomed Microdevices*, 14(5), 895-906.
- Falconnet, D., Csucs, G., Grandin, H. M. and Textor, M. (2006) 'Surface engineering approaches to micropattern surfaces for cell-based assays', *Biomaterials*, 27(16), 3044-3063.
- Finney, L., Mandava, S., Ursos, L., Zhang, W., Rodi, D., Vogt, S., Legnini, D., Maser, J., Ikpatt, F. and Olopade, O. I. (2007) 'X-ray fluorescence microscopy reveals large-scale relocalization and extracellular translocation of cellular copper during angiogenesis', *Proceedings of the National Academy of Sciences*, 104(7), 2247-2252.
- Fischer, S., Loncar, J., Zaja, R., Schnell, S., Schirmer, K., Smital, T. and Luckenbach, T. (2011) 'Constitutive mRNA expression and protein activity levels of nine ABC efflux transporters in seven permanent cell lines derived from different tissues of rainbow trout (*Oncorhynchus mykiss*)', *Aquat Toxicol*, 101(2), 438-46.
- Franke, W. W., Grund, C., Kuhn, C., Jackson, B. W. and Illmensee, K. (1982) 'Formation of cytoskeletal elements during mouse embryogenesis: III. Primary mesenchymal cells and the first appearance of vimentin filaments', *Differentiation*, 23(1-3), 43-59.
- Gaborski, T. R., Snyder, J. L., Striemer, C. C., Fang, D. Z., Hoffman, M., Fauchet, P. M. and McGrath, J. L. (2010) 'High-performance separation of nanoparticles with ultrathin porous nanocrystalline silicon membranes', *ACS nano*, 4(11), 6973-6981.
- Geppert, M., Sigg, L. and Schirmer, K. (2016) 'A novel two-compartment barrier model for investigating nanoparticle transport in fish intestinal epithelial cells', *Environmental Science: Nano*, 3(2), 388-395.
- Griep, L., Wolbers, F., De Wagenaar, B., ter Braak, P. M., Weksler, B., Romero, I. A., Couraud, P., Vermes, I., van der Meer, A. D. and van den Berg, A. (2013) 'BBB on

- chip: microfluidic platform to mechanically and biochemically modulate blood-brain barrier function', *Biomedical microdevices*, 15(1), 145-150.
- Grosell, M., Farrell, A. P. and Brauner, C. J. (2011) *The multifunctional gut of fish*, ELSEVIER.
- Günzel, D., Zakrzewski, S. S., Schmid, T., Pangalos, M., Wiedenhoef, J., Blasse, C., Ozboda, C. and Krug, S. M. (2012) 'From TER to trans-and paracellular resistance: lessons from impedance spectroscopy', *Annals of the New York Academy of Sciences*, 1257(1), 142-151.
- Handy, R. D., Henry, T. B., Scown, T. M., Johnston, B. D. and Tyler, C. R. (2008) 'Manufactured nanoparticles: their uptake and effects on fish—a mechanistic analysis', *Ecotoxicology*, 17(5), 396-409.
- Harris, J. H. (1995) 'The use of fish in ecological assessments', *Austral Ecology*, 20(1), 65-80.
- Harris, S. G. and Shuler, M. L. (2003) 'Growth of endothelial cells on microfabricated silicon nitride membranes for an in vitro model of the blood-brain barrier', *Biotechnology and Bioprocess Engineering*, 8(4), 246-251.
- Hay, E. D. (1995) 'An overview of epithelio-mesenchymal transformation', *Cells Tissues Organs*, 154(1), 8-20.
- Heileman, K., Daoud, J. and Tabrizian, M. (2013) 'Dielectric spectroscopy as a viable biosensing tool for cell and tissue characterization and analysis', *Biosensors and bioelectronics*, 49, 348-359.
- Henry, O. Y., Villenave, R., Crouce, M. J., Leineweber, W. D., Benz, M. A. and Ingber, D. E. (2017) 'Organs-on-chips with integrated electrodes for trans-epithelial electrical resistance (TEER) measurements of human epithelial barrier function', *Lab on a Chip*, 17(13), 2264-2271.
- Herrmann, H., Munick, M., Brettel, M., Fouquet, B. and Markl, J. (1996) 'Vimentin in a cold-water fish, the rainbow trout: highly conserved primary structure but unique assembly properties', *Journal of cell science*, 109(3), 569-578.
- Hoess, A., Teuscher, N., Thormann, A., Aurich, H. and Heilmann, A. (2007) 'Cultivation of hepatoma cell line HepG2 on nanoporous aluminum oxide membranes', *Acta Biomaterialia*, 3(1), 43-50.
- Hoess, A., Thormann, A., Friedmann, A., Aurich, H. and Heilmann, A. (2010) 'Co-Cultures of Primary Cells on Self-Supporting Nanoporous Alumina Membranes', *Advanced Engineering Materials*, 12(7), B269-B275.
- Hoess, A., Thormann, A., Friedmann, A. and Heilmann, A. (2012) 'Self-supporting nanoporous alumina membranes as substrates for hepatic cell cultures', *Journal of Biomedical Materials Research Part A*, 100A(9), 2230-2238.

- Hoffmann, O. I., Ilmberger, C., Magosch, S., Joka, M., Jauch, K.-W. and Mayer, B. (2015) 'Impact of the spheroid model complexity on drug response', *Journal of biotechnology*, 205, 14-23.
- Hoyle, I. and Handy, R. (2005) 'Dose-dependent inorganic mercury absorption by isolated perfused intestine of rainbow trout, *Oncorhynchus mykiss*, involves both amiloride-sensitive and energy-dependent pathways', *Aquat Toxicol*, 72(1), 147-159.
- Hubatsch, I., Ragnarsson, E. G. and Artursson, P. (2007) 'Determination of drug permeability and prediction of drug absorption in Caco-2 monolayers', *Nat Protoc*, 2(9), 2111-9.
- Huh, D., Leslie, D. C., Matthews, B. D., Fraser, J. P., Jurek, S., Hamilton, G. A., Thorneloe, K. S., McAlexander, M. A. and Ingber, D. E. (2012a) 'A human disease model of drug toxicity-induced pulmonary edema in a lung-on-a-chip microdevice', *Sci Transl Med*, 4(159), 159ra147.
- Huh, D., Matthews, B. D., Mammoto, A., Montoya-Zavala, M., Hsin, H. Y. and Ingber, D. E. (2010) 'Reconstituting organ-level lung functions on a chip', *Science*, 328(5986), 1662-8.
- Huh, D., Torisawa, Y. S., Hamilton, G. A., Kim, H. J. and Ingber, D. E. (2012b) 'Microengineered physiological biomimicry: Organs-on-Chips', *Lab on a Chip*, 12(12), 2156-2164.
- Imura, Y., Asano, Y., Sato, K. and Yoshimura, E. (2009) 'A microfluidic system to evaluate intestinal absorption', *Anal Sci*, 25(12), 1403-7.
- Ingerslev, H. C., Ossum, C. G., Lindenstrom, T. and Nielsen, M. E. (2010) 'Fibroblasts Express Immune Relevant Genes and Are Important Sentinel Cells during Tissue Damage in Rainbow Trout (*Oncorhynchus mykiss*)', *Plos One*, 5(2).
- James, M. O., Altman, A. H., Morris, K., Kleinow, K. M. and Tong, Z. (1997) 'Dietary modulation of phase 1 and phase 2 activities with benzo(a)pyrene and related compounds in the intestine but not the liver of the channel catfish, *Ictalurus punctatus*', *Drug Metab Dispos*, 25(3), 346-54.
- Jang, K. J. and Suh, K. Y. (2010) 'A multi-layer microfluidic device for efficient culture and analysis of renal tubular cells', *Lab on a Chip*, 10(1), 36-42.
- Jani, A. M. M., Losic, D. and Voelcker, N. H. (2013) 'Nanoporous anodic aluminium oxide: Advances in surface engineering and emerging applications', *Progress in Materials Science*, 58(5), 636-704.
- Jud, C., Ahmed, S., Muller, L., Kinnear, C., Vanhecke, D., Umehara, Y., Frey, S., Liley, M., Angeloni, S., Petri-Fink, A. and Rothen-Rutishauser, B. (2015) 'Ultrathin Ceramic Membranes as Scaffolds for Functional Cell Coculture Models on a Biomimetic Scale', *Bioresearch Open Access*, 4(1), 457-468.

- Jutfelt, F. (2011) 'Barrier function of the gut', *Encyclopedia of fish physiology: from genome to environment*. Academic Press, San Diego, 1322-1331.
- Kalluri, R. (2003) 'Basement membranes: Structure, assembly and role in tumour angiogenesis', *Nature Reviews Cancer*, 3(6), 422-433.
- Kawano, A., Haiduk, C., Schirmer, K., Hanner, R., Lee, L. E. J., Dixon, B. and Bols, N. C. (2011) 'Development of a rainbow trout intestinal epithelial cell line and its response to lipopolysaccharide', *Aquaculture Nutrition*, 17(2), E241-E252.
- Kelly, B. C., Gobas, F. A. and McLachlan, M. S. (2004) 'Intestinal absorption and biomagnification of organic contaminants in fish, wildlife, and humans', *Environmental Toxicology and Chemistry*, 23(10), 2324-2336.
- Kenzaoui, B. H., Angeloni, S., Overstolz, T., Niedermann, P., Chapuis Bernasconi, C., Liley, M. and Juillerat-Jeanneret, L. (2013) 'Transfer of ultrasmall iron oxide nanoparticles from human brain-derived endothelial cells to human glioblastoma cells', *ACS Appl Mater Interfaces*, 5(9), 3581-6.
- Kenzaoui, B. H., Bernasconi, C. C., Hofmann, H. and Juillerat-Jeanneret, L. (2012) 'Evaluation of uptake and transport of ultrasmall superparamagnetic iron oxide nanoparticles by human brain-derived endothelial cells', *Nanomedicine*, 7(1), 39-53.
- Kim, H. J., Huh, D., Hamilton, G. and Ingber, D. E. (2012) 'Human gut-on-a-chip inhabited by microbial flora that experiences intestinal peristalsis-like motions and flow', *Lab on a Chip*, 12(12), 2165-74.
- Kim, H. J. and Ingber, D. E. (2013) 'Gut-on-a-Chip microenvironment induces human intestinal cells to undergo villus differentiation', *Integr Biol (Camb)*, 5(9), 1130-40.
- Klapper, W., Heidorn, K., Kühne, K. and Parwaresch, R. (1998) 'Telomerase activity in 'immortal'fish', *FEBS letters*, 434(3), 409-412.
- Komatsu, K., Tsutsui, S., Hino, K., Araki, K., Yoshiura, Y., Yamamoto, A., Nakamura, O. and Watanabe, T. (2009) 'Expression profiles of cytokines released in intestinal epithelial cells of the rainbow trout, *Oncorhynchus mykiss*, in response to bacterial infection', *Developmental & Comparative Immunology*, 33(4), 499-506.
- Konishi, S., Fujita, T., Hattori, K., Kono, Y. and Matsushita, Y. (2015) 'An openable artificial intestinal tract system for the in vitro evaluation of medicines', *Microsystems & Nanoengineering*, 1, 15015.
- Kruegel, J. and Miosge, N. (2010) 'Basement membrane components are key players in specialized extracellular matrices', *Cellular and Molecular Life Sciences*, 67(17), 2879-2895.

- Kuiper, S., Van Rijn, C., Nijdam, W. and Elwenspoek, M. C. (1998) 'Development and applications of very high flux microfiltration membranes', *Journal of Membrane Science*, 150(1), 1-8.
- Kunze, A., Giugliano, M., Valero, A. and Renaud, P. (2011) 'Micropatterning neural cell cultures in 3D with a multi-layered scaffold', *Biomaterials*, 32(8), 2088-98.
- Kwong, R. W., Andrés, J. A. and Niyogi, S. (2010) 'Molecular evidence and physiological characterization of iron absorption in isolated enterocytes of rainbow trout (*Oncorhynchus mykiss*): implications for dietary cadmium and lead absorption', *Aquat Toxicol*, 99(3), 343-350.
- Kwong, R. W. and Niyogi, S. (2008) 'An in vitro examination of intestinal iron absorption in a freshwater teleost, rainbow trout (*Oncorhynchus mykiss*)', *J Comp Physiol B*, 178(8), 963-75.
- Kwong, R. W. and Niyogi, S. (2009) 'The interactions of iron with other divalent metals in the intestinal tract of a freshwater teleost, rainbow trout (*Oncorhynchus mykiss*)', *Comp Biochem Physiol C Toxicol Pharmacol*, 150(4), 442-9.
- Kwong, R. W. and Niyogi, S. (2012) 'Cadmium transport in isolated enterocytes of freshwater rainbow trout: interactions with zinc and iron, effects of complexation with cysteine, and an ATPase-coupled efflux', *Comp Biochem Physiol C Toxicol Pharmacol*, 155(2), 238-46.
- Langan, L. M., Arossa, S., Owen, S. F. and Jha, A. N. (2017) 'Assessing the impact of benzo [a] pyrene with the in vitro fish gut model: an integrated approach for ecogenotoxicological studies', *Mutation Research/Genetic Toxicology and Environmental Mutagenesis*.
- Le-The, H., Tibbe, M., Loessberg-Zahl, J., do Carmo, M. P., van der Helm, M., Bomer, J., van den Berg, A., Leferink, A., Segerink, L. and Eijkel, J. (2018) 'Large-scale fabrication of free-standing and sub- $\mu\text{m}$  PDMS through-hole membranes', *Nanoscale*, 10(16), 7711-7718.
- Le Ferrec, E., Chesne, C., Artusson, P., Brayden, D., Fabre, G., Gires, P., Guillou, F., Rousset, M., Rubas, W. and Scarino, M.-L. (2001) 'In vitro models of the intestinal barrier', *Atla*, 29, 649-668.
- LeBleu, V. S., Macdonald, B. and Kalluri, R. (2007) 'Structure and function of basement membranes', *Exp Biol Med (Maywood)*, 232(9), 1121-9.
- Lee, W. and Park, S.-J. (2014) 'Porous anodic aluminum oxide: anodization and templated synthesis of functional nanostructures', *Chemical reviews*, 114(15), 7487-7556.
- Leeuwen, C. J. v. (2007) *Risk Assessment of Chemicals*, 2nd ed., Bilthoven, Netherlands: Springer.

- Leonard, E. M., Nadella, S. R., Bucking, C. and Wood, C. M. (2009) 'Characterization of dietary Ni uptake in the rainbow trout, *Oncorhynchus mykiss*', *Aquat Toxicol*, 93(4), 205-16.
- Liang, E., Chessic, K. and Yazdanian, M. (2000) 'Evaluation of an accelerated Caco-2 cell permeability model', *Journal of pharmaceutical sciences*, 89(3), 336-345.
- Lilienblum, W., Dekant, W., Foth, H., Gebel, T., Hengstler, J., Kahl, R., Kramer, P.-J., Schweinfurth, H. and Wollin, K.-M. (2008) 'Alternative methods to safety studies in experimental animals: role in the risk assessment of chemicals under the new European Chemicals Legislation (REACH)', *Archives of toxicology*, 82(4), 211-236.
- Lokka, G., Austbo, L., Falk, K., Bjerkas, I. and Koppang, E. O. (2013) 'Intestinal morphology of the wild Atlantic salmon (*Salmo salar*)', *J Morphol*, 274(8), 859-76.
- Ma, S. H., Lepak, L. A., Hussain, R. J., Shain, W. and Shuler, M. L. (2005) 'An endothelial and astrocyte co-culture model of the blood-brain barrier utilizing an ultra-thin, nanofabricated silicon nitride membrane', *Lab on a Chip*, 5(1), 74-85.
- Malhão, F., Urbatzka, R., Navas, J., Cruzeiro, C., Monteiro, R. and Rocha, E. (2013) 'Cytological, immunocytochemical, ultrastructural and growth characterization of the rainbow trout liver cell line RTL-W1', *Tissue and Cell*, 45(3), 159-174.
- Marx, U. (2012) 'Trends in Cell Culture Technology', *New Technologies for Toxicity Testing*, 745, 26-46.
- Meissner, R., Eker, B., Kasi, H., Bertsch, A. and Renaud, P. (2011) 'Distinguishing drug-induced minor morphological changes from major cellular damage via label-free impedimetric toxicity screening', *Lab on a Chip*, 11(14), 2352-61.
- Merrifield, D., Dimitroglou, A., Bradley, G., Baker, R. and Davies, S. (2009) 'Soybean meal alters autochthonous microbial populations, microvilli morphology and compromises intestinal enterocyte integrity of rainbow trout, *Oncorhynchus mykiss* (Walbaum)', *Journal of Fish Diseases*, 32(9), 755-766.
- Minghetti, M., Drieschner, C., Bramaz, N., Schug, H. and Schirmer, K. (2017) 'A fish intestinal epithelial barrier model established from the rainbow trout (*Oncorhynchus mykiss*) cell line, RTgutGC', *Cell Biol Toxicol*, 33(6), 539-555.
- Minghetti, M. and Schirmer, K. (2016) 'Effect of media composition on bioavailability and toxicity of silver and silver nanoparticles in fish intestinal cells (RTgutGC)', *Nanotoxicology*, 10(10), 1526-1534.
- Minghetti, M., Schnell, S., Chadwick, M. A., Hogstrand, C. and Bury, N. R. (2014) 'A primary Fish Gill Cell System (FIGCS) for environmental monitoring of river waters', *Aquat Toxicol*, 154, 184-192.

- Morigi, M., Zoja, C., Figliuzzi, M., Foppolo, M., Micheletti, G., Bontempelli, M., Saronni, M., Remuzzi, G. and Remuzzi, A. (1995) 'Fluid shear stress modulates surface expression of adhesion molecules by endothelial cells', *Blood*, 85(7), 1696-1703.
- Nehilla, B. J., Nataraj, N., Gaborski, T. R. and McGrath, J. L. (2014) 'Endothelial vacuolization induced by highly permeable silicon membranes', *Acta Biomaterialia*, 10(11), 4670-4677.
- Nishiyama, H., Suga, M., Ogura, T., Maruyama, Y., Koizumi, M., Mio, K., Kitamura, S. and Sato, C. (2010) 'Atmospheric scanning electron microscope observes cells and tissues in open medium through silicon nitride film', *Journal of structural biology*, 169(3), 438-449.
- Ojo, A. A. and Wood, C. M. (2007) 'In vitro analysis of the bioavailability of six metals via the gastro-intestinal tract of the rainbow trout (*Oncorhynchus mykiss*)', *Aquat Toxicol*, 83(1), 10-23.
- Organization, W. H. (1998) 'Aluminium' in *Guidelines for Drinking-Water Quality*, 2nd ed. 6-15.
- Ossum, C. G., Hoffmann, E. K., Vijayan, M., Holt, S. and Bols, N. (2004) 'Characterization of a novel fibroblast-like cell line from rainbow trout and responses to sublethal anoxia', *Journal of Fish Biology*, 64(4), 1103-1116.
- Ostaszewska, T., Dabrowski, K., Palacios, M. E., Olejniczak, M. and Wieczorek, M. (2005) 'Growth and morphological changes in the digestive tract of rainbow trout (*Oncorhynchus mykiss*) and pacu (*Piaractus mesopotamicus*) due to casein replacement with soybean proteins', *Aquaculture*, 245(1-4), 273-286.
- Pariselli, F., Sacco, M. and Rembges, D. (2009) 'An optimized method for in vitro exposure of human derived lung cells to volatile chemicals', *Experimental and Toxicologic Pathology*, 61(1), 33-39.
- Parkinson, L. G., Giles, N. L., Adcroft, K. F., Fear, M. W., Wood, F. M. and Poinern, G. E. (2009) 'The Potential of Nanoporous Anodic Aluminium Oxide Membranes to Influence Skin Wound Repair', *Tissue Engineering Part A*, 15(12), 3753-3763.
- Pereira, C., Araújo, F., Barrias, C. C., Granja, P. L. and Sarmiento, B. (2015) 'Dissecting stromal-epithelial interactions in a 3D in vitro cellularized intestinal model for permeability studies', *Biomaterials*, 56, 36-45.
- Poinern, G. E. J., Ali, N. and Fawcett, D. (2011) 'Progress in Nano-Engineered Anodic Aluminum Oxide Membrane Development', *Materials*, 4(3), 487-526.
- Powell, D. W., Pinchuk, I. V., Saada, J. I., Chen, X. and Mifflin, R. C. (2011) 'Mesenchymal cells of the intestinal lamina propria', *Annu Rev Physiol*, 73, 213-37.

- Press, B. and Di Grandi, D. (2008) 'Permeability for intestinal absorption: Caco-2 assay and related issues', *Current drug metabolism*, 9(9), 893-900.
- Puliafito, A., Hufnagel, L., Neveu, P., Streichan, S., Sigal, A., Fygenson, D. K. and Shraiman, B. I. (2012) 'Collective and single cell behavior in epithelial contact inhibition', *Proceedings of the National Academy of Sciences*, 109(3), 739-744.
- Rakers, S., Klinger, M., Kruse, C. and Gebert, M. (2011) 'Pros and cons of fish skin cells in culture: long-term full skin and short-term scale cell culture from rainbow trout, *Oncorhynchus mykiss*', *European journal of cell biology*, 90(12), 1041-1051.
- Ramadan, Q., Jafarpoorchehab, H., Huang, C., Silacci, P., Carrara, S., Koklu, G., Ghaye, J., Ramsden, J., Ruffert, C., Vergeres, G. and Gijs, M. A. (2013) 'NutriChip: nutrition analysis meets microfluidics', *Lab on a Chip*, 13(2), 196-203.
- Ring, E., Peckys, D., Dukes, M., Baudoin, J. and De Jonge, N. (2011) 'Silicon nitride windows for electron microscopy of whole cells', *Journal of microscopy*, 243(3), 273-283.
- Rogal, J., Probst, C. and Loskill, P. (2017) 'Integration concepts for multi-organ chips: how to maintain flexibility?!', *Future science OA*, 3(2), FSO180.
- Rovida, C. and Hartung, T. (2009) 'Re-evaluation of animal numbers and costs for in vivo tests to accomplish REACH legislation requirements for chemicals - a report by the transatlantic think tank for toxicology (t(4))', *ALTEX*, 26(3), 187-208.
- Sandvik, M., Horsberg, T. E., Skaare, J. U. and Ingebrigtsen, K. (1998) 'Comparison of dietary and waterborne exposure to benzo a pyrene: bioavailability, tissue disposition and CYP1A1 induction in rainbow trout *Oncorhynchus mykiss*', *Biomarkers*, 3(6), 399-410.
- Schirmer, K. (2006) 'Proposal to improve vertebrate cell cultures to establish them as substitutes for the regulatory testing of chemicals and effluents using fish', *Toxicology*, 224(3), 163-183.
- Schirmer, K., Chan, A., Greenberg, B., Dixon, D. and Bols, N. (1997) 'Methodology for demonstrating and measuring the photocytotoxicity of fluoranthene to fish cells in culture', *Toxicology in vitro*, 11(1-2), 107-119.
- Schmitt, P., Wacyk, J., Morales-Lange, B., Rojas, V., Guzmán, F., Dixon, B. and Mercado, L. (2015) 'Immunomodulatory effect of cathelicidins in response to a  $\beta$ -glucan in intestinal epithelial cells from rainbow trout', *Developmental & Comparative Immunology*, 51(1), 160-169.
- Schnaitman, C. A. (1971) 'Solubilization of the cytoplasmic membrane of *Escherichia coli* by Triton X-100', *Journal of bacteriology*, 108(1), 545-552.

- Schug, H., Begnaud, F., Debonneville, C., Berthaud, F., Gimeno, S. and Schirmer, K. (in preparation) 'TransFER: a new device to measure the transfer of volatile and hydrophobic organic chemicals across an in vitro intestinal fish cell barrier'.
- Seltana, A., Basora, N. and Beaulieu, J. F. (2010) 'Intestinal epithelial wound healing assay in an epithelial–mesenchymal co-culture system', *Wound Repair and Regeneration*, 18(1), 114-122.
- Semple, S., Vo, N., Li, A., Pham, P., Bols, N. and Dixon, B. (2017) 'Development and use of an Arctic charr cell line to study antiviral responses at extremely low temperatures', *Journal of Fish Diseases*.
- Shah, P., Fritz, J. V., Glaab, E., Desai, M. S., Greenhalgh, K., Frachet, A., Niegowska, M., Estes, M., Jäger, C. and Seguin-Devaux, C. (2016) 'A microfluidics-based in vitro model of the gastrointestinal human–microbe interface', *Nature communications*, 7, 11535.
- Shaker, A. and Rubin, D. C. (2010) 'Intestinal stem cells and epithelial–mesenchymal interactions in the crypt and stem cell niche', *Translational Research*, 156(3), 180-187.
- Simon-Assmann, P., Bouziges, F., Arnold, C., Haffen, K. and Kedinger, M. (1988) 'Epithelial-mesenchymal interactions in the production of basement membrane components in the gut', *Development*, 102(2), 339-347.
- Simon-Assmann, P., Turck, N., Sidhoum-Jenny, M., Gradwohl, G. and Kedinger, M. (2007) 'In vitro models of intestinal epithelial cell differentiation', *Cell Biol Toxicol*, 23(4), 241-56.
- Sorrell, J. M. and Caplan, A. I. (2009) 'Fibroblasts-a diverse population at the center of it all', *Int Rev Cell Mol Biol*, 276, 161-214.
- Srinivasan, B., Kolli, A. R., Esch, M. B., Abaci, H. E., Shuler, M. L. and Hickman, J. J. (2015) 'TEER measurement techniques for in vitro barrier model systems', *Journal of laboratory automation*, 20(2), 107-126.
- Stadnicka-Michalak, J., Schirmer, K. and Ashauer, R. (2015) 'Toxicology across scales: Cell population growth in vitro predicts reduced fish growth', *Science Advances*, 1(7).
- Stadnicka-Michalak, J., Tanneberger, K., Schirmer, K. and Ashauer, R. (2014) 'Measured and Modeled Toxicokinetics in Cultured Fish Cells and Application to In Vitro - In Vivo Toxicity Extrapolation', *Plos One*, 9(3).
- Stadnicka-Michalak, J., Weiss, F. T., Fischer, M., Tanneberger, K. and Schirmer, K. (2018) 'Biotransformation of benzo(a)pyrene by three rainbow trout (*Onchorhynchus mykiss*) cell lines and extrapolation to derive a fish bioconcentration factor', *Environmental Science & Technology*.

- Stadnicka, J., Schirmer, K. and Ashauer, R. (2012) 'Predicting concentrations of organic chemicals in fish by using toxicokinetic models', *Environmental Science & Technology*, 46(6), 3273-80.
- Streit, B. (1998) 'Bioaccumulation of contaminants in fish', *EXS*, 86, 353-87.
- Striemer, C. C., Gaborski, T. R., McGrath, J. L. and Fauchet, P. M. (2007) 'Charge-and size-based separation of macromolecules using ultrathin silicon membranes', *Nature*, 445(7129), 749.
- Sundell, K., Jutfelt, F., Agustsson, T., Olsen, R. E., Sandblom, E., Hansen, T. and Bjornsson, B. T. (2003) 'Intestinal transport mechanisms and plasma cortisol levels during normal and out-of-season parr-smolt transformation of Atlantic salmon, *Salmo salar*', *Aquaculture*, 222(1-4), 265-285.
- Sundell, K. and Sundh, H. (2012) 'Intestinal fluid absorption in anadromous salmonids: importance of tight junctions and aquaporins', *Frontiers in physiology*, 3, 388.
- Sung, J. H. and Shuler, M. L. (2009) 'Prevention of air bubble formation in a microfluidic perfusion cell culture system using a microscale bubble trap', *Biomedical microdevices*, 11(4), 731-738.
- Tan, L. and Schirmer, K. (2017) 'Cell culture-based biosensing techniques for detecting toxicity in water', *Curr Opin Biotechnol*, 45, 59-68.
- Tanneberger, K., Knöbel, M., Busser, F. J., Sinnige, T. L., Hermens, J. L. and Schirmer, K. (2012) 'Predicting fish acute toxicity using a fish gill cell line-based toxicity assay', *Environmental Science & Technology*, 47(2), 1110-1119.
- Tanneberger, K., Knobel, M., Busser, F. J. M., Sinnige, T. L., Hermens, J. L. M. and Schirmer, K. (2013) 'Predicting Fish Acute Toxicity Using a Fish Gill Cell Line-Based Toxicity Assay', *Environmental Science & Technology*, 47(2), 1110-1119.
- Tanneberger, K., Rico-Rico, A., Kramer, N. I., Busser, F. J., Hermens, J. L. and Schirmer, K. (2010) 'Effects of solvents and dosing procedure on chemical toxicity in cell-based in vitro assays', *Environmental Science & Technology*, 44(12), 4775-81.
- Tong, H. D., Jansen, H. V., Gadgil, V. J., Bostan, C. G., Berenschot, E., van Rijn, C. J. and Elwenspoek, M. (2004) 'Silicon nitride nanosieve membrane', *Nano letters*, 4(2), 283-287.
- van der Helm, M. W. (2018) *Electrical and microfluidic technologies for organs-on-chips Mimicking blood-brain barrier and gut tissues*, unpublished thesis (PhD), University of Twente, Netherlands.
- van der Helm, M. W., Odijk, M., Frimat, J.-P., van der Meer, A. D., Eijkel, J. C., van den Berg, A. and Segerink, L. I. (2016) 'Direct quantification of transendothelial electrical resistance in organs-on-chips', *Biosensors and bioelectronics*, 85, 924-929.

- van der Helm, M. W., Odijk, M., Frimat, J.-P., van der Meer, A. D., Eijkel, J. C., van den Berg, A. and Segerink, L. I. (2017) 'Fabrication and Validation of an Organ-on-chip System with Integrated Electrodes to Directly Quantify Transendothelial Electrical Resistance', *Journal of visualized experiments: JoVE*, (127).
- van der Meer, A. D. and van den Berg, A. (2012) 'Organs-on-chips: breaking the in vitro impasse', *Integr Biol (Camb)*, 4(5), 461-70.
- van Midwoud, P. M., Verpoorte, E. and Groothuis, G. M. (2011) 'Microfluidic devices for in vitro studies on liver drug metabolism and toxicity', *Integr Biol (Camb)*, 3(5), 509-21.
- Visco, V., Bava, F. A., d'Alessandro, F., Cavallini, M., Ziparo, V. and Torrisi, M. R. (2009) 'Human colon fibroblasts induce differentiation and proliferation of intestinal epithelial cells through the direct paracrine action of keratinocyte growth factor', *Journal of cellular physiology*, 220(1), 204-213.
- Vlassioug, I., Apel, P. Y., Dmitriev, S. N., Healy, K. and Siwy, Z. S. (2009) 'Versatile ultrathin nanoporous silicon nitride membranes', *Proc Natl Acad Sci U S A*, 106(50), 21039-44.
- Vo, N., Bender, A., Lee, L., Lumsden, J., Lorenzen, N., Dixon, B. and Bols, N. (2015) 'Development of a walleye cell line and use to study the effects of temperature on infection by viral haemorrhagic septicaemia virus group IVb', *Journal of Fish Diseases*, 38(2), 121-136.
- von Martels, J. Z., Sadabad, M. S., Bourgonje, A. R., Blokzijl, T., Dijkstra, G., Faber, K. N. and Harmsen, H. J. (2017) 'The role of gut microbiota in health and disease: in vitro modeling of host-microbe interactions at the aerobic-anaerobic interphase of the human gut', *Anaerobe*, 44, 3-12.
- Wallace, K. N., Akhter, S., Smith, E. M., Lorent, K. and Pack, M. (2005) 'Intestinal growth and differentiation in zebrafish', *Mechanisms of development*, 122(2), 157-173.
- Walton, K. D., Mishkind, D., Riddle, M. R., Tabin, C. J. and Gumucio, D. L. (2018) 'Blueprint for an intestinal villus: Species-specific assembly required', *Wiley Interdisciplinary Reviews: Developmental Biology*.
- Wang, Y., Ahmad, A. A., Sims, C. E., Magness, S. T. and Allbritton, N. L. (2014) 'In vitro generation of colonic epithelium from primary cells guided by microstructures', *Lab on a Chip*, 14(9), 1622-1631.
- Whittamore, J. M. (2012) 'Osmoregulation and epithelial water transport: lessons from the intestine of marine teleost fish', *Journal of Comparative Physiology B*, 182(1), 1-39.
- Widder, M. W., Brennan, L. M., Hanft, E. A., Schrock, M. E., James, R. R. and Schalie, W. H. (2015) 'Evaluation and refinement of a field-portable drinking water toxicity sensor utilizing electric cell-substrate impedance sensing and a fluidic biochip', *Journal of Applied Toxicology*, 35(7), 701-708.

- Wilson, J. and Castro, L. (2010) 'Morphological diversity of the gastrointestinal tract in fishes' in *Fish physiology* Elsevier, 1-55.
- Wilson, R. W. (2012) 'Aluminum' in Inc., E., ed., *Homeostasis and Toxicology of Non-Essential Metals*, 1st ed.67-123.
- Wu, S. M., Wildhaber, F., Vazquez-Mena, O., Bertsch, A., Brugger, J. and Renaud, P. (2012) 'Facile fabrication of nanofluidic diode membranes using anodic aluminium oxide', *Nanoscale*, 4(18), 5718-5723.
- Xu, Y., Xie, X., Duan, Y., Wang, L., Cheng, Z. and Cheng, J. (2016) 'A review of impedance measurements of whole cells', *Biosensors and bioelectronics*, 77, 824-836.
- Yasugi, S. (1993) 'Role of Epithelial-Mesenchymal Interactions in Differentiation of Epithelium of Vertebrate Digestive Organs', *Development, growth & differentiation*, 35(1), 1-9.
- Yu, J., Carrier, R. L., March, J. C. and Griffith, L. G. (2014) 'Three dimensional human small intestine models for ADME-Tox studies', *Drug discovery today*, 19(10), 1587-1594.
- Zeuner, A., Todaro, M., Stassi, G. and De Maria, R. (2014) 'Colorectal cancer stem cells: from the crypt to the clinic', *Cell stem cell*, 15(6), 692-705.
- Zheng, W., Wang, Z., Zhang, W. and Jiang, X. (2010) 'A simple PDMS-based microfluidic channel design that removes bubbles for long-term on-chip culture of mammalian cells', *Lab on a Chip*, 10(21), 2906-2910.

## Glossary

<b>AAO</b>	Anodized aluminum oxide
<b>AC</b>	Alternating current
<b>ALD</b>	Atomic layer deposition
<b>BCF</b>	Bio-concentration factor
<b>BSA</b>	Bovine serum albumin
<b>Caco-2</b>	Human colon carcinoma cell line
<b>Col1A1</b>	Collagen 1A1
<b>DAPI</b>	4',6-Diamidino-2-phenylindol
<b>DC</b>	Direct current
<b>EC<sub>50</sub></b>	Half maximal effective concentration
<b>ECIS</b>	Electric cell substrate for impedance sensing
<b>EDTA</b>	Ethylenediaminetetraacetic acid
<b>EVOM</b>	Epithelial Voltometer
<b>FBS</b>	Fetal bovine serum
<b>GIT</b>	Gastrointestinal tract
<b>HF</b>	High frequency
<b>KOH</b>	Potassium hydroxide
<b>L-15</b>	Leibovitz's L-15 medium
<b>LF</b>	Low frequency
<b>LPCVD</b>	low pressure chemical vapour deposition
<b>LY</b>	Lucifer yellow
<b>PBS</b>	Phosphate buffered saline
<b>PC</b>	Polycarbonate
<b>PDMS</b>	Polydimethylsiloxane
<b>PET</b>	Polyethylene terephthalate
<b>pnc-Si</b>	Porous nanocrystalline silicon
<b>Pt</b>	platinum
<b>REACH</b>	Registration, Evaluation, Authorization and Restriction of Chemicals
<b>RTgutF</b>	Rainbow Trout gut Fibroblast
<b>RTgutGC</b>	Rainbow Trout gut Germany Canada
<b>SDS</b>	Sodium dodecyl sulfate
<b>SEM</b>	Scanning electron microscopy

## Glossary

---

<b>Si-Chip</b>	Silicon chip with integrated aluminum oxide membrane
<b>SiN</b>	Silicon nitride
<b>SiN<sub>Flow</sub> Chip</b>	Silicon chip with integrated silicon nitride membrane for flow application
<b>TEER</b>	Trans-epithelial electrical resistance
<b>TEM</b>	Transmission electron microscopy
<b>Z</b>	Impedance
<b>ZO-1</b>	Zonula Occludens-1

## Curriculum Vitae CAROLIN DRIESCHNER



**Address:** Kreuzbühlstr. 37, 8600 Dübendorf, Switzerland  
**E-Mail:** carolin.drieschner@eawag.ch  
**Date of birth:** October 14, 1984  
**Nationality:** German

**Languages:** German (native), English (excellent), Spanish (fair), French (basics)  
**Interests:** Science, photography, outdoor sports, traveling

### EDUCATION

---

- Since Apr 2013 *Interdisciplinary Ph.D. in microtechnology & environmental toxicology at EPFL and Eawag, Switzerland*
- Supervision: Prof. Kristin Schirmer – Department of environmental toxicology (Eawag) and Prof. Philippe Renaud – Microsystems laboratory 4 (EPFL)
  - Doctoral school: Biotechnology & Bioengineering (EPFL)
  - Project: “What is the role of the fish intestine as environment-organism barrier? Mechanistic investigations using fish intestinal cells on chip”
- 2004 - 2011 *BSc and MSc in biological sciences, University of Konstanz, Germany*
- ERASMUS for 1 Semester at University of La Laguna, Spain
  - External master thesis in environmental toxicology at Eawag, Switzerland

### RESEARCH EXPERIENCE

---

- Since Apr 2013 **Ph.D. candidate**
- Microchip development and application for *in vitro* cell-based assays
  - 2 journal publications
  - Oral presentation at SETAC Europe Nantes 2016 conference, France
- May 2011 – Aug 2012 **Research assistant** – *Department of environmental toxicology and department of aquatic ecology, Eawag, Switzerland*
- Projects: (1) Studying effects of tracers used in hydrology on *Daphnia spp.*; (2) Basic research on ABC-Transporters in *Daphnia spp.*
- Oct 2010 – Apr 2011 **Master thesis** – *Department of environmental toxicology, Eawag, Switzerland*
- Project: Development and characterization of a piscine intestinal barrier model using the fish cell line RTgutGC
- Apr 2010 – Jun 2010 **Research internship** – *Department of toxicology, University of La Laguna, Spain*
- Project: Analyzing heavy metals in different fish species from the Canary Islands, Spain by Atomic Absorption Spectroscopy
- Dec 2007 – Mar 2008 **Bachelor Thesis** – *Department of human and environmental toxicology, University of Konstanz, Germany*
- Project: Impacts of pharmaceuticals on the germ cell migration in zebrafish embryo

## TECHNICAL SKILLS

---

### Software

Adobe Photoshop, Adobe Lightroom, CleWin, EndNote, GraphPad prism, KLayout, MS Word, MS Excel, MS PowerPoint, SolidWorks

### Life science

- Cell biology: Culture of human and fish cell lines, immunocytochemistry, confocal microscopy, electrical resistance measurement of cells (impedance spectroscopy, TEER), Viability assays
- Ecology: Culture of *Daphnia spp.*
- Molecular biology: DNA cloning, RNA & DNA purification, western blot, PCR
- Toxicology: Chemical exposure of aquatic organisms (zebrafish embryo, daphnia) and fish cell lines, range-finding test, dose-response curve

### Microtechnology

- Cleanroom fabrication: Ultrathin permeable membranes (alumina, silicon nitride), planar electrodes, PDMS molds, PDMS spin coating, scanning electron microscopy
- Microsystem engineering: Microfluidic bioreactor, laser cutting, PDMS molding

## PUBLICATIONS

---

**Drieschner, C.**; Minghetti, M.; Wu, S.; Renaud, P.; Schirmer, K., Ultrathin Alumina Membranes as Scaffold for Epithelial Cell Culture from the Intestine of Rainbow Trout. *ACS applied materials & interfaces* **2017**, 9 (11), 9496-9505.

Minghetti, M.; **Drieschner, C.**; Bramaz, N.; Schug, H.; Schirmer, K., A fish intestinal epithelial barrier model established from the rainbow trout (*Oncorhynchus mykiss*) cell line, RTgutGC. *Cell biology and toxicology* **2017**, 33 (6), 539-555.

## CONFERENCES

---

**Drieschner, C.**, Renaud, P., Schirmer, K. (2016) 'Fish-gut-on-chip: Development of novel in vitro system of the fish intestine', SETAC Europe, Nantes, France. (Talk)

**Drieschner, C.**, Minghetti, M., Renaud, P., Schirmer, K. (2015) 'Fish-gut-on-chip: Development of a novel in vitro system of the fish intestine', NanoBioTech, Montreux, Switzerland. (Poster)

**Drieschner, C.**, Minghetti, M., Renaud, P., Schirmer, K. (2015) 'Fish-gut-on-chip: Development of ultrathin support for intestinal cell culture from rainbow trout', SETAC Europe, Barcelona, Spain. (Poster)

**Drieschner, C.**, Renaud, P., Schirmer, K. (2014) 'Development of a microfluidic bioreactor for culture and analysis of the piscine intestinal cell line RTgutGC', SETAC Europe, Basel, Switzerland. (Poster)

